Wet adhesion properties of oilseed proteins stimulated by chemical and physical interactions and bonding

by

Haijing Liu

B.S., Henan University of Technology, P. R. China, 2010
M.S., Chinese Academy of Agricultural Sciences, P. R. China, 2013

AN ABSTRACT OF A DISSERTATION

submitted in partial fulfillment of the requirements for the degree

DOCTOR OF PHILOSOPHY

Department of Grain Science and Industry
College of Agriculture

KANSAS STATE UNIVERSITY
Manhattan, Kansas

2017

Abstract

The ecological and public health liabilities related with consuming petroleum resources have inspired the development of sustainable and environmental friendly materials. Plant protein, as a byproduct of oil extraction, has been identified as an economical biomaterial source and has previously demonstrated excellent potential for commercial use. Due to the intrinsic structure, protein-based materials are vulnerable to water and present relatively low wet mechanical properties. The purpose of this study focuses on increasing protein surface hydrophobicity through chemical modifications in order to improve wet mechanical strength. However, most of the water sensitive groups (WSG), such as amine, carboxyl, and hydroxyl groups, are also attributed to adhesion. Therefore, the goal of this research is to reduce water sensitive groups to an optimum level that the modified soy protein presents good wet adhesion and wet mechanical strength.

In this research, we proposed two major approaches to reduce WSG: 1). By grafting hydrophobic chemicals onto the WSGs on protein surface; 2). By interacting hydrophobic chemicals with the WSGs. For grafting, undecylenic acid (UA), a castor oil derivative with 11-carbon chain with a carboxyl group at one end and naturally hydrophobic, was used. Carboxyl groups from UA reacted with amine groups from protein and converted amines into ester with hydrophobic chains grafting on protein surface. The successful grafting of UA onto soy protein isolate (SPI) was proved by both Infrared spectroscopy (IR) and ninhydrin test. Wood adhesive made from UA modified soy protein had reached the highest wet strength of 3.30 ± 0.24 MPa with fiber pulled out, which was 65% improvement than control soy protein. Grafting fatty acid chain was verified to improve soy protein water resistance.

For interaction approach, soy oil with three fatty acid chains was used to modify soy protein. Soy oil was first modified into waterborne polyurethanes (WPU) to improve its compatibility and reactivity with aqueous protein. The main forces between WPU and protein were hydrogen bonding, hydrophobic interactions, and physical entanglement. Our results showed that WPU not only increased protein surface hydrophobicity with its fatty acid chains but also enhanced the three-dimensional network structure in WPU-SPI adhesives. WPU modification had increased wet adhesion strength up to 3.81 ± 0.34 MPa with fiber pulled out compared with 2.01 ± 0.46 MPa of SPI. Based on IR and thermal behavior changes observed by DSC, it was inferred that a new crosslinking network formed between WPU and SPI.

To exam if the UA and WPU technologies developed using soy protein are suitable for other plant proteins, we selected camelina protein because camelina oil has superior functional properties for jet fuels and polymers. Like soy protein, camelina protein is also highly water sensitive. However, simply applied UA and WPU to camelina protein following the same methods used for soy proteins, we did not obtain the same good adhesion results compared to what we achieved with soy protein. After protein structure analysis, we realized that camelina protein is more compact in structure compared to soy protein that made it weak in both dry and wet adhesion strength. Therefore, for camelina protein, we unfolded its compact structure with Polymericamine epichlorohydrine (PAE) first to improve flexible chains with more adhesion groups for future reaction with UA or WPU. PAE with charged groups interacted camelina protein through electrostatic interaction and promoted protein unfolding to increase reactivity within protein subunits and between protein and wood cells. Therefore, the wet adhesion strength of camelina protein was improved from zero to 1.30 ± 0.23 MPa, which met the industrial standard for plywood

adhesives in terms of adhesion strength. Then the wet adhesion strength of camelina protein was further improved after applying UA and WPU into the PAE modified camelina protein. In addition, we also found PAE unfolding significantly improved the dry adhesion strength of camelina protein from 2.39 ± 0.52 to 5.39 ± 0.50 MPa with 100% wood failure on two-layer wood test.

Camelina meal which is even more economical than camelina protein was studied as wood adhesive. Through a combination of PAE and laccase modification method, the wet adhesion strength of camelina meal was improved as high as 1.04 ± 0.19MPa, which also met industrial standards for plywood adhesives.

The results of this study had proven successful modification of oilseed protein to increase water resistance and wet mechanical strength. We have gained in-depth understanding of the relationship between protein structure and wet adhesion strength. The successful modification of plant proteins meeting the industrial needs for bio-adhesives will promote the development of eco-friendly and sustainable materials.

Wet adhesion properties of oilseed proteins stimulated by chemical and physical interactions and bonding

by

Haijing Liu

B.S., Henan University of Technology, P. R. China, 2010
M.S., Chinese Academy of Agricultural Sciences, P. R. China, 2013

A DISSERTATION

submitted in partial fulfillment of the requirements for the degree

DOCTOR OF PHILOSOPHY

Department of Grain Science and Industry
College of Agriculture

KANSAS STATE UNIVERSITY
Manhattan, Kansas

2017

Approved by:

Major Professor
Xiuzhi Susan Sun

Copyright

Abstract

The ecological and public health liabilities related with consuming petroleum resources have inspired the development of sustainable and environmental friendly materials. Plant protein, as a byproduct of oil extraction, has been identified as an economical biomaterial source and has previously demonstrated excellent potential for commercial use. Due to the intrinsic structure, protein-based materials are vulnerable to water and present relatively low wet mechanical properties. The purpose of this study focuses on increasing protein surface hydrophobicity through chemical modifications in order to improve wet mechanical strength. However, most of the water sensitive groups (WSG), such as amine, carboxyl, and hydroxyl groups, are also attributed to adhesion. Therefore, the goal of this research is to reduce water sensitive groups to an optimum level that the modified soy protein presents good wet adhesion and wet mechanical strength.

In this research, we proposed two major approaches to reduce WSG: 1). By grafting hydrophobic chemicals onto the WSGs on protein surface; 2). By interacting hydrophobic chemicals with the WSGs. For grafting, undecylenic acid (UA), a castor oil derivative with 11-carbon chain with a carboxyl group at one end and naturally hydrophobic, was used. Carboxyl groups from UA reacted with amine groups from protein and converted amines into ester with hydrophobic chains grafting on protein surface. The successful grafting of UA onto soy protein isolate (SPI) was proved by both Infrared spectroscopy (IR) and ninhydrin test. Wood adhesive made from UA modified soy protein had reached the highest wet strength of 3.30 ± 0.24 MPa with fiber pulled out, which was 65% improvement than control soy protein. Grafting fatty acid chain was verified to improve soy protein water resistance.

For interaction approach, soy oil with three fatty acid chains was used to modify soy protein. Soy oil was first modified into waterborne polyurethanes (WPU) to improve its compatibility and reactivity with aqueous protein. The main forces between WPU and protein were hydrogen bonding, hydrophobic interactions, and physical entanglement. Our results showed that WPU not only increased protein surface hydrophobicity with its fatty acid chains but also enhanced the three-dimensional network structure in WPU-SPI adhesives. WPU modification had increased wet adhesion strength up to 3.81 ± 0.34 MPa with fiber pulled out compared with 2.01 ± 0.46 MPa of SPI. Based on IR and thermal behavior changes observed by DSC, it was inferred that a new crosslinking network formed between WPU and SPI.

To exam if the UA and WPU technologies developed using soy protein are suitable for other plant proteins, we selected camelina protein because camelina oil has superior functional properties for jet fuels and polymers. Like soy protein, camelina protein is also highly water sensitive. However, simply applied UA and WPU to camelina protein following the same methods used for soy proteins, we did not obtain the same good adhesion results compared to what we achieved with soy protein. After protein structure analysis, we realized that camelina protein is more compact in structure compared to soy protein that made it weak in both dry and wet adhesion strength. Therefore, for camelina protein, we unfolded its compact structure with Polymericamine epichlorohydrine (PAE) first to improve flexible chains with more adhesion groups for future reaction with UA or WPU. PAE with charged groups interacted with camelina protein through electrostatic interaction and promoted protein unfolding to increase reactivity within protein subunits and between protein and wood cells. Therefore, the wet adhesion strength of camelina protein was improved from zero to 1.30 ± 0.23 MPa, which met the industrial standard for plywood

adhesives in terms of adhesion strength. Then the wet adhesion strength of camelina protein was further improved after applying UA and WPU into the PAE modified camelina protein. In addition, we also found PAE unfolding significantly improved the dry adhesion strength of camelina protein from 2.39 ± 0.52 to 5.39 ± 0.50 MPa with 100% wood failure on two-layer wood test.

Camelina meal which is even more economical than camelina protein was studied as wood adhesive. Through a combination of PAE and laccase modification method, the wet adhesion strength of camelina meal was improved as high as 1.04 ± 0.19 MPa.

The results of this study had proven successful modification of oilseed protein to increase water resistance and wet mechanical strength. We have gained in-depth understanding of the relationship between protein structure and wet adhesion strength. The successful modification of plant proteins meeting the industrial needs for bio-adhesives will promote the development of eco-friendly and sustainable materials, which also met industrial standards for plywood adhesives.

Table of Contents

List of Figures xiv

List of Tables xvii

Abbreviations xix

Acknowledgements xx

Chapter 1. Introduction 1

1.1 Research needs 1

1.2 Objectives and goals 3

1.2.1 Objectives 3

1.2.2 Long-term goals 4

1.3 Rationale and significance 4

1.3.1 Structural basis 4

1.3.2 Hypotheses on polyelectrolyte and fatty acyl chains stimulating protein structure 5

1.3.3 Hypotheses on the structure-mechanical properties relationship 7

1.4 Literature review 7

1.4.1 Protein structure and denaturation mechanism 7

1.4.2 Protein-based adhesives and modification methods 9

1.4.3 Studies on protein-polyelectrolyte interactions and implications 12

1.4.4 Studies on protein-fatty acyl chains interactions and implications 14

1.5 Reference 16

Chapter 2. Improved water resistance of Undecylenic Acid (UA) modified Soy Protein Isolates (SPI) based adhesive 22

2.1 Abstract 22

2.2 Introduction 22

2.3 Materials and methods: 23

2.3.1 Materials 23

2.3.2 Preparation of UA modified SPI adhesives 24

2.3.3 Instruments 24

2.4 Result and Discussion 26

2.4.1 Structure and reactivity analysis 26

2.4.2 Thermal properties 27

2.4.3 Rheology properties 28

2.4.4 Characterize of aggregates in SPI adhesives 29

2.4.5 Shear adhesion strength 31

2.5 Conclusions 31

2.6 Reference 32

2.7 Figures and Tables 35

Chapter 3. Soy-oil-based waterborne polyurethane improved wet strength of soy protein adhesives on wood 46

3.1 Abstract 46

3.2 Introduction 46

3.3 Materials and Methods 48

3.3.1 Materials 48

3.3.2 Characterization 49

3.4 Results and Discussion 52

3.4.1 FTIR spectra of SPI, WPU and their mixtures 52

3.4.2 Contact angle 52

3.4.3 Water resistance of WPU-SPI film curing on glass plate 53

3.4.4 Viscosity analysis 53

3.4.5 Thermal properties analysis 54

3.4.6 Thermogravimetric analysis (TGA) 55

3.4.7 Particle size distribution and morphology of WPU-SPI adhesives 56

3.4.8 Dry and wet strength wood specimens 57

3.5 Conclusions 58

3.6 Reference 59

3.7 Figures and Tables 61

Chapter 4. Camelina protein enhanced by polyelectrolyte interaction and its plywood bonding properties 75

4.1 Abstract 75

4.2 Introduction 75

4.3 Experimental Section 77

4.3.1 Materials 77

4.3.2 Characterization 77

4.3.3 Preparation of Camelina Protein 81

4.3.4 Preparation of modified camelina protein based adhesives 81

4.4 Results and Discussion 82

4.4.1 Molecular weight of control and modified camelina protein studied by size extraction chromatography (SEC) 82

4.4.2 IR spectra of control and modified camelina protein 83

4.4.3 Viscosities of control and modified camelina protein 84

4.4.4 Microstructures of control and modified camelina proteins 85

4.4.5 Particle size analysis 86

4.4.6 Turbidity 86

4.4.7 Thermal degradation analysis of control and modified camelina protein 87

4.4.8 Wood bonding performance of camelina protein based adhesives 87

4.5 Conclusion 90

4.6 Reference 90

4.7 Figures and tables 94

Chapter 5. Adhesion and physicochemical properties of camelina meal with different modification 105

5.1 Abstract 105

5.2 Introduction 105

5.3 Materials and methods 107

5.3.1 Materials 107

5.3.2 Preparation of modified camelina meal based adhesives 107

5.3.3 Wood bonding strength tests 107

5.3.4 Characterization 109

5.4 Results and discussion 110

5.4.1 Bonding strength of camelina meal based wood adhesive 110

5.4.2 Synergistic effect of PAE with laccase on adhesion strength of camelina meal 110

5.4.3 FTIR analysis of control and modified camelina meal 110

5.4.4 Rheology properties of control and modified camelina meal 111

5.4.5 Thermal degradation analysis of control and modified camelina meal 111

5.4.6 Differential scanning chromatography (DSC) study of camelina meal 112

5.5 Conclusion 112

5.6 Reference 113

5.7 Figures and Tables 115

Chapter 6. Conclusion and future outlook 123

6.1 Conclusion 123

6.2 Recommendation 125

List of Figures

Figure 2.1 Schematic illustration of amidation mechanism between UA and SPI 35

Figure 2.2 FTIR spectra of SPI, UA, and UA modified SPI 36

Figure 2.3 TGA curves for control SPI and SPI modified with UA at concentration of 3%, 5%, 7%, and 10% 37

Figure 2.4 DSC thermogram of UA modified SPI based adhesives 39

Figure 2.5 Viscosity of UA modified SPI based adhesives 40

Figure 2.6 Elastic and Viscous modulus of UA modified SPI adhesives 41

Figure 2.7 AFM tapping phase image of SPI, 5%UA and 10% UA modified SPI samples. 42

Figure 3.1 Proposed chemical scheme of possible interactions between WPU and SPI: covalent linkage; hydrogen bond; hydrophobic interaction; physical entanglement 61

Figure 3.2 FTIR spectra of SPI, WPU, and WPU-SPI 62

Figure 3.3 Contact angle of WPU-SPI blended adhesives as a function of WPU content 63

Figure 3.4 WPU-SPI blended samples' solid lost in water 63

Figure 3.5 Apparent viscosity of WPU0002-SPI blended adhesives as affected by shear rate 64

Figure 3.6 Apparent viscosity of WPU0500-SPI blended adhesives as affected by shear rate 65

Figure 3.7 DSC thermogram of SPI, WPU, and WPU-SPI blends. Graph on left is the first scan; graph on right is the second scan. 66

Figure 3.8 DTGA curves of WPU, SPI, and WPU-SPI blend 67

Figure 3.9 Particle size distribution of SPI, WPU0500, and WPU0500-SPI adhesives 68

Figure 3.10 Particle size distribution of SPI, WPU0002, and WPU0002-SPI adhesives 68

Figure 3.11 TEM images: A: SPI; B:WPU0002;C:WPU0500;D:WPU0002-SPI; E:WPU0500-SPI 70

Figure 3.12 Wet shear bond strength of WPU-SPI blended adhesives 72

Figure 3.13 Wood surface after dry and wet bond strength test 72

Figure 4.1 SEC molecular weight distribution of C, CP, CUP, and CWP 94

Figure 4.2 SEC molecular weight distribution of C, CPT, and CT 95

Figure 4.3 Total SEC peak area of control and modified camelina protein 95

Figure 4.4 IR spectra of PAE, C, and CP 96

Figure 4.5 The infrared absorbance of camelina protein with different modification 96

Figure 4.6 Shear rate dependent viscosities of camelina protein adhesives with different formulations 97

Figure 4.7 TEM images of camelina protein and sample modified with PAE 98

Figure 4.8 SEM images of CP and PAE treated CP 98

Figure 4.9 Particle size distributions of camelina protein adhesives with different formulations 99

Figure 4.10 Derivate thermal degradation analysis curves of control and modified camelina proteins 100

Figure 5.1 FTIR spectra of control and modified camelina meal 115

Figure 5.2 Shear rate dependent viscosities of control and modified camelina meal adhesives 116

Figure 5.3 Derivate thermal degradation analysis curves of control and modified camelina meals 116

Figure 5.4 DSC of control and modified camelina meal 117

List of Tables

Table 2.1 Contents of amino groups in samples with different UA amounts 44

Table 2.2 Degradation peak temperature of control SPI and SPI modified with UA at percentage of 3%, 5%, 7%, and 10%. 44

Table 2.3 Denaturation temperatures and enthalpy of SPI slurry with different UA content 44

Table 2.4 Particle size distribution of SPI, 5% UA and 10% UA modified SPI. 45

Table 2.5 Tapping phase contrast of SPI and UA modified SPI 45

Table 2.6 Dry and wet shear adhesion strength of UA modified SPI adhesives 45

Table 3.1 Peak temperatures and enthalpy change for DSC thermogram 73

Table 3.2 Dry shear bond strength of WPU-SPI blended adhesives 74

Table 4.1 The turbidity of camelina protein adhesives with different formulation 101

Table 4.2 Derivative thermogravimetric peaks temperature data of control and modified camelina proteins 101

Table 4.3 Two layer cherry wood adhesion strength of camelina protein modified with different amount PAE at neutral pH 102

Table 4.4 Two layer cherry wood adhesion strength of camelina protein modified with 10% PAE at different pH 102

Table 4.5 Synergistic effect of PAE with UA on two layer yellow pine wood adhesion performance at pH8 102

Table 4.6 Synergistic effect of PAE with WPU on two layer yellow pine wood adhesion performance at pH8 103

Table 4.7 Synergistic effect of PAE with T on two layer yellow pine wood adhesion performance at Ph4.5 and Ph8 103

Table 4.8 Three layer wood test results of selected adhesive formulations and literature reference data 104

Table 5.1 Two layer cherry wood adhesion strength of camelina meal modified with different amount PAE at neutral pH 118

Table 5.2 Three layer yellow pine wood adhesion strength of modified camelina meal 119

Table 5.3 Derivative thermal degradation peaks of control and modified camelina meal 121

Table 5.4 DSC peaks of control and modified camelina meal 122

Abbreviations

Abbreviation	Definition
WSGs	Water sensitive groups
UA	Undecylenic acid
SPI	Soy protein isolate
IR	Infrared spectroscopy
WPU	Waterborne polyurethane
PAE	Polymericamine epichlorohydrine
PSSNa	Sodium polystyrenesulfonate
GH	Guanidine hydrochloride
PF	Phenol formaldehyde
NaCl	Sodium chloride
$NaSO_4$	Sodium sulfate
$NaSO_3$	Sodium sulfite
BSA	Bovine serum albumin
PAA	Poly (acrylic acid)
HEL	Hen egg white lysozyme
PDADMAC	Poly (diallyldimethylammonium chloride)
FTIR	Fourier transform infrared spectroscopy
TGA	Thermogravimetric analysis
DSC	Differential scanning calorimetry
AFM	Atomic force microscopy
EDC	Carbodiimide hydrochloride
IPDI	Isophorone diisocyanate
DMPA	Dime thylol propionic acid
TEA	Trimethylamine
TEM	Transmission electron microscopy
T	Tetrakis (hydroxylmethyl)phosphonium chloride
DCM	Defatted camelina meal
SEC	Size exclusion chromatography
HPLC	High performance liquid chromatography
SDS	Sodium dodecyl sulfate
SEM	Scanning electron microscopy
C	Camelina protein
CP	Camelina protein + PAE
CWP	Camelina protein + WPU + PAE
CUP	Camelina protein + UA + PAE
CT	Camelina protein + T
CTP	Camelina protein + T + PAE
CM	Camelina meal

Acknowledgements

First of all, I would like to give all the praise to God, almighty creator and redeemer. Thank God for guiding my research project and my daily life.

Thank the financial support from the USDA-NIFA Biomass Research and Development Initiative Program (Grant no. 2012-10006-20230).

Sincerely appreciate goes to my major advisor, Dr. Susan Xiuzhi Sun. I feel grateful to be recruited by her. Without Dr. Sun's valuable and patient academic leading and suggestions, I can't finish this degree. Her continuous passion, perseverance, and wisdom for work and life have greatly encouraged me for professional development together with my everyday life. I specially want to thank Dr. Donghai Wang, Dr. Yongcheng Shi, Dr. Stefan Bossmann, and Dr. Praveen Vadlani, who serve as supervisory committee and give their valuable suggestions. Great thanks goes to Dr. Viktor Chikan for his time to serve as outside chair.

I am grateful to all the lab mates in Biomaterial and Technology Lab with whom I have been pleasure to work during my PhD project. I want to give my special thanks to Dr. Yonghui Li, Dr. Guangyan Qi, and Dr. Cong Li, for their precious advices and technical support at the beginning and during the whole research project. Thanks also go to our department secretary Mrs. Susan Kelly and Mrs. Terri Mangiaracino for their administrating support. I also would like to thank all the other members in Grain Science and Industrial Department for their friendship and help.

Last but not least, I would like to give my grateful thanks to my families. I warmly thank my parents and my parents in law for their support in every aspect of life. Thank my lovely son for just being there. My devout appreciation goes to my husband for his tasty cooking, patience, encouragement, and unconditional love. Without the love and understanding from all my families, it is not possible for me to complete my degree.

Chapter 1. Introduction

1.1 Research needs

Progress in research and development of petroleum-based resins had shown great success since the 1940s. Such resins meet many industrial applications like paint, printing ink, adhesives, and rubber for tough conditions (1). However, they also bring concerns about human health and natural environment. For example, condensation resins based on formaldehyde are traditional wood adhesives and are believed to cause human carcinogens (2). Non-renewable reservoir and growing environmental concerns from traditional petroleum resources have led to the desire for more biodegradable and renewable materials. Protein, as a byproduct of oil extraction, has been identified as a common economical biomaterial source. Proteins are made up of different polypeptide chains and these polypeptide chains fold into unique 3-dimensional structures mainly by hydrophobic interaction and hydrogen bonding in aqueous solution. Interactions between protein and substrate surface together with the intermolecular and intramolecular cross-linking of single protein contribute to the mechanical strength to support structure. The relative insolubility, resistance to proteolytic hydrolysis, or other chemical dissolution decide the durability of proteins (3). Most of the oilseed proteins are globular in water with the polar and charged amino acids on the surface and hydrophobic amino acids buried inside. Therefore, protein based adhesive are vulnerable to water penetration. The poor performance of wet adhesion strength from protein's hydrophilic nature has limited its potential industrial applications. There is a strong necessity to improve the water resistance and cohesion of protein based adhesives.

While soy protein based wood adhesives and particle boards have already shown the successful application in the commercial market, camelina which contains 40% of the protein in its defatted meal, hasn't been extensively used and could potentially serve as a new primary source of protein. Compared with soy protein, camelina protein is more economical and doesn't cause potential political and economic concerns regarding famine. Camelina would be useful new resources to replace soy protein in biomaterial field. Based on the similarity of amino acid composition between soy protein and camelina protein and the fact that the adhesion strength of camelina protein is

much lower than soy protein, it is suggested that compact 3D conformation of camelina protein hinders its adhesion property.

Altering tertiary protein conformation will potentially change its physicochemical properties including rheology, thermal stability, and mechanical strength. To make such compact globular proteins into adhesive, the bonds and interactions shaping proteins' structures need to be broken. Only with flexible and interwoven polypeptide chains can proteins attach to solid surface and distribute the concentration of stresses generated at the interface into the bulk (4).

A few studies had shown that unfolding protein tertiary structure with urea, guanidine hydrochloride, sodium dodecyle sulfate would make the polypeptide chains more flexible and have a high degree of entanglements and crosslinked structure (5-7). Strengthening the crosslinking and hydrophobicity of protein will improve its adhesion properties. Grafting hydrophobic chains, 2-octen-1-ylsuccinic anhydride and undecylenic acid, onto amino acid residues improved the wet adhesion strength of soy protein based adhesive (8.9) However, how to achieve unfolding and crosslinking while increasing the hydrophobicity at the same time? In the proposed study, the polyelectrolyte is introduced into protein solution to open the dense globular structure and then built a new crosslinking network through ionic interactions and covalent bonds to strengthen the original protein structure. The fatty acyl chains will also be introduced into protein structure to increase surface hydrophobicity. The synergetic effect between polyelectrolytes and fatty acyl chains will also be studied.

Polyelectrolyte chemicals bear electrolyte groups either cations or anions with different chain lengths and other functional groups in the main chain. Protein-polyelectrolyte interactions arise from interactions between a three-dimensional fixed and heterogeneously charged protein with a flexible charged chain strand. Strong bonding is formed through electrostatic interactions among charged groups and hydrophobic interactions among hydrophobic segments of the polyelectrolyte and hydrophobic patches of proteins (10.11) Therefore, the three-dimensional network of protein adhesive will be strengthened. To further increase hydrophobicity, aliphatic chains would be introduced into the protein-polyelectrolyte system. In summary, this project aims at a thorough understanding of how to change globular proteins into adhesives and how polyelectrolyte and

aliphatic chemicals influence protein structures as well as how to accomplish the optimum formula for oilseed proteins based adhesives.

1.2 Objectives and goals

1.2.1 Objectives

Our previous study proved that physiochemical properties of protein could be influenced by altering the interactions which stabilize the three-dimensional structure of protein. The unfolding and crosslinking of globular protein make it work better as adhesives. The task of this research is to investigate and verify our hypothesis that 1) polyelectrolytes could stimulate protein unfold and rebuild a new crosslinking network; 2) introduce fatty acyl chains into protein could increase system hydrophobicity. Both the interactions between the protein and polyelectrolytes, protein and aliphatic chemicals improve the wet adhesion strength of protein adhesive. We will study how polyelectrolyte and aliphatic chemicals interact with protein and the crosslinking structures in the hybrid system. We want to develop protein-based adhesives with enhanced mechanical strength and easy handling rheology properties. The specific objectives are:

Objective 1: Investigate the chemical reaction pathway of fatty acyl chains grafting onto protein and study modified protein structures and physiochemical properties. Hypothesis: Covering protein with hydrophobic fatty acyl chains will prevent water penetrate into and dissolve protein.

Objective 2: Study the interactions between protein and oil based polyurethane in aqueous condition. Hypothesis: Waterborne polyurethane has the hydrophilic and hydrophobic segment, which could interact and improve protein structure through covalent and noncovalent bonds.

Objective 3: Investigate the mechanisms of how polyelectrolytes interact with protein and characterize the properties of modified protein (molecular weight, particle size, morphology, thermal stability and mechanical strength). Hypothesis: polyelectrolytes stimulate protein unfolding through electrostatic and hydrophobic interactions and then form a new crosslinking complex.

Objective 4: Study the synergetic effect of polyelectrolyte-hydrophobic chains on protein structure and optimize protein adhesive formula and investigate the structure-property

relationship. Hypothesis: densely crosslinked structure with higher hydrophobicity will benefit thermal stability and both dry and wet adhesion strength.

1.2.2 Long-term goals

Our long-term goal is to develop efficient technologies to modify oilseed protein into a reliable adhesive with improved performance on wet adhesion. The modified protein based adhesives should be great substitutes for petroleum-derived adhesive resins. This will dramatically relieve the stress on fossil resources and alleviate environment pollution and then benefit human being in the long run. Also, the knowledge and methodology we gain from the proposed research will be applied to other scientific studies to exploit more protein-based biomaterials.

1.3 Rationale and significance

1.3.1 Structural basis

Proteins, formed from sequences of monomer amino acids, are specific polymers with three dimension arrangement of atoms. Proteins fold into different spatial conformations stabilized by non-covalent interactions including hydrogen bonding, ionic interactions, hydrophobic packing and van der waals forces (12). The oilseed proteins usually fold into a compact globular structure driven mainly by hydrophobic interactions which bury the hydrophobic residues inside. The interactions between amino acids play a vital role in protein folding and the formation of protein complex structures. Other external factors such as solvent, ionic strength, pH, and thermal or pressure conditions could significantly influence native protein structure. With the disruption of the forces stabilizing native state, protein will unfold or form aggregation and lose its bio-functionality. For example, water molecules play a major role in protein folding and protein interactions through their structural association with protein particularly at the two interface (13). Acid/pH can promote protein unfolding and make it go through a H^+ linked conformational transitions with a change in residue binding affinity (14).

Polyelectrolytes are macromolecules with either anionic or cationic charged functional groups, thus they have both the properties of electrolytes (dissociate in aqueous solution) and polymers (high molecular weight with repeating structures). The charged chains play the fundamental role

in determining polyelectrolyte spatial structure, stability and the interactions with other molecular assemblies. The conformation of polyelectrolyte chains decides many physical properties like viscosity, thermal stability. When polyelectrolyte dissolve in aqueous dispersion, it can interact with solute particles result in either stability or instability of the dispersion. Acrylamide is usually used to synthesis polyelectrolyte (15). By monitoring the polymerized condition of acrylamide, the chain length, charge group position and density, and even the aqueous conformation of polyacrylamide could be controlled. The polyelectrolyte can absorb on dispersion particles through physical entangling and covalent bonding. The polypeptide can also consider as polyelectrolyte when it is charged by tuning pH condition. It is possible to synthesis polyacrylamide based polyelectrolyte and used to modify the spatial structure of protein.

1.3.2 Hypotheses on polyelectrolyte and fatty acyl chains stimulating protein structure

Electrostatic interactions serve as an essential role in the binding of charged chemicals with protein. The initial electrostatic association would form a salt bridge or hydrogen bonding between protein and polyelectrolyte, which promote protein to unfold partially and gain more conformational flexibility and molecular mobility. Therefore, the hydrophobic sites are easier to access and, in turn, allow the hydrophobic chain of polyelectrolyte to interact with internal hydrophobic sites of protein after the initial electrostatic attraction. What's more, the functional groups on polyelectrolyte side chain could self-crosslink or crosslink with amino residuals during the curing process. With all the interactions, a reinforced three-dimensional crosslinking network is built within protein based adhesive. The hydrophobicity of polyelectrolyte modified protein system could be increased or decreased compared with native protein. It is hypothesized that increasing the hydrophobic groups on protein surface will benefit the water resistant after protein curing. Long chain aliphatic chemicals are suitable hydrophobic agents which can be grafted onto amino residuals through covalent bond (like amide bond formed between carboxyl and amine groups) or non-covalent linkage such as electrostatic and hydrophobic interactions.

The previous studies proved that the initial interaction between surfactants and proteins is dominantly ionic. The ionic surfactants (for example, sodium dodecyl sulfate) first binds to group with opposite charge on protein through electrostatic interactions and when initial binding site are

saturated, binding of more surfactant lead to the cluster that starts to unfold protein. The unfolded protein provides more hydrophobic binding patches and the binding change to the cooperative pattern. (16-18). It is reported that when covering the original positively charged lysine residues with negatively-charged citraconyl or neutral acetyl groups, the binding between oleic acid (negative charged) with bovine a-lactalbumin was eliminated (10). The authors believed electrostatic interactions between positive charged basic groups and the negatively charged carboxylate group were as important as the hydrophobic interactions between protein hydrophobic sites and aliphatic tails of oleic acid. The binding of polyelectrolyte to proteins is also initiated by charged groups but within a three-dimensional structure and a long flexible chain. Proteins undergoe a series of conformational changes as bending toward the direction of more unfolded structure. By varying the solution condition, soluble polyelectrolyte-protein complex formed (19). This process is too diverse to be simply accommodated in one model. Whether this complex could further crosslink under curing conditions is influenced by many factors including charge density on both polyelectrolyte and protein, ionic strength, stoichiometry ratio. The binding of sodium polystyrenesulfonate (PSSNa, negative charge) to lysozyme (globular, positively charged) stimulated the progressively unfolding of lysozyme with an initial strong electrostatic binding and then hydrophobic interaction. The short chain polyelectrolyte with protein excess formed local shrunk but no network while the long chain polyelectrolyte still keeps part of the original network within PSSNa but are partially shrunk due to cross-linking by lysozyme (20). Some studies on soy protein adhesives demonstrated it reacted with various chemicals. When grafted hydrophobic long chain structure, 2-octen-1-ylsuccinic anhydride and undecylenic acid, the rheology and thermal properties were changed, and the wet adhesion strength improved (8, 9). The grafting hydrophobic structure on protein surface will increase its water resistance but at the same time decrease its self-crosslinking and reaction with other components. Our previous study found that positively charged polymericamine-eppichlorohydrine could modify camelina protein structure and increase its mechanical strength. Given all the potential results, further study on the mechanism of how polyelectrolyte could unfold oilseed protein (soy and camelina) and form a desirable crosslinking network and the influence on physiochemical properties is necessary.

1.3.3 Hypotheses on the structure-mechanical properties relationship

The physiochemical properties of protein-based biomaterials are primarily established upon by the intrinsic amino acid sequence and peptide spatial conformation. It is found that β-sheet structures contribute to increased adhesion and water resistance in soy protein, the hydrophobic residue sequence leads to highly ordered secondary and tertiary structure than hydrophilic sequences, but they also promote aggregations (21-23). When soy protein polymerize with poly(ethylene glycol) in a loosely cross-linked network, both polymer and protein have been fully solvated, enabling 96% water content and formed hydrogel systems (24). The highly crosslinked structure tend to have larger molecular weight and stronger tensile strength. The synergistic crosslinking of poly(vinyl alcohol) hydrogel with natural gelation can significantly change its physical properties to meet the requirement of vasculature (25). Hydrophobic and electrostatic interaction mainly control the polymer self-assembly. Therefore, we hypothesize that polyelectrolyte and aliphatic chemicals could disturb protein conformation by breaking down old hydrophobic and electrostatic forces and build new crosslinking interactions. The mechanical strength of modified protein adhesives should be altered according to their structure changes.

1.4 Literature review

1.4.1 Protein structure and denaturation mechanism

Proteins are a kind of polymers made up of amino acids. Each protein is a specifical polypeptide sequence with its secondary and tertiary, even quaternary structure. The primary structure is the amino acid sequence connecting by the peptide bonds. The secondary structure refers to highly regular local sub-structures. Principally α-helices, β-sheets, and random coil or loops structure are the main types of secondary structure. These secondary structures are stabilized by hydrogen bonds between the main-chain peptide atoms. The tertiary structure refers to the spatial arrangement of a single polypeptide chain, wherein secondary structure segments into a compact three-dimensional folded form with hydrophilic groups located on the exterior protein surface and most of the hydrophobic groups buried inside to exclude water. The main strength to stabilize tertiary structure is a hydrophobic interaction between amino residues. The quaternary structure is the spatial arrangement of a multi-subunit protein and how the subunits fit together. The quaternary structure is stabilized by disulfide bonds and non-covalent interactions including hydrogen bonds, salt

bridges, and Van der Waals' force. Hydrophobic interactions and ionic networks are considered necessary for protein stability under varied denaturation condition (26).

Protein denaturation means a process in which such quaternary, tertiary and secondary structures are damaged by the application of some external physical stress like heating, radiation, ultrasound or chemical compounds such as strong acid or base, an organic solvent, salts. Such process occurs when the external stress is strong enough to disrupt the bonding interactions responsible for the secondary and tertiary structures. During a denaturation process, hydrogen bonds, salt bridges, disulfide bonds, and non-polar hydrophobic interactions are destroyed. Since denaturation reactions are not forceful enough to break the peptide bonds, the primary structure (sequence of amino acids) remains the same after a denaturation process (26). Usually, the protein can still keep its bioactivity when losing its quaternary structure because the folding of the reactive site is still retained. Denatured proteins have various characteristics, like losing solubility, communal aggregation (aggregation of hydrophobic groups), and changes in rheology properties. In most cases, denaturation is irreversible when removing the influence factors. After denaturation, proteins tend to form aggregation and crosslink into the new network.

Urea and guanidine hydrochloride (GH) are the most commonly used denaturation agents. It believes that urea upsets the hydrogen-bonding network of the solvent around hydrophobic side chains and provides better solvation environment for non-polar amino acid. Another explanation of urea denaturation is directly interacting with protein and comparing with intramolecular hydrogen bonding (27-29). Urea competes with water both as a hydrogen bond donor and acceptor (30). For larger biomolecule, the denaturation requires a high concentration of urea (>10M, for irreversible denaturation) and the association of urea with the protein-water system is based on enhancement of hydrophobic interactions (31). GH, in particular, tends to interact with hydrophobic regions of protein through its flat, nonpolar surface while exposing its polar charged edges to the solvent. In high GH concentration, the electrostatic interaction between Gdm+ and the charged residues as well as the peptide backbone is the primary mechanism for destabilizing protein structure (32, 33). At extreme pH, proteins have lower stability compared with neutral or near isoelectric point pH. Acids and bases increase the unfavorable electrostatic interactions resulting in the decreased stability (34). As might be expected, acids and bases disrupt salt bridges

held together by ionic charges (35). There are alterations in ionic interactions with the protein interactions of the chain with water molecules and exposure of hydrophobic residues under extreme pH (36). Heat and high pressure are basic physical unfolding methods for protein. It is known that the hydrophobic interactions in native protein structure are disturbed under heating or high-pressure conditions (37, 38). Recently, the study of chignolin concluded that heating caused protein transferred to a higher entropy state with larger moving space. During pressure denaturation, water approaches those not well hydrated hydrophobic residues and broke hydrophobic contacts. (39). After denaturation, protein molecule has unfolding structures and imbalanced attractive and repulsive forces of particles, which generates protein aggregation. Protein aggregation can be further developed into gelation (40, 41). Physiochemical properties including viscosity, solubility, thermal stability and mechanical strength could be modified through protein denaturation.

1.4.2 Protein-based adhesives and modification methods

In the ancient centuries, proteins like gelation and casein had been used as adhesive. After the successful development of synthetic polymers at the beginning of twenty century, protein based adhesive were abandoned by industry because the issue of water sensitivity and high price. However, petroleum derived polymers bear the drawbacks of non-degradable and toxic. Considering the natural environment and human health, more and more researchers focus on bio-based adhesives. Oilseed protein like soy and camelina proteins are byproducts of oil extraction and usually treated as animal feed. Innovate oilseed protein into value added biomaterials such as film and adhesive could bring more profit to farmers. Soy is the most promising and inexpensive raw material for wood adhesives. The timber industry lowers costs and eliminates emission with soy. Hydrolyzed soy proteins added to phenol formaldehyde (PF) resins provide cost reduction without degrading performance. Soy-based products represent one alternative to urea-based products for interior applications where legislation now restricts emissions of formaldehyde. Commercial products are available, for instance, Columbia Company had converted the soy adhesive patent from Oregon State University into decorative plywood panels under the Pure Bond name (42).

From a structure perspective, gelatin and casein have relatively large, flexible and interwoven polymer chains which can firmly attach to a solid surface by adsorption. The protein network distributes the concentration of stresses generated at the interface into the polymer bulk and away from the surface and saving the bond (43). In native state, most of the proteins are globular and compact structure. In aqueous form, most of the nonpolar residuals of globular protein are buried inside by hydrophobic interaction while the polar parts contact with water. The oilseed proteins are storage proteins with globular shapes. Soy protein has two major components, β -conglycinin (7S) and glycinin (11S), accounting for more than 70% of the total protein in soybean. β-conglycinin and glycinin are both macromolecules with a mass of 150–360 kDa (44). Camelina protein is a mixture of albumins, globulins, and glutelins with different solubility (45). Both soy and camelina protein are rich of amino residuals containing carboxyl (-COOH), amine ($-NH_2$), hydroxyl (-OH), and thiol (-SH). These functional groups are good adhesion groups absorbing onto the substrate surface and available for many reactions such as esterification, alkylation and therefore, provide many potential modification methods.

The inherently amino acid composition of oilseed protein are suitable for application in adhesives but to utilize and improve the properties, the specific bonds and interactions in native protein need to be broken to make a loose structure with more flexible crosslinking in further adhesive curing process (4). Solvent polarity, pH, chemicals, temperature, and pressure, are the major methods to modify protein. Salts like sodium chloride (NaCl), sodium sulfate ($NaSO_4$), and sodium sulfite ($NaSO_3$), could change the ionic environment and decrease protein adhesion strength at high concentration by interacting with charged polar amino residuals. Low concentration salts can decrease protein adhesive viscosity without influence on adhesion strength (46). The study of pH conditions concludes that the optimum pH for soy protein isolate to gain the maximum adhesion strength is in the range of 5.0 to 6.7 (47). Another study on alkali-modified soy protein found that moderate alkaline condition pH ten at 50 ℃ improved the adhesive strength compared with unmodified protein (48). The isoelectric pH for soy protein is around 4.5 and at higher pH condition, protein can be charged and partly unfolding. The charged and unfolding protein has a higher surface polarity which will benefit the bonding between wood and protein. Since the adhesive performance depends on both the adhesiveness and cohesiveness of protein, too much unfolding will weaken the cohesiveness of protein resulting in lower bond strength. The

temperature, ionic strength, and other factors will also affect the protein unfolding and confirmation, so the optimum condition is different for a different system. Urea and gluanidine hydrochloride (GH) are the chemical unfolding agents for protein. At low urea concentration, for soy protein, a certain amount of secondary structure changed to β-sheet and enhanced adhesion strength. While in high concentration, urea-unfolded protein structure too much to the random coil and reduced adhesion strength. GH has a similar effect of unfolding protein like urea. More hydrophobic groups were exposed, and protein secondary structure was rearranged with urea and GH treatment, which enhanced water resistance as well as adhesion strength (49-51).

There are several studies found that increasing hydrophobicity could enhance the wet adhesion strength. Under alkaline and trypsin hydrolysis condition, the globular soy protein was open to linear structure and expose more hydrophobic residuals and had improved water resistance (52). Grafting hydrophobic chains onto protein surface through covalent linkage could also increase the system hydrophobicity and water resistance. 2-octen-1-ylsuccinic anhydride and undecylenic acid were both grafted onto soy protein and the aliphatic chains form a hydrophobic layer on the protein surface and prevent water penetrating into the interface between protein and wood (8, 9). Crosslinking is another direction to modify the physicochemical properties of protein. Crosslinking agents are chemicals with multiple functional groups which can link polypeptide together or with other chemicals through covalent bonds. 3-aminopropyltriethoxysilane was used to crosslink inorganic calcium silicate hydrate with soy protein and the entangled and interwoven polymeric structure promoted the attachment to the solid surface, which consequently improved the bonding strength between protein molecules (53). Glutaraldehyde crosslinked proteins through reaction with amino groups and increased protein molecular weight and changed native protein conformation. The mild crosslinking enhanced cohesiveness and then improve bond strength but too much crosslinking resulted in rigid protein structure which damaged wettability and decreased dry and wet adhesion strength (54).

Ionic interaction and hydrogen bonding also play a major role in protein network formation. The phosphorylation of soy protein stimulated charged phosphorus groups to form ionic interaction and hydrogen bonds with polypeptide chains which enhanced the protein structure and wet adhesion strength to meet the interior used hardwood plywood and particleboard (55). Polyamide-

epichlorohydrin and soy protein molecules formed revisable complexation through ionic interactions at pH range from 4.0 to 9.0. The complexation improved the wet adhesion strength of soy protein adhesive by enhanced the crosslinking network and stabilized the structure (56). Blending with synthetic resin is another way to improve the performance of the protein-based adhesive. For example, the polyamidoamine-epichlorohydrin resin and formaldehyde based latex improved the water resistance of soy adhesive. On the other hand, adding soy protein to formaldehyde resin could reduce the emission (57, 58).

In summary, to make proteins better adhesives, the protein should be unfolded to make the polypeptide chains more flexible and then easier to attached on a wood substrate. Protein unfolding will explore more hydrophobic residuals and enhance water resistance. Mild crosslinking help stabilizes the protein structure and also benefit the adhesion strength. The previous studies on modification methods give us advise on further improving oilseed protein structure to get higher strength and water resistance.

1.4.3 Studies on protein-polyelectrolyte interactions and implications

Polyelectrolytes are polymers with positive or negative charged groups on side chains. There are many synthetic polyelectrolytes like poly(sodium styrene sulfonate) and polyacrylic acid and natural polyelectrolytes like polypeptides, glycosaminoglycans, and DNA. The electrolyte groups dissociate at an aqueous solution and affect solution's ionic strength and further influence other properties such as electrical conductivity. The charged groups on linear polyelectrolyte will repel each other and cause a complicated polymer conformation. Polyelectrolytes can be used to modify flow and stability properties of aqueous solutions and gels. In food formulation, polyelectrolytes including pectin, carrageenan, alginates and carboxymethyl cellulose are used to concrete mixtures. Polyelectrolytes can also destabilize a suspension and initiate flocculation. Proteins interact strongly with both biological and synthetic polyelectrolytes. Interactions of synthetic polyelectrolytes and protein have been studied as the technology in enzyme immobilization, protein separation, sensor development and stimuli-responsive systems. Many studies had been down to investigate and implicate the interaction between protein and polyelectrolytes.

The binding of protein to polyelectrolytes are considered as nonspecific, low affinity and nonselective binding. The initial force for protein-polyelectrolyte interaction is ionic interaction, and this force stimulates protein unfolding to explore more hydrophobic patches to interact with the hydrophobic parts on polyelectrolytes (59). The ionic strength and counterions strongly modulate the binding process. The anisotropy of electrostatic domains on protein surface plays a key role in determining the ionic strength dependence of its binding to polyelectrolytes. Through the study of hydrophobically modified polyacid binding to different proteins, the authors found out that the charge heterogeneity presence near the binding sites on proteins and inhomogeneous distributions of Coulomb potential at the protein surface can tune the overall affinity (60). When the polyelectrolytes have densely charged groups, it could affect the secondary structures of binding protein, decreasing of α-helix and increasing of β-sheet when studied using bovine serum albumin (BSA) and hen egg white lysozyme (HEL) upon (61). After binding with poly(diallyldimethylammonium chloride) (PDADMAC), the dynamic surface elasticity changed since the formation of BSA-PDADMAC complex with a surface activity higher than that of native BSA (62). On the other hand, the structure of polyelectrolytes such as chain length, charged group distribution affect the microstructures of protein-polyelectrolyte complex. High molecular weight PDADMAC binding with BSA resulted in increased viscosity (63). The BSA-chitosan complex showed much greater zero-shear viscosities and relaxation times than BSA- PDADMAC complex. The existence of dense and somewhat interconnected domains formed by the clustering of protein-polyelectrolyte aggregates of variable degrees of desolvation explained for rheology properties change. For chitosan-BSA, domains appear to occupy larger coacervate volume fractions and are more interconnected but less dense (64).

The bovine serum albumin (BSA) was the model protein to study protein immobilization by polyelectrolyte brushes. Poly(acrylic acid) (PAA) was grafted on spherical brushes and then PAA tails bonded with BSA through positive and negative charge interaction at low salts concentration. The adsorption of BSA dramatically decreased at high salt concentration because at higher level ionic strength the pH and salt concentration within the brush and BSA was the same, and steric repulsion became operative, and no adsorption took place. This binding property makes polyelectrolyte brushes suitable carrier particles for protein (65). Another application for protein-polyelectrolyte interaction is protein separation. Protein and polyelectrolyte firstly form soluble

complexes before coacervation. The phase separation is a result of the aggregation of nearly neutral polyions which is influenced by many factors. The study of BSA-polyelectrolyte poly(dimethyldially1ammo- nium chloride) system showed that soluble complex formed in the pH range between 4.6 to 7.4. When pH lower than 4.6, coulombic repulsive forces between positively charged protein and positively charged polyelectrolyte prevent the formation of complexes and protein departed as separate entities in the solution. When pH higher than 7.4, coacervate occurred. The protein and polyelectrolyte molecular concentration and ratio both affected the phased boundary pH (66, 67).

Based on all the previous studies, proteins are very active to interact with the polyelectrolyte. The microstructure of protein-polyelectrolyte complex decides the physical properties like viscosity, surface elasticity, thermal stability and aqueous solubility. Varying the structure of polyelectrolytes can achieve the aim to modify the protein conformation.

1.4.4 Studies on protein-fatty acyl chains interactions and implications

Long chain aliphatic compounds including fatty acids, fatty alcohol, lipids, and other hydrocarbons. They can interact with protein covalently through the chemical reactions on headgroups or noncovalently through special binding motifs on proteins. In bio-system, lipids can bind to specific protein to meet the need of bio-functions. For instance, the protein-lipid mixture can promote rapid surface film formation, which is thought to be critical for normal lung surfactant function (68). Proteins inserting into the lipids bilayer in biological membranes is the model for long protein chain aliphatic compounds interaction. Both the structure and conformation of protein and lipid fatty acyl chains contribute to successful binding. Lipid fatty acyl chains distort to match the rough surface of membrane protein. The presence of a rigid protein surface will reduce the extent of the emotional fluctuations of the chains, and the chains will have to tilt and become conformationally disordered to maximize contact with protein surface (69). While from the protein perspective, proteins make use of a variety of structural motifs to anchor them to lipid membranes. For example, some particular amino acid sequence could encode for enzymatic attachment of lipid moieties that target the protein to a lipid bilayer. The inherent secondary and tertiary structures of the proteins could also be used to bind lipids. Such structures include target specific domains like the C1 domain that binds diacylglycerol, the pleckstrin homology domain that binds

phosphoinositides like PIP2 and PIP3, and FYVE domains that bind PIP3 (70). The study of Golgi complex also demonstrated that lipid-protein interactions rely on the abilities of certain protein domains to recognize specific lipids. The interactions are unique to the head groups of the phospholipids and in a few cases through specifically interacting with the phospholipid acyl chains (71).

Analysis of X-ray diffraction, electron crystallography, and NMR data over 100 specific lipid binding sites on membrane proteins demonstrated that lipids bind non-covalently to proteins through their headgroups, acyl chains, or binding are mediated by the entire lipid molecules. The dominant forces to stabilize such binding are polar interactions and van der Waals force (72). Xie and the coworkers did an experiment to prove that electrostatic interactions between the positively charged basic groups on a-lactalbumin and the negatively charged carboxyl groups on oleic acid play an essential role in the binding of oleic acid with α lactalbumin in the HAMLET-like complex (20). Another study found that the hydrophobic segments in membrane protein are the bridges for the interaction between protein and lipid acyl chains. It is also possible that proteins change the orientation of hydrophobic and hydrophilic side chains and the lipids stretch acyl chains or assembling to meet the binding process (73). Many factors including lipid chain length, lipid packing, fluidity, surface charge density, and protein conformation play an important role in the protein-lipid interaction.

Binding desire fatty acyl chains on protein could change the physicochemical properties especially the water absorption of protein. Almond and walnut oil were used to modify protein films by emulsification. The hydrophobic character of protein film was enhanced (74, 75). Epoxy soybean oil was used as a cross-linking agent to improve the water resistance as well as the tensile strength of soy protein-based films (76) 2-octen-1-ylsuccinic anhydride with eight carbon chain and undecylenic acid with ten carbon chain were grafted on to soy protein through reaction with amine groups to improve the wet adhesion strength of soy protein adhesives (8,9). The hydrophobic nature of fatty acyl chains benefits the water resistance of protein.

1.5 Reference

1. Zohuriaan-Mehr, M. J., & Omidian, H. Petroleum Resins: An Overview. Journal of Macromolecular Science, Part C: Polymer Reviews, 2000, 40(1), 23–49
2. International Agency for Research on Cancer, 15 June 2004, Press release no. 153
3. Silverman, H. G., & Roberto, F. F. Understanding marine mussel adhesion. Marine Biotechnology, 2007, 9(6), 661-681.
4. Van Der Leeden, M. C., Rutten, A. A. C. M., & Frens, G. How to develop globular proteins into adhesives. Journal of Biotechnology, 2000, (00)00238-8.
5. Mo, X., & Sun, X. Thermal and mechanical properties of plastics molded from urea-modified soy protein isolates. Journal of the American Oil Chemists' Society, 2001, 78(8), 867-872.
6. Zhong, Z. K., & Sun, X. S. Thermal and mechanical properties and water absorption of sodium dodecyl sulfate-modified soy protein (11S). Journal of Applied Polymer Science, 2001, 81(1), 166-175.
7. Zhong, Z. K., & Sun, X. S. Thermal and mechanical properties and water absorption of guanidine hydrochloride-modified soy protein (11S). Journal of Applied Polymer Science, 2000, 78(5), 1063-1070.
8. Qi, G., Li, N., Wang, D., & Sun, X. S. Physicochemical properties of soy protein adhesives modified by 2-octen-1-ylsuccinic anhydride. Industrial Crops and Products, 2013, 46, 165-172.
9. Liu, H., Li, C., & Sun, X. S. Improved water resistance in undecylenic acid (UA)-modified soy protein isolate (SPI)-based adhesives. Industrial Crops and Products, 2015, 74, 577-584.
10. Chodankar, S., Aswal, V. K., Kohlbrecher, J., Vavrin, R., & Wagh, A. G. Structural study of coacervation in protein-polyelectrolyte complexes. Physical Review E, 2008, 78(3), 031913.
11. Fan, Y., Tang, S., Thomas, E. L., & Olsen, B. D. Responsive Block Copolymer Photonics Triggered by Protein–Polyelectrolyte Coacervation. American Chemistry Socisty *NANO*, 2014, 8(11), 11467-11473.
12. H. Stephen Stoker. General Organic and Biological Chemistry. Cengage Learning. 2012, p. 371.
13. Hong, S., & Kim, D. Interaction between bound water molecules and local protein structures: A statistical analysis of the hydrogen bond structures around bound water molecules. Proteins: Structure, Function and Bioinformatics,2016, 84(1) 43–51. http://doi.org/10.1002/prot.24953
14. Fitch, C. A., Whitten, S. T., Hilser, V. J., & García-Moreno E, B. Molecular mechanisms of pH-driven conformational transitions of proteins: Insights from continuum

electrostatics calculations of acid unfolding. Proteins: Structure, Function and Genetics, 2006, 63(1), 113–126. http://doi.org/10.1002/prot.20797

15. Rabiee, A., Ershad-Langroudi, A., & Jamshidi, H. Polyacrylamide-based polyampholytes and their applications. Reviews in Chemical Engineering, 2014, 30(5), 501–519. http://doi.org/10.1515/revce-2014-0004.
16. Jones, M. A theoretical approach to the binding of amphipathic molecules to globular proteins. Biochemical Journal, 1975,151, 109–114.
17. Dobrynin, A. V., Colby, R. H., & Rubinstein, M. Polyampholytes. Journal of Polymer Science, *Part B: Polymer Physics*, 2004, 42(19), 3513–3538. http://doi.org/10.1002/polb.20207.
18. Oakes, J. Protein–surfactant interactions. Nuclear magnetic resonance and binding isotherm studies of interactions between bovine serum albumin and sodium dodecyl sulphate. Journal of the Chemical Society, Faraday Transactions 1: Physical Chemistry in Condensed Phases, 1974, 70, 2200-2209.
19. Otzen, D. Protein-surfactant interactions: A tale of many states. Biochimica et Biophysica Acta - Proteins and Proteomics, 2001, 1814(5), 562–591. http://doi.org/10.1016/j.bbapap.2011.03.003.
20. Xie, Y., Min, S., Harte, N. P., Kirk, H., O'Brien, J. E., Voorheis, H. P., & Hun Mok, K. Electrostatic interactions play an essential role in the binding of oleic acid with α-lactalbumin in the HAMLET-like complex: A study using charge-specific chemical modifications. Proteins: Structure, Function, and Bioinformatics, 2013, 81(1), 1-17.
21. Cousin, F., Gummel, J., Ung, D., & Boué, F. Polyelectrolyte-protein complexes: structure and conformation of each specie revealed by SANS. Langmuir, 2005, 21(21), 9675-9688.
22. Shen, X., Mo, X., Moore, R., Frazier, S. J., Iwamoto, T., Tomich, J. M., & Sun, X. S. Adhesion and structure properties of protein nanomaterials containing hydrophobic and charged amino acids. Journal of Nanoscience and Nanotechnology, 2006, 6(3), 837-844.
23. Mo, X., Hiromasa, Y., Warner, M., Al-Rawi, A. N., Iwamoto, T., Rahman, T. S., & Tomich, J. M. Design of 11-residue peptides with unusual biophysical properties: Induced secondary structure in the absence of water. Biophysical Journal, 2008, 94(5), 1807-1817.
24. Maruyama, N., Adachi, M., Takahashi, K., Yagasaki, K., Kohno, M., Takenaka, Y., & Utsumi, S. Crystal structures of recombinant and native soybean β-conglycinin β homotrimers. European Journal of Biochemistry, 2001, 268(12), 3595-3604.
25. Shingel, K. I., & Faure, M. P. Structure-property relationships in poly (ethylene glycol)-protein hydrogel systems made from various proteins. Biomacromolecules, 2005, 6(3), 1635-1641.
26. Stepanenko, O. V., Marabotti, A., Kuznetsova, I. M., Turoverov, K. K., Fini, C., Varriale, A. D'Auria, S. Hydrophobic interactions and ionic networks play an important role in thermal stability and denaturation mechanism of the porcine odorant-binding protein.

Proteins: Structure, Function and Genetics, 2008, 71(1), 35–44. http://doi.org/10.1002/prot.21658

27. Caballero-Herrera, A., Nordstrand, K., Berndt, K. D., & Nilsson, L. Effect of urea on peptide conformation in water: molecular dynamics and experimental characterization. Biophysical Journal, 2005, 89(2), 842-857.
28. Smith, L. J., Jones, R. M., & van Gunsteren, W. F. Characterization of the denaturation of human α-lactalbumin in urea by molecular dynamics simulations. Proteins: Structure, Function, and Bioinformatics, 2005, 58(2), 439-449.
29. Frank, H. S., & Franks, F. Structural approach to the solvent power of water for hydrocarbons; urea as a structure breaker. The Journal of Chemical Physics, 1968, 48(10), 4746-4757.
30. Smith, L. J., Jones, R. M., & van Gunsteren, W. F. Characterization of the denaturation of human α-lactalbumin in urea by molecular dynamics simulations. Proteins: Structure, Function, and Bioinformatics, 2005, 58(2), 439-449.
31. Muthuselvi, L., Miller, R., & Dhathathreyan, A. How does urea really denature myoglobin. Chemical Physics Letters, 2008, 465(1-3), 126–130. http://doi.org/10.1016/j.cplett.2008.09.037.
32. Mayr, L. M., & Schmid, F. X. Stabilization of a protein by guanidinium chloride. Biochemistry, 1993, 32(31), 7994-7998.
33. O'Brien, E. P., Dima, R. I., Brooks, B., & Thirumalai, D. Interactions between hydrophobic and ionic solutes in aqueous guanidinium chloride and urea solutions: lessons for protein denaturation mechanism. Journal of the American Chemical Society, 2007, 129(23), 7346-7353.
34. Anderson, D. E., Becktel, W. J., & Dahlquist, F. W. pH-induced denaturation of proteins: a single salt bridge contributes 3-5 kcal/mol to the free energy of folding of T4 lysozyme. Biochemistry, 1990, 29(9), 2403-2408.
35. Ophardt, C. E. Denaturation of Protein. Virtual chembook. Elmhurst college.2003
36. Selvakumar, P., Sharma, N., Tomar, P. P. S., Kumar, P., & Sharma, A. K. Structural insights into the aggregation behavior of Murraya koenigii miraculin-like protein below pH 7.5. Proteins: Structure, Function, and Bioinformatics, 2014, 82(5), 830-840.
37. Denmat, M., Anton, M., & Gandemer, G. Protein denaturation and emulsifying properties of plasma and granules of egg yolk as related to heat treatment. Journal of Food Science, 1999, 64(2), 194-197.
38. Grigera, J. R., & McCarthy, A. N. The behavior of the hydrophobic effect under pressure and protein denaturation. Biophysical Journal, 2010, 98(8), 1626-1631.
39. Okumura, H. Temperature and pressure denaturation of chignolin: Folding and unfolding simulation by multibaric-multithermal molecular dynamics method. Proteins: Structure, Function, and Bioinformatics, 2012, 80(10), 2397-2416.

40. Berli, C. L., Deiber, J. A., & Añón, M. C. Heat-induced phenomena in soy protein suspensions. Rheometric data and theoretical interpretation. Journal of Agricultural and Food Chemistry, 1999, 47(3), 893-900.

41. Vasbinder, A. J., van de Velde, F., & de Kruif, C. G. Gelation of casein-whey protein mixtures. Journal of Dairy Science, 2004, 87(5), 1167-1176.

42. http://www.adhesivesmag.com/blogs/14-adhesives-blog/post/88951-advantages-of-soy-based-adhesives.

43. Pizzi A., Mittal K.L. Handbook of adhesive technology, Revised and Expanded, Marcel Dekker New York. 1994

44. Yuan, D. B., Min, W., Yang, X. Q., Tang, C. H., Huang, K. L., Guo, J., & Jun-Ru, Q. I. An improved isolation method of soy β-conglycinin subunits and their characterization. Journal of the American Oil Chemists' Society, 2010, 87(9), 997-1004.

45. Li, N., Qi, G., Sun, X. S., Wang, D., Bean, S., & Blackwell, D. Isolation and characterization of protein fractions isolated from camelina meal. Transactions of the ASABE, 2014, 57(1), 169-178.

46. Kalapathy, U., Hettiarachchy, N. S., Myers, D., & Rhee, K. C. Alkali-modified soy proteins: effect of salts and disulfide bond cleavage on adhesion and viscosity. Journal of the American Oil Chemists' Society, 1996, 73(8), 1063-1066.

47. Mo, X., & Sun, X. S. Soy proteins as plywood adhesives: formulation and characterization. Journal of Adhesion Science and Technology, 2013, 27(18-19), 2014-2026.

48. Zhang, Z., & Hua, Y. Urea-modified soy globulin proteins (7S and 11S): effect of wettability and secondary structure on adhesion. Journal of the American oil Chemists' Society, 2007, 84(9), 853-857.

49. Huang, W., & Sun, X. Adhesive properties of soy proteins modified by urea and guanidine hydrochloride. Journal of the American Oil Chemists' Society, 2000, 77(1), 101-104.

50. Zhong, Z., Sun, X. S., Fang, X., & Ratto, J. A. Adhesive strength of guanidine hydrochloride—modified soy protein for fiberboard application. International Journal of Adhesion and Adhesives, 2002, 22(4), 267-272.

51. Hettiarachchy, N. S., Kalapathy, U., & Myers, D. J. Alkali-modified soy protein with improved adhesive and hydrophobic properties. Journal of the American Oil Chemists' Society, 1995, 72(12), 1461-1464.

52. Kim, M. J., & Sun, X. S. Adhesion properties of soy protein crosslinked with organic calcium silicate hydrate hybrids. Journal of Applied Polymer Science, 2014, 131(17).

53. Wang, Y., Mo, X., Sun, X. S., & Wang, D. Soy protein adhesion enhanced by glutaraldehyde crosslink. Journal of Applied Polymer Science, 2007, 104(1), 130-136.

54. Zhu, D., & Damodaran, S. Chemical phosphorylation improves the moisture resistance of soy flour-based wood adhesive. Journal of Applied Polymer Science, 2014, 131(13).

55. Zhong, Z., Sun, X. S., & Wang, D. Isoelectric pH of polyamide–epichlorohydrin modified soy protein improved water resistance and adhesion properties. Journal of Applied Polymer Science, 2007, 103(4), 2261-2270.

56. Gui, C., Wang, G., Wu, D., Zhu, J., & Liu, X. Synthesis of a bio-based polyamidoamine-epichlorohydrin resin and its application for soy-based adhesives. International Journal of Adhesion and Adhesives, 2013, 44, 237-242.

57. Qi, G., & Sun, X. S. Soy protein adhesive blends with synthetic latex on wood veneer. Journal of the American Oil Chemists' Society, 2011, 88(2), 271-281.

58. Lorenz, L. F., Conner, A. H., & Christiansen, A. W. The effect of soy protein additions on the reactivity and formadehyde emissions of urea-formaldehyde adhesive resins. Forest Products Journal, 1999, 49(3), 73.

59. Cousin, F., Gummel, J., Ung, D., & Boué, F. Polyelectrolyte-protein complexes: structure and conformation of each specie revealed by SANS. Langmuir, 2005, 21(21), 9675-9688.

60. Seyrek, E., Dubin, P. L., Tribet, C., & Gamble, E. A. Ionic strength dependence of protein-polyelectrolyte interactions. Biomacromolecules, 2003, 4(2), 273-282.

61. Schwinte, P., Ball, V., Szalontai, B., Haikel, Y., Voegel, J. C., & Schaaf, P. Secondary structure of proteins adsorbed onto or embedded in polyelectrolyte multilayers. Biomacromolecules, 2002, 3(6), 1135-1143.

62. Milyaeva, O. Y., Noskov, B. A., Lin, S. Y., Loglio, G., & Miller, R. Influence of polyelectrolyte on dynamic surface properties of BSA solutions. Colloids and Surfaces A: Physicochemical and Engineering Aspects, 2014, 442, 63-68.

63. Bohidar, H., Dubin, P. L., Majhi, P. R., Tribet, C., & Jaeger, W. Effects of protein-polyelectrolyte affinity and polyelectrolyte molecular weight on dynamic properties of bovine serum albumin-poly (diallyldimethylammonium chloride) coacervates. Biomacromolecules, 2005, 6(3), 1573-1585.

64. Kayitmazer, A. B., Strand, S. P., Tribet, C., Jaeger, W., & Dubin, P. L. Effect of polyelectrolyte structure on protein-polyelectrolyte coacervates: Coacervates of bovine serum albumin with poly (diallyldimethylammonium chloride) versus chitosan. Biomacromolecules, 2007, 8(11), 3568-3577.

65. Wittemann, A., Haupt, B., & Ballauff, M. Adsorption of proteins on spherical polyelectrolyte brushes in aqueous solution. Physical Chemistry Chemical Physics, 2003, 5(8), 1671-1677.

66. Mattison, K. W., Brittain, I. J., & Dubin, P. L. Protein-polyelectrolyte phase boundaries. Biotechnology Progress, 1995, 11(6), 632-637.

67. Chodankar, S., Aswal, V. K., Kohlbrecher, J., Vavrin, R., & Wagh, A. G. Structural study of coacervation in protein-polyelectrolyte complexes. Physical Review E, 2008, 78(3), 031913.

68. Hawgood, S., Benson, B.J., Hamilton, R.L. Effects of a surfactant-associated protein and calcium-ions on the structure and surface-activity of lung surfactant lipids. Biochemistry, 1985, 24, 184-190.

69. East, J.M., Melville, D., Lee, A.G. Exchange-rates and numbers of annular lipids for the calcium and magnesium-ion dependent adenosine-triphosphatase. Biochemistry 1985, 24, 2615-2623.

70. Lemmon, M.A. Membrane recognition by phospholipid-binding domains. Nature Reviews Molecular Cell Biology, 2008, 9, 99-111.

71. De Matteis, M.A., Godi, A. Protein-lipid interactions in membrane trafficking at the Golgi complex. Biochimica Et Biophysica Acta-Biomembranes, 2004,1666, 264-274.

72. Yeagle, P.L. Non-covalent binding of membrane lipids to membrane proteins. Biochimica Et Biophysica Acta-Biomembranes, 2014, 1838, 1548-1559.

73. Killian, J.A. Hydrophobic mismatch between proteins and lipids in membranes. Biochimica Et Biophysica Acta-Reviews on Biomembranes, 1998, 1376, 401-416.

74. Galus, S., & Kadzińska, J. Whey protein edible films modified with almond and walnut oils. Food Hydrocolloids, 2016, 52, 78-86.

75. McHugh, T. H. Protein-lipid interactions in edible films and coatings. Food Nahrung, 2000, 44(3), 148-151.

76. Xia, C., Wang, L., Dong, Y., Zhang, S., Shi, S. Q., Cai, L., & Li, J. Soy protein isolate-based films cross-linked by epoxidized soybean oil. RSC Advances, 2015, 5(101), 82765-82771.

Chapter 2. Improved water resistance of Undecylenic Acid (UA) modified Soy Protein Isolates (SPI) based adhesive

2.1 Abstract

Soy protein has showed great potential as renewable and environment-friendly adhesives. However, poor water resistance of soy protein adhesive has limited its application as high performance wood adhesive. This work focused on development and characterization of UA modified soy proteins to improve their water resistance. The reaction between amine groups from protein and carboxyl groups from undecylenic acid was proposed to be the main chemical pathway for grafting, which was proved by Ninhydrin test and Fourier Transform Infrared Spectroscopy (FTIR). Thermal study of thermogravimetric analysis (TGA) and Differential scanning calorimetry (DSC) showed that UA modification led to less thermal stable state because of protein unfolding and less protein-protein cross linkages. The increased attractive force between carbon chains of UA and residues of protein resulted in higher viscosity and dynamic modulus. Atomic force microscopy (AFM) images indicated the changes in particle size and surface properties. Wet strengths of modified soy protein adhesives were significantly improved by 35% to 62%, compared with SPI of 2.02 MPa wet strength. Undecylenic acid with hydrophobic carbon chains and reactive carboxyl groups is an ideal bio-based modifier for soy protein.

2.2 Introduction

The main adhesives used in wood composites are petroleum-based resins including phenol-formaldehyde and urea-formaldehyde. However, formaldehyde-based resins not only damage environment but are also a human carcinogen (1). The demand to find renewable and environment-friendly substitutions for petrochemicals is urgent. Soybean is widely planted across the world which makes it one of the most promising biodegradable and renewable resources for adhesives, packaging, and labeling industries (2). However, the poor water resistance of soy protein based adhesives limits their developments (3). Soy protein contains two major compositions β-conglycinin (7S) and glycinin (11S), accounting for more than 70% of the total protein in soybean. Glycinin and β-conglycinin are both macromolecules with a mass of 150-360kDa (4). There are 20 different kinds of amino acid residues with varieties of functional groups on the side chains of polypeptides including carboxyl (-COOH), amino ($-NH_2$), hydroxyl (-OH), and thiol (-SH). Such

functional groups are available for many chemical reactions like esterification and alkylation. Modifications of soy protein affect its surface and inner structures, which results in changes of physical and mechanical properties of soy protein adhesives (5).

In the past decades, lots of chemical modifications of soy protein adhesives were carried out to improve water resistance. Most of them focused on unfolding protein and making the hydrophobic subunits exposed (6, 7, 8). Qi et al, used sodium bisulfide modified soy protein to react with 2-octen-1-ylsuccinic anhydride, which needed two steps to finish the modification (9). Our study focused on one step modification of simple soy protein isolate (SPI) to improve the water resistance. Only undecylenic acid (UA) was used to react with SPI and the pH was kept consistently at 10.0. UA is derived from castor oil by cracking under pressure and it is widely used in pharmaceuticals, cosmetics and perfumery (10, 11). UA has 10 carbons in its aliphatic chain with C=C double bond and carboxyl group on each end [$CH_2CH(CH_2)_8COOH$]. The long hydrophobic aliphatic chain is supposed to be water unfavorable.

In the present work, we confirmed reaction between UA and SPI through FTIR and ninhydrin test. The objectives of this study were to improve water resistance of soy protein based adhesives through grafting hydrophobic chains and characterize physical and mechanical properties such as thermal, rheological and adhesion strength of modified adhesives.

2.3 Materials and methods:

2.3.1 Materials

Defatted soy flour was purchased from Cargill (Cedar Rapids, IA) and was used for extraction of soy protein isolate (SPI). SPI was precipitated at pH 4.5 and redissolved at pH 7.6, then freeze-dried (freeze dryer, Model 6211-0459; The Virtis Company. Inc., Gardiner. NY). The dried SPI was milled into powder, with 95% passed through U.S. #100 mesh. The freeze-dried SPI powder sample had a protein content of 85.6% and moisture content of 8%.

Undecylenic acid (UA, 99%), 1-ethyl-3-[3-dimethylaminopropul] carbodiimide hydrochloride (EDC, 99%) and Ninhydrin reagent solution were purchased from Sigma-Aldrich. Cherry wood

veneers with dimensions of 50 mm × 127 mm × 5mm (width × length × thickness) were provided by Veneer One (Oceanside, NY).

2.3.2 Preparation of UA modified SPI adhesives

2g SPI powder was suspended in 14.6ml deionized water and stirred for 1hr to make uniform, 12% solid content slurries. Adjusted pH of SPI slurry to 10 ± 0.1 with 2mol/L sodium hydroxide using a digital pH analyzer. Then, UA was added to SPI slurry and pH of the slurry was maintained at 10.0 by adding sodium hydroxide. EDC (30 wt% of UA) was added to the slurry together with UA to active carboxyl group (-COOH). The mixture of SPI slurry and UA was stirred for 5 h at room temperature (23 ℃). Varying UA content to be 0, 3%, 5%, 7%, and 10% on dry base of SPI, a series of UA modified SPI adhesives were prepared.

2.3.3 Instruments

2.3.3.1 Infrared spectroscopy

SPI and UA modified SPI samples were freeze dried and grounded into fine powder for IR analysis. The IR spectra were recorded by PerkinElmer Spectrum 100 FTIR spectrometer (Waltham, MA) in MID-IR range (4000-600 cm^{-1}) with a Universal ATR (attenuated total reflectance) sampling device. Each sample was scanned 32 times at a resolution of 2 cm^{-1}. Data from ATR is converted to sample transmission data.

2.3.3.2 Qualitative analysis of amino (-NH2) group

Based on the reaction between amino group and ninhydrin, the concentration of amino group can be tested by the changes in absorbance at 570 nm. 1 ml Ninhydrin reagent solution was used to mix with each sample (2 ml, samples were diluted 200 times to ensure absorbance at 570 nm under 1.0) and then placed samples into boiling water bath for 10 min. Cooled to room temperature and added 5 ml 95% ethanol to each sample. Read absorbance at 570 nm and the concentration of amino group was determined by comparison of the 570 nm absorbance with standard curve (Glycine solution was used to make the standard curve. $Y=0.0859x-0.0004$, $R^2=0.9988$, Y: concentration of amino group; X: absorbance) (12, 13).

2.3.3.3 Thermogravimetric analysis (TGA)

SPI and UA modified SPI slurries were freeze dried and then the decomposition temperature of dry samples were determined using TGA (PerkinElmer Pyris1 TGA, Norwalk, CT). For each sample, about 5 mg was loaded in the pan and heated from 25 to 700 ℃ at a rate of 10 ℃/min under nitrogen atmosphere. Onset (To) and peak temperatures (Tp) were calculated by TGA software.

2.3.3.4 Differential Scanning Calorimetry (DSC)

Thermal denaturation of SPI and UA modified SPI (slurry with 12% solid content) were measured visa differential scanning calorimeter (Q200, TA instrument, Schaumburg, IL). About 10 mg samples were hermetically sealed in Tzero aluminum hermetic pans. Sample temperature was held at 20 ℃ for 1 min and then scanned from 20 to 150 ℃ with a heating rate of 10℃/min.

2.3.3.5 Rheology properties

Apparent viscosity of SPI and UA modified SPI slurries were measured by a Bohlin CVOR150 rheometer (Malvern Instruments, Southborough, MA) with a parallel plate (PP20, 20 mm plate diameter and 500 μm gap). Shear rate was 25 S^{-1} and testing temperature was 23℃.To prevent dehydration during testing, a thin layer of silicone oil was spread over the circumference of the sample.

Dynamic oscillatory shear measurements were carried out using the same rheometer. Constant strain of 0.01 and an angular frequency of 0.63 rad/s were used. Samples were heated from 20 to 75 ℃ at a heating rate of 3 ℃/min. A thin layer of silicone oil was spread over the circumference of the sample to prevent evaporation of water. Elastic modulus (G') and viscous modulus (G'') were continuously recorded.

2.3.3.6 Atomic Force Microscopy (AFM)

Tapping-mode AFM was used to obtain height and phase imaging data on an Innova AFM from BRUKER. Silicon probes with 125 μm long cantilevers were used at their fundamental resonance frequencies which typically varied from 200 to 400 KHz depending on the cantilever. Samples were prepared by diluting protein slurry to 10 μg /ml and then put them onto freshly cleaved mica. Nitrogen gas was used to dry the samples and resulted in particles fixed to the mica surface.

2.3.3.7 Particle size analysis

The 12% solid content SPI and UA modified SPI slurries were used for particle size analysis directly. Laser scattering particle size distribution analyzer LA-910 from HORIBA company were used to record and calculate particle size distribution.

2.3.3.8 Wood specimen preparation and shear strength measurements

Cherry wood were preconditioned in chamber (Electro Tech Systems, Inc., Glenside, PA) at 23 ℃ and 50% RH for a week before use. About 600 μl SPI adhesive slurry was brushed onto each end of the cherry wood piece with dimensions of 127 mm × 20 mm (length × width). Wood pieces were allowed to rest at room temperature for 15 min and then assembled and pressed with a hot press at 170 ℃, 1.4 MPa for 10 min. Wood samples were removed and cooled at room temperature and then stored in chamber at 23 ℃ and 50% RH.

The wood assemblies were preconditioned in a 23℃ and 50% RH chamber for 1 day and cut into 5 pieces with dimensions of 50 mm × 20 mm (length × width), then further conditioned for 2 days before dry strength test. According to ASTM Standard Method D2339-98 at a crosshead speed of 1.6 mm/min (14), wood specimens were tested with an Instron Tester (Model 4465, Canton, MA). Adhesion strength was recorded as stress at the maximum load. Wood failure was estimated in accordance with the standard method for estimating the percentage of wood failure in adhesive-bonded joints (15). Results in this paper were the average of five duplicates.

Water resistance of the wood assemblies was measured on the basis of ASTM Standard Methods D1183-96 and D1151-00 (16, 17). The specimens after cutting were soaked into water at room temperature for 48 h. The wet strength was tested immediately after soaking.

2.4 Result and Discussion

2.4.1 Structure and reactivity analysis

Carboxyl groups of UA and amino groups of SPI can carry out amidation. Fig.1 shows the possible chemical pathway with carbodiimide hydrochloride (EDC) as catalyst to active carboxyl group. EDC reacts with a carboxyl group first and forms an amine reactive O-acylisourea intermediate that quickly reacts with an amino group to form an amide bond (16).

Fig.2 showed the FTIR spectra of SPI, UA, and UA modified SPI. The characteristic peaks of control SPI are amide I at 1634 cm^{-1} corresponding to C=O stretching vibration (80%) with minor contribution of C-N stretching vibration and amide II at 1514 cm^{-1} arising from N-H bending (60%) as well as C-N stretching vibration (40%) (18, 19). The broad peak at 3283 cm^{-1} responded for the N-H stretching vibration of protein. The characteristic peak of carboxyl group in UA was at 1706 cm^{-1} from C=O stretching and long aliphatic carbon chain was characterized by $–CH_2$ and –CH3 stretching at 2925 and 2855 cm^{-1} respectively (20). For the spectrum of UA modified SPI (SPI:UA = 4:1, weight ratio), the characteristic peak of carboxylic acid at 1706 cm^{-1} disappeared indicating –COOH participated in reaction with $–NH_2$. The position of amide II peak moved to higher wavenumber 1559 $cm^{-1}$and the relative intensity between amide II and amide I increased compared with unmodified SPI. Since the reaction between –COOH from UA and $–NH_2$ from SPI would generate new C-N vibration, changes in amide II peaks demonstrated this reaction.

Free amino groups in SPI slurry before and after reaction with UA were tested by ninhydrin reagent. The concentrations of amino groups and percentages of reacted amino groups in different samples were shown in Table 1. With the increasing of UA amount involved in reaction, the concentration of amino group dropped from 8.25 to 0.86 μmol/ml. For sample with a weight ratio of SPI:UA=1:1, 89.57% amino groups were grafted with UA. Amino test together with FTIR spectrum were strong evidences for reaction between carboxyl group from UA and amino group from SPI.

2.4.2 Thermal properties

Fig. 3 shows derivative weight loss curves as a function of temperature for SPI based adhesives with different UA contents. The peak temperatures of each sample in TGA were summarized in Table 2. Control SPI experienced three stages weight loss degradation. In the first stage, from 36.6 ℃ to 103.8 ℃, weight loss was due to evaporation of free and bonded water. The second stage was associated with protein degradation from 283.9 ℃ to 360.3 ℃. During the degradation, non-covalent bonds including intermolecular and intramolecular hydrogen bonds, electrostatic bonds and losing of hydrophobic interaction were firstly decomposed, and then covalent bonds between C-N, C (O)-NH, C (O)-NH_2 and $–NH_2$ of amino acid residues were broken with increasing heating temperature. Protein backbone was totally decomposed and released various gases such as CO_2,

CO, and NH3 (21, 22). The third degradation peak at 499.8 to 544.4 ℃ indicated a protein composition with higher decomposition temperature. Long time alkali treatment could unfold protein structure and exposed more reactive side groups such as amino, carboxyl, and hydroxyl which were responsible for crosslinking reactions (23, 24). UA modified samples had similar water lost peak as that of control. But there was only one protein degradation peak from around 270 to 350 ℃. One possible reason for the thermal stability change is that UA prefers to react with $–NH_2$ groups on unfolded protein surface and thus the cross linkages due to protein-protein interaction decreased. Another reason maybe that hydrophobic interaction between aliphatic chains of UA and protein promotes the rupture of low-energy inter-molecular bonds that maintain protein conformation and disrupt the continuity of protein matrix, resulting in unfolding and less thermal stability (25).

DSC study showed that thermal denaturation of pure SPI slurry at pH 10 was characterized by one major peak at 76.9 ℃. Usually, soy protein has two denaturation peaks at around 75 and 90 ℃ responding to β-conglycinin globulin (7S) and glycinin globulin (11S) respectively. 11S can converts to 2S or 7S in alkali condition (26). Since inHyd our research the control SPI had a long time alkali treatment, only 7S denaturation peak was found. The Td of 3% and 5% UA modified SPI moved to lower temperature and enthalpy increased. For 7% and 10% UA modified samples, only small peaks were found at around 70 ℃. Reaction between UA and amino groups of SPI converted the positive charged groups into neutral residues, thus the electrostatic repulsion was weakened and tended to gather to larger aggregates (27). However, the reaction between UA and active amino groups on protein could unfold polypeptide chains and dissociate aggregates. Introducing long alky chains on protein would enhance hydrophobic interaction among different polypeptides. The association of polypeptides led to a more thermal stable state while dissociation led to a less thermal stable state. The completion between association and dissociation explained changes in denaturation temperature and enthalpy of modified SPI slurry.

2.4.3 Rheology properties

The apparent viscosities of SPI with different UA modification at single shear rate (25 S^{-1}) were summarized in Fig.5. Modified samples had higher viscosity, which firstly increased from 227.67 to 843.00 cP and then jumped to 5623.33 cP. 3%, 5%, and 7% UA modified SPI adhesives still

had good flow-ability while viscosity of sample with 10% UA was too viscous to handle. The long hydrophobic carbon chains of UA might attract the hydrophobic groups of protein, thus the attractive force (hydrophobic interaction) between different protein particles increased which resulted in higher viscosity. After adding UA, the concentration of the slurry also increased which was another possible reason for the higher viscosity (28, 29).

Fig. 6 showed the dynamic viscoelasticity of control and UA modified SPI samples. The elastic modulus (G') and loss modules (G'') were recorded as a function of temperature. Viscoelastic properties of different SPI slurry were well characterized by elastic modulus (G') and loss modulus (G''). The G' and G'' of UA modified SPI were both higher than control sample and increased with UA amount. These data indicated that after UA modification the protein slurry formed stiffer and more solid cross linkage than control. This result was consistent with viscosity changes. We hypothesized that the hydrophobic interaction between alkyl chain of UA and amino acid residues led to the increase in viscosity and modulus. Due to the increased intra- and intermolecular attractive force, probably as a result of hydrophobic interaction and hydrogen bonding, the molecular networks were strengthened. As temperature increased, molecular movements increased and protein matrix became soft. Thus, the modulus decreased with increasing temperature.

2.4.4 Characterize of aggregates in SPI adhesives

Compared to control SPI, UA modified SPI have different aggregate structures due to the introduction of alkane chains, which may cause the difference in viscoelastic behaviors. AFM, as a powerful instrument to detect the contact response between tip and sample, can be used to describe the differences of viscoelastic behaviors among samples by phase imaging. Phase imaging reflects the energy dissipation involved in the contact between the tip and the sample, which depends on a number of factors, including such features as viscoelasticity, surface energy hysteresis and long-range interfacial interactions. Especially viscoelasticity, which varies remarkably based on the setting oscillation amplitude (30, 31, 32). For mixed samples, it is easy to get contrast in the phase. In this study, line scans were carried out after getting tapping phase images to give information on phase contrast.

Fig.6 was the AFM tapping phase image of control and UA modified samples. A lot of large aggregates were found in SPI image. But aggregates in modified samples became much smaller. To quantify the changes in true adhesive samples, particle size distributions of different UA modified samples were measured. As was shown in Fig.7, SPI had three peaks in its particle size distribution curve while UA modified samples only had the first two peaks at smaller size. There were much more particles larger than 500 μm in SPI than in UA modified samples. Table 4 gave more quantitative information on this. The median number of SPI was 90.3 μm and this data dropped to 78.0 and 75.9 μm after 5% and 10% UA modification respectively, which indicated that SPI had higher frequency in larger particle sizes while modified sample had higher frequency in smaller sizes. The mean particle size of SPI was 162.7 μm while for modified samples, the mean size were only 116.2 and 101.3 μm for 5% and 10% UA respectively. The mode number (particle size at highest frequency) of control sample was also bigger than modified samples. The particle size distributions had good consistency with AFM image. Because UA reacted with amino groups on protein surface, the cross linkages due to protein-protein interaction decreased. Thus, less large aggregates were formed after modification.

Table 5 gave the phase contrast data under different setpoints. Setpoint is a measure of force applied by the tip to the sample, which is controlled by certain amplitude of oscillation of the cantilever. At setpoint 1v, the phase contrast of SPI was 3.4 while this number changed to 2.8 and 1.8 for setpoints at 2 and 3.5 respectively. The big changes of contrast indicated that SPI sample surface was sensitive to forces attacked on it. While for modified samples, the contrasts stayed around 6 under setpoint 1 and 2V and dropped to 4.2 at setpoint 3.5V. Under the same setpoint, phase contrasts of modified sample were about two times of that of control, which meant modified samples had stronger hysteretic quality. 5% and 10% UA modified samples had similar phase contrasts, which indicated that they were similar in surface physical properties. After grafting UA on SPI, the aliphatic chain could interact with protein surface through hydrophobic force or hydrogen bonds. The folded structures of SPI changed and resulted in changes of properties such as viscoelasticity and adhesion.

2.4.5 Shear adhesion strength

Both SPI and UA modified adhesives had great performance on dry shear adhesion strength, showing in Table 6. UA had little influence on dry shear strength, all samples exhibiting 100% cohesive wood failure. The wet strength of UA modified SPI adhesives were improved from 2.04 MPa to 3.3 MPa at UA amount up to 10%. The fiber of the wood specimen was pulled out from the glued wood surface for 10% UA modified sample. As a result of UA grafted onto SPI through reaction with $-NH_2$, the conformation of protein might change which could increase contact surface areas between protein and wood and then benefit adhesion strength. At the same time, hydrophilic amino groups were replaced by hydrophobic aliphatic hydrocarbon chains which enhanced the hydrophobic interactions among protein molecules. Poor wet strength of protein based adhesives is due to cavities between protein and wood surface formed when hydrophilic groups of protein dissolve into water. Introducing hydrophobic chains on protein could decrease its water solubility. In addition, UA is totally not water soluble and thus the hydrophobic aliphatic chains prevent water penetrating into the interfacial surface of adhesive and wood. The decrease of hollow cavities could be the main reason for increased water resistance of UA modified SPI adhesives.

2.5 Conclusions

UA was successfully grafted on soy protein through reaction between –COOH and $–NH_2$ under facile condition, confirmed by the disappearance of carbonyl peak at 1706 cm^{-1} in FTIR spectra and decreased amino group concentration tested through ninhydrin reagent. The less thermal stability after UA modification was detected by denature and degradation peak changes in DSC and TGA curves. Increased viscoelastic properties demonstrated the unfolding of protein during reaction. AFM image and particle size distribution proved the dissociation and less protein to protein cross-linkage after grafting UA. AFM phase contrast information also proved viscoelastic properties changes in UA modified samples. UA modification significantly improved wet shear adhesion strength by 35%-62%. The oily nature and long hydrophobic alkyl chains of UA prevented water penetration, which mainly contributed to the significant water resistance improvement.

2.6 Reference

1. International Agency for Research on Cancer, 15 June 2004, Press release no. 153
2. Zhong, Z., Sun, X.S., Fang, X., Ratto, J.A., 2002. Adhesive strength of guanidine hydrocholoride-modified soy protein for fiberboard application. Int. J. Adhes. 22, 267–272; Qi, G., Sun, X.S., 2010. Peel adhesion properties of modified soy protein adhesive on a glass panel. Ind. Crop Prod. 32, 208–212
3. Kumar R., Choudhary V., Mishra S., and Varma I.K., Adhesive and plastics based on soy protein products, Industrial Crops and Products, 2002(16)155-172
4. Thanh, V. H.; Shibasaki, K. β-Conglycinin from soy proteins: isolation and immunological and physicochemical properties of the monomeric forms. Biochim. Biophys. Acta 1977, 490, 370–384
5. Zhu, L., 2006. Studies of soy protein adhesive performance on the effects of pH, amino acid group, and temperature. PhD diss. Manhattan, KS: Kansas State University,Department of Grain Science and Industry
6. Huang, W., Sun, X.S., 2000. Adhesive properties of soy proteins modified by sodium dodecyl sulfate and sodium dodecylbenzene sulfonate. J. Am. Oil Chem. Soc. 77,705–708
7. Rogers, J., Geng, X., Li, K., 2004. Soy-based adhesives with 1, 3- Dichloro-2-propanol as a curing agent. Wood Fiber. Sci. 36, 186–194
8. Qi, G., Li, N., Wang, D., Sun, X.S., 2012. Physicochemical properties of soy protein adhesives obtained by in situ sodium bisulfite modification during acid precipitation. J. Am. Oil Chem. Soc. 89, 301–312
9. Qi G., Li N., Wang D., and Sun, X.S., 2013, Physicochemical properties of soy protein adhesives modified by 2-octen-1-ylsyccinic anhydride, Industrial Crops and Products 46, 165-172
10. "United States International Trade Commission Memorandum" (PDF). USITC. Archived from the original on 2006-09-24. Retrieved 2007-01-02. - see page 2 of link
11. Lemuel P. Ereaux and Gibson E. Craig (1949). "Undecylenic Acid in Psoriasis". Can Med Assoc J. 61 (4): 361–364. PMC 1591667. PMID 18140580).
12. Moore, S., et al., Chromatography of amino acids on sulfonated polystryrene resins. An improved system. Analytical Chemistry., 30, 1185-1190, 1985
13. Virender K. Sarin, Stephen B. H. Kent, James P. Tam, and R. B. Merrifield, Quantitative Monitoring of Solid- Phase Peptide Synthesis by the Ninhydrin Reaction, Analytical Biochemistry 117, 147-157(1981)).
14. Annual Book of ASTM Standards (2002) D2339-98. ASTM International, West Conshohocken 15.06:158–160

15. Standard practice for estimating the percentage of wood failurein adhesive bonded joints. In Annual Book of ASTM Standards; ASTM International: West Conshohocken, PA, 2002; 15.06, D5266-99, p 443

16. Grabarek Z. and Gergely J., Zero-length crossing procedure with the use of active esters. Analytical Biochemistry 1990, 185:131-5

17. Annual Book of ASTM Standards (2002) D1151-00. Vol. 15.06, ASTM International, West Conshohocken, pp 67–6919

18. Thanh VH, Okubo K., and Shibasaki K., Major proteins of soy seeds. A straightforward fraction and their characterization heterogeneity of beta-conglycinin. Journal of Agricultural Food Chemistry 1976, 24:1117–1121

19. Stuart B., Introduction and applications. In: Ando, D.J. (Ed.), Biological applications of infrared spectroscopy. West Sussex, England, 1997, pp. 127–131

20. Jackson Michael and Mantsch Henry H., The use and misuse of FTIR spectroscopy in the determination of protein structure, 1995, Critical Reviews in Biochemistry and Molecular Biology, 30(2):95-120

21. Olga Gershevitz and Chaim N. Sukenik, In situ FTIR-ATR and titration of carboxylic acid-terminated SAMs, 2004, Journal of American Chemistry society, 126, 482-483

22. V.Schmidt, C. Giacomelli, V. Soldi*, Thermal stability of films formed by soy protein isolate-sodium dodecyl sulfate, Polymer Degradation and Stability 87(2005) 25-31, 2005,87,25-31

23. Das SN, Routray M, Nayak PL (2008) Spectral, thermal andmechanical properties of furfural and formaldehyde cross-linked soy protein concentrate: a comparative study. Polym Plastic Technol Eng 47:567–582

24. Hettiarachchy N.S., Kalapathy U., and Myers D.J., Alkali-Modified soy protein with improved adhesive and hydrophobic properties, JAOCS 1996 vol.72. no.12, 1461-1465

25. Mo X, Sun X. Thermal and mechanical properties of plastics molded form sodium dodecyl sulfate-modified soy bean protein isolates. J Polym Environ 2000;8(4):161e6.)

26. V. Schmidt, C.Giacomelli, and V.Soldi, Thermal stability of films formed by soy protein isolate-sodium dodecyl sulfate, polymer, degradation and stability, 2005(87):25-31

27. Catriona M. M. Lakenmond, Harmen H. J. de Jongh, Martin Hessing, Harry Gruppen and Alphons G. J. Voragen, Soy Glycinin: Influence of pH and Ionic Strength on Solubility and Molecular Structure at Ambient Temperatures, 2000, Agricultural and Food Chemistry, Vol 48,(6)1985-1990

28. Achouri, A., Zhang, W., Xu, S., 1998. Enzymatic hydrolysis of soy protein isolate and effect of succinylation on the functional properties of resulting protein hydrolysates. Food. Res. Int. 31, 617–623.

29. Per M. Claesson and Hugo K. Christenson, Very long range attractive forces between uncharged hydrocarbon and fluorocarbon surfaces in water, Journal Physics and Chemistry, 1988,92,1650-1655

30. Garcia R., G ómez, C.J., Martinez N.F., Patil S., Dietz C., and Magerle R., Identification of Nanoscale Dissipation Processes by Dynamic Atomic Force Microscopy, Physical Review letters, 2006, 7 July week ending 016103-1-016103-4

31. Ludovic Berthier and Gilles Tarijus, The role of attractive forces in viscous liquids, Journal of Chmical Physics, 2011, 134, 214503-1-1

32. Peter Eaton, and Paul West, Atomic Force Microscopy, Oxford University Press, 2010, Chapter 3, Page 49-57

33. Theory of phase imaging: Cleveland, J. P., et al, Apply. Physics. Letter. 1998, 72, 2613-2615

2.7 Figures and Tables

Figure 2.1 Schematic illustration of amidation mechanism between UA and SPI

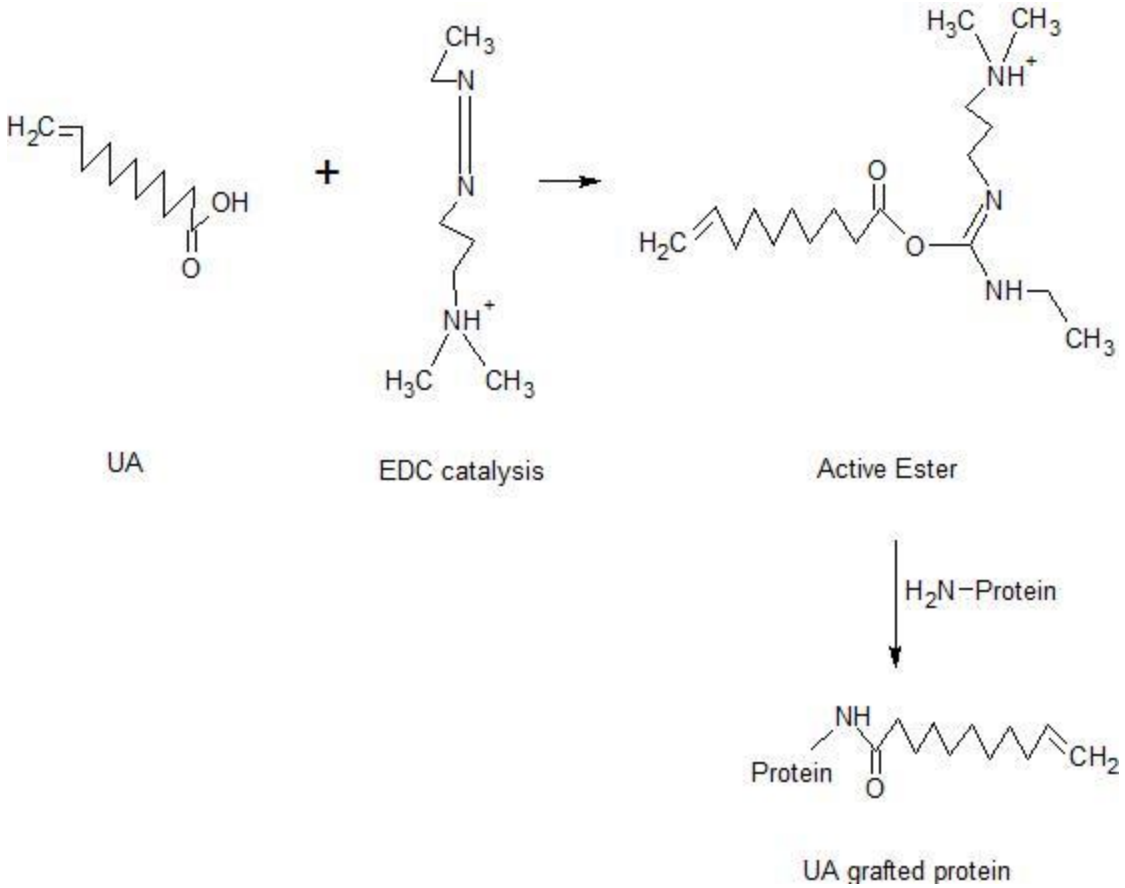

Figure 2.2 FTIR spectra of SPI, UA, and UA modified SPI

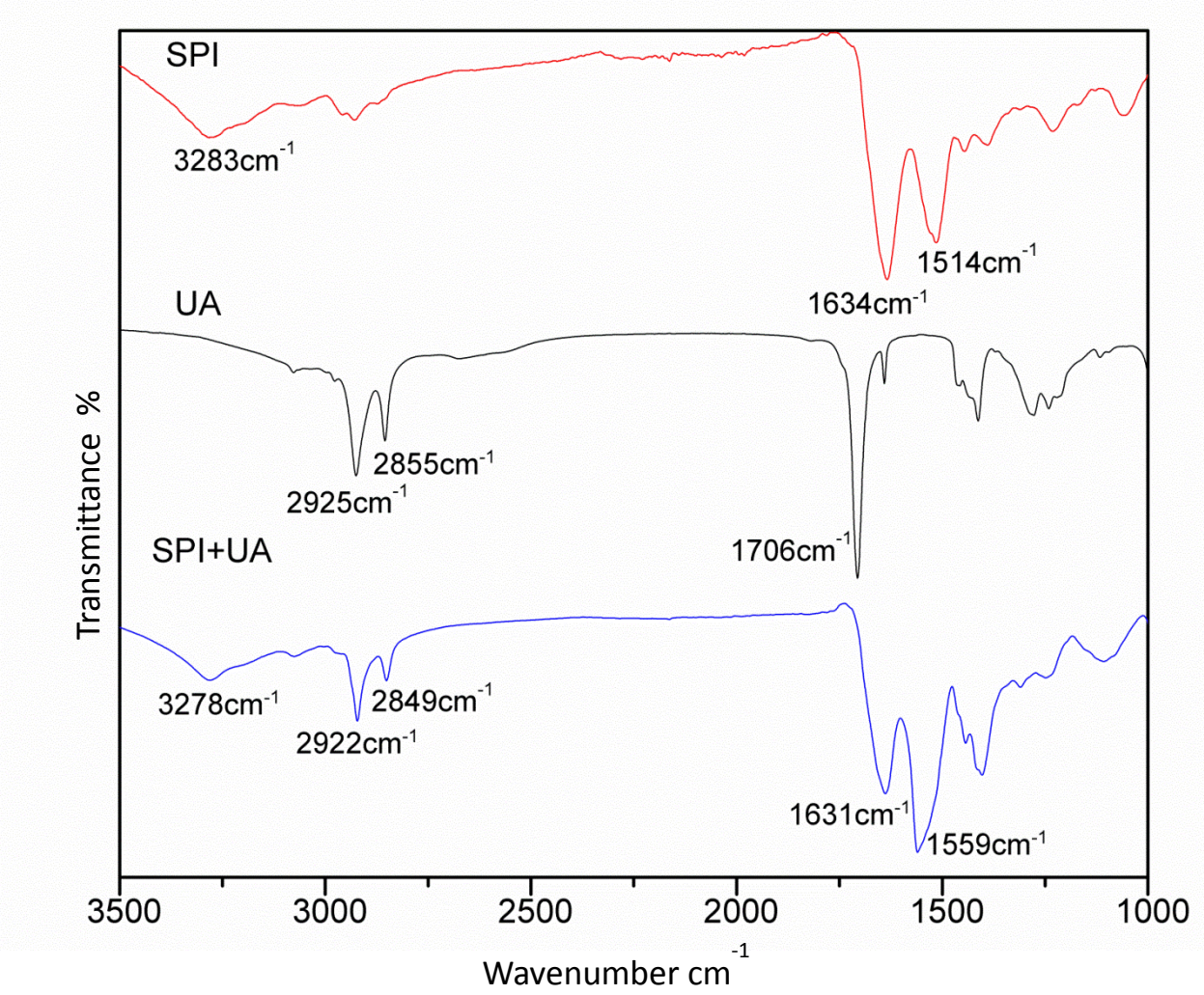

Figure 2.3 TGA curves for control SPI and SPI modified with UA at concentration of 3%, 5%, 7%, and 10%

Note: Measured at a heating rate of 10 ℃/min under nitrogen atmosphere

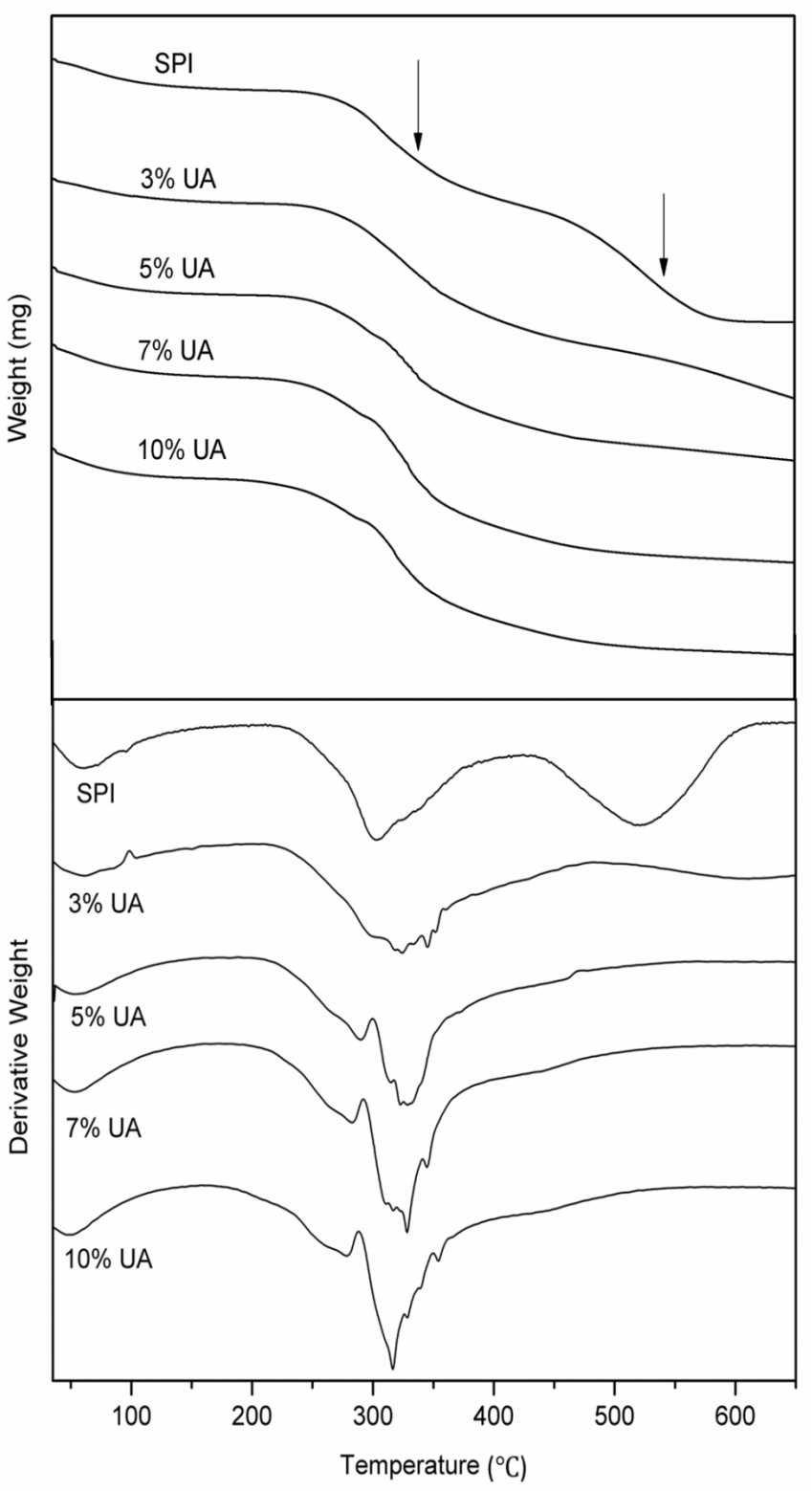

Figure 2.4 DSC thermogram of UA modified SPI based adhesives

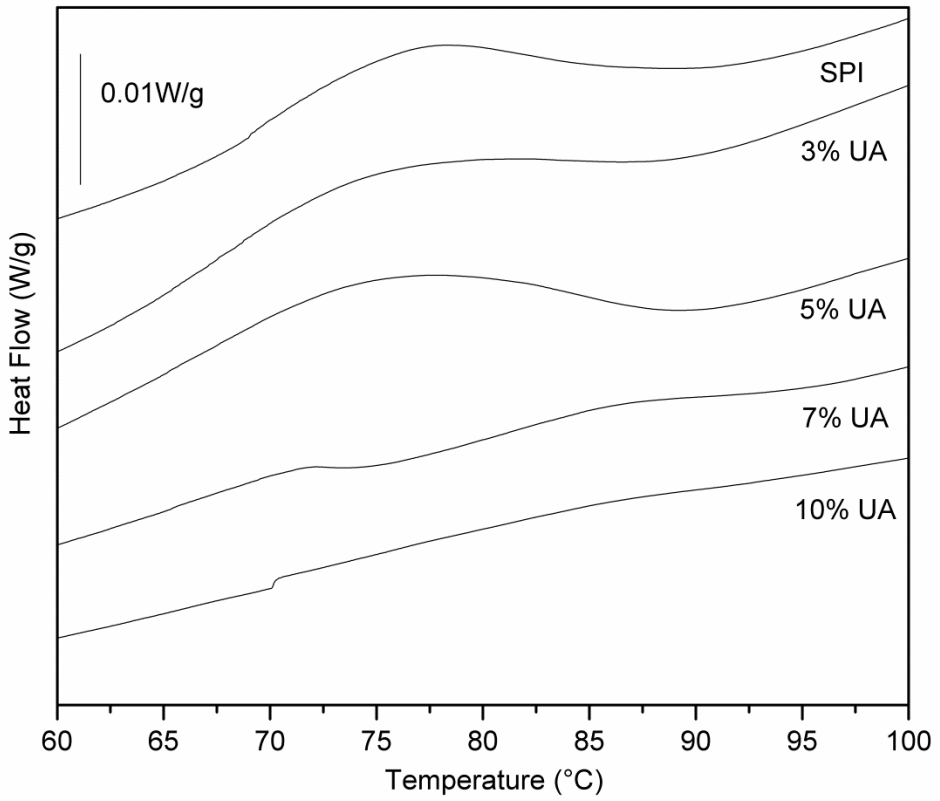

Figure 2.5 Viscosity of UA modified SPI based adhesives

Note: Data are average of three dulpicates and A, B, C means signicantly different, $\alpha < 0.05$, same letter means not significantly different

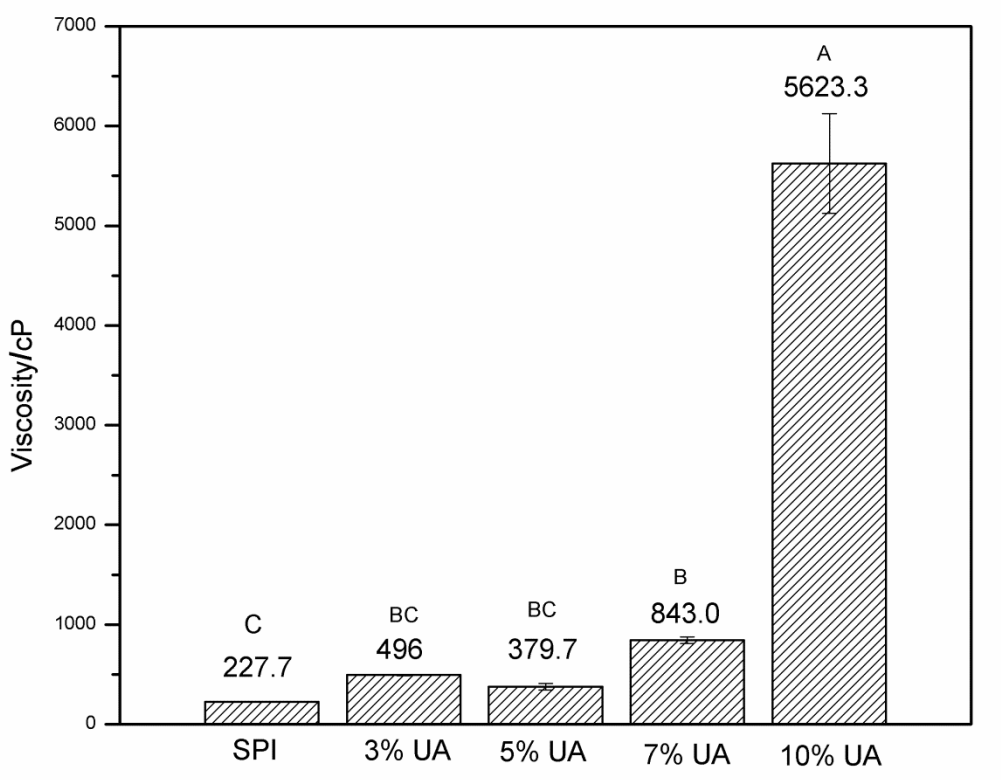

Figure 2.6 Elastic and Viscous modulus of UA modified SPI adhesives

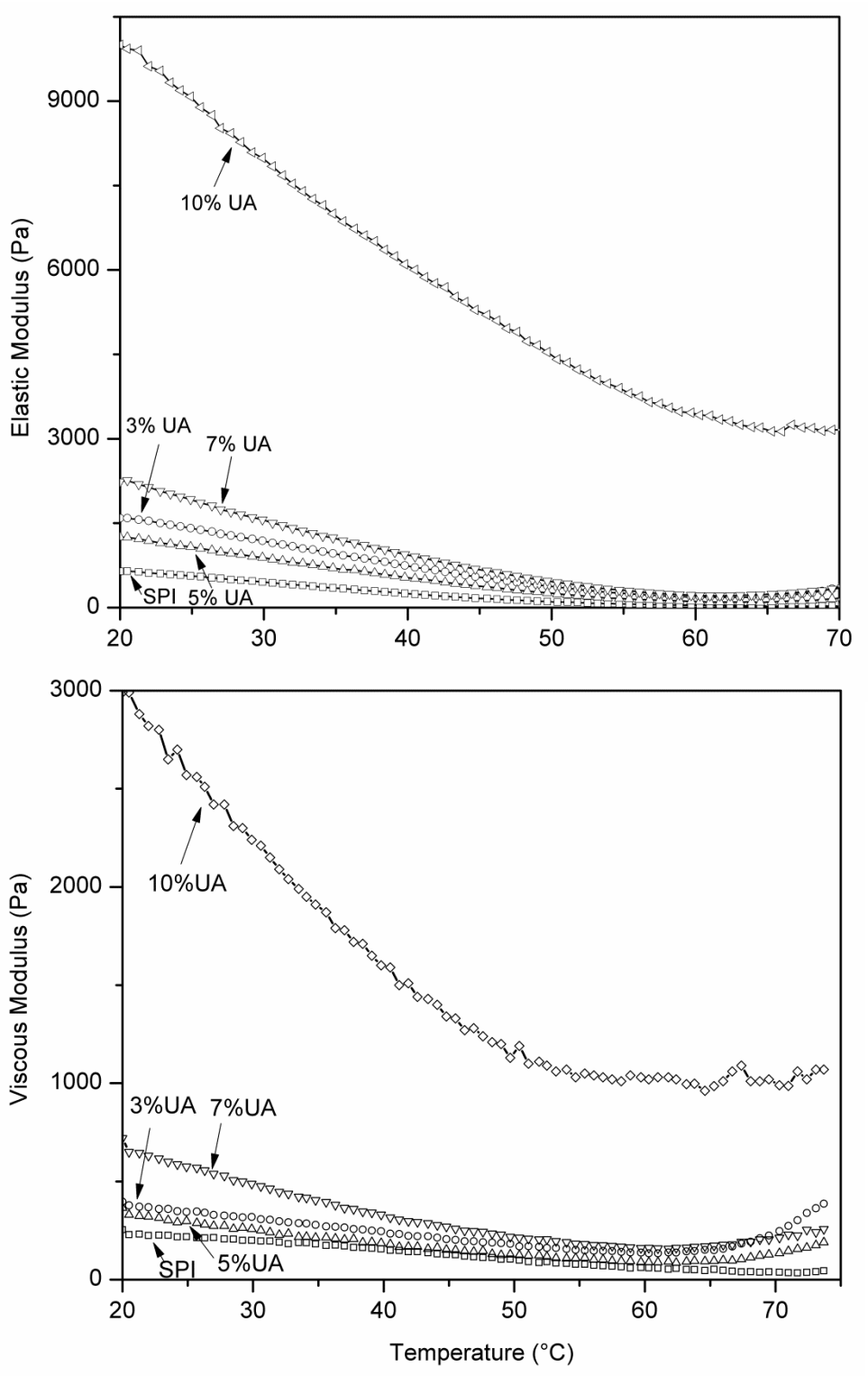

Figure 2.7 AFM tapping phase image of SPI, 5%UA and 10% UA modified SPI samples.

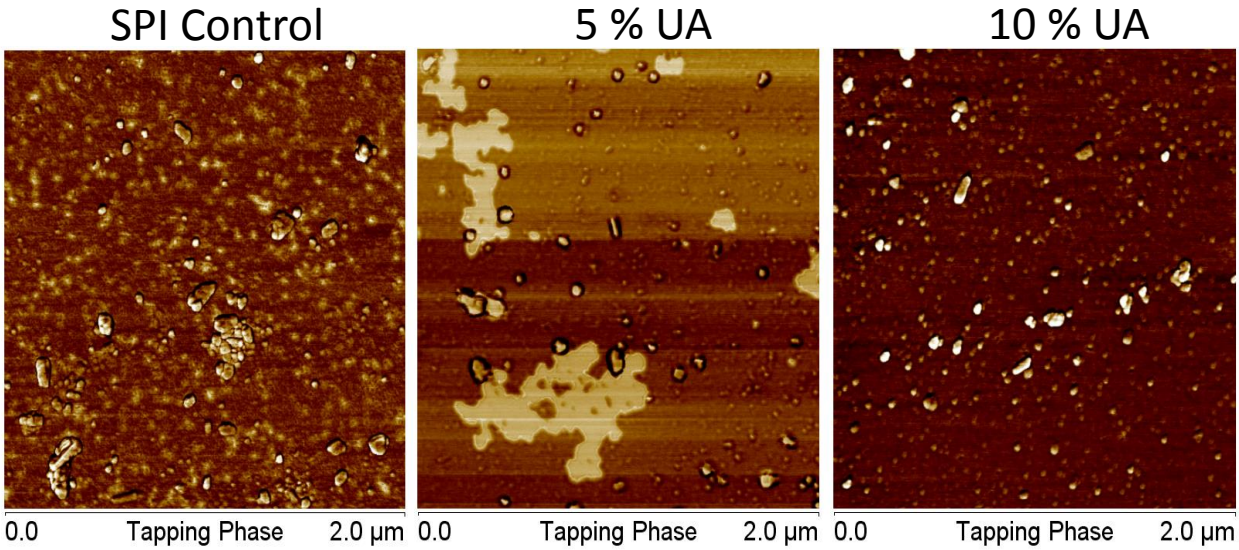

Figure 2.8 Particle size distribution of SPI and UA modified SPI

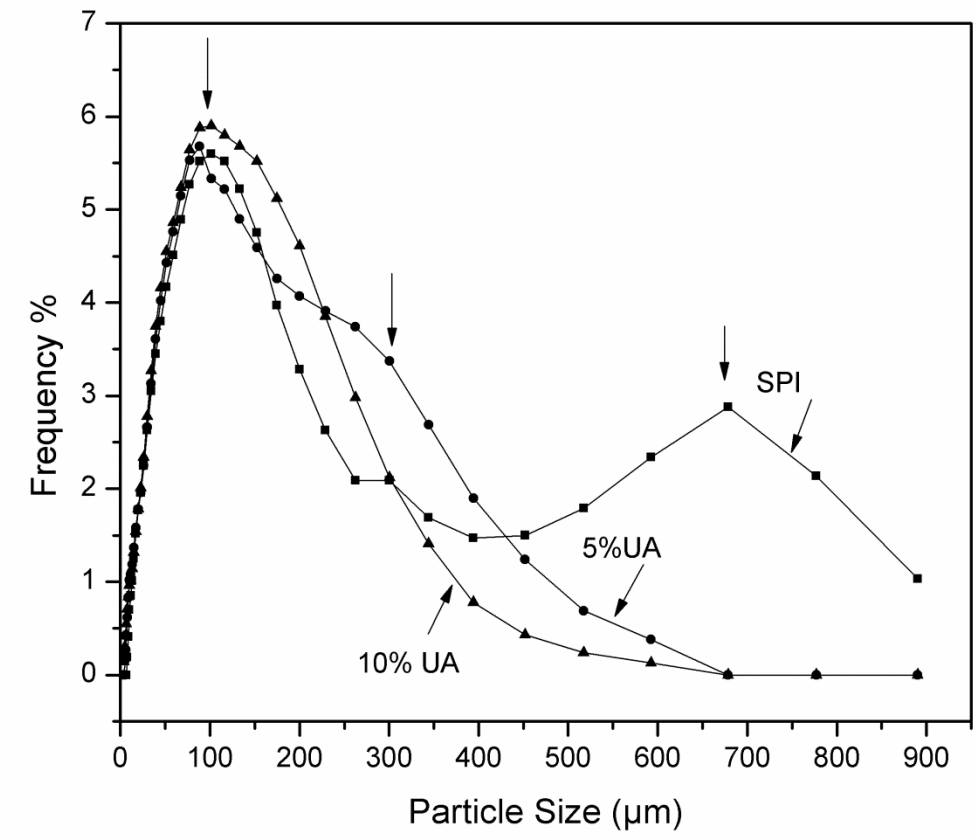

Table 2.1 Contents of amino groups in samples with different UA amounts

Sample ID	SPI	SPI:UA 4:1	SPI:UA 3:1	SPI:UA 1:1
Amino concentration (μmol/ml)	8.25 ±0.12	4.63 ± 0.06	2.66 ± 0.12	0.86 ± 0.05
Reacted amino group %		43.85± 0.04	67.80±0.03	89.57 ± 0.04

Note: SPI:UA weight ratio on dry base. Data are the average of two duplicates.

Table 2.2 Degradation peak temperature of control SPI and SPI modified with UA at percentage of 3%, 5%, 7%, and 10%.

UA %	Peak 1(℃)			Peak 2(℃)			Peak 3(℃)		
	T_o	T_e	T_{peak}	T_o	T_e	T_{peak}	T_o	T_e	T_{peak}
0	36.6	103.8	61.3	283.9	360.3	302.4	500.0	544.5	521.4
3%	26.9	96.1	61.7	279.5	363.3	324.1	-	-	-
5%	29.6	92.2	52.9	298.0	357.3	328.5	-	-	-
7%	27.3	86.4	53.6	291.3	345.8	328.3	-	-	-
10%	27.3	72.8	50.2	288.5	332.5	316.4	-	-	-

Note: T_o, onset temperature of a peak; T_e end temperature of a peak

Table 2.3 Denaturation temperatures and enthalpy of SPI slurry with different UA content

UA %	T_d (℃)	ΔH_{d1}(J/g)
0	76.98	2.07
3	75.02	2.32
5	75.23	4.46
7	71.27	0.43
10	70.04	0.159

Table 2.4 Particle size distribution of SPI, 5% UA and 10% UA modified SPI.

	Median (μm)	Mode (μm)	Mean (μm)
SPI	92.4 ± 2.9	88.7 ± 8.7	158.8 ± 5.5
5% UA	78.0 ± 4.9	82.7 ± 0.1	116.2 ± 1.4
10% UA	75.9 ± 3.2	88.7 ± 8.5	101.3 ± 0.7

Note: Data were the average of two parallel experiments.

Table 2.5 Tapping phase contrast of SPI and UA modified SPI

Setpoint (V)	1	2	3.5
SPI	3.4	2.8	1.8
5% UA	6	6	4.2
10% UA	6.5	6	4.2

Table 2.6 Dry and wet shear adhesion strength of UA modified SPI adhesives

UA	Dry strength (MPa)	WCF	Wet strength (MPa)	WCF
0%	5.991±0.788	100%	$2.038±0.177^{C}$	0
3%	5.243±0.724	100%	$2.748±0.314^{B}$	0
5%	6.103±0.635	100%	$2.701±0.106^{B}$	0
7%	5.940±0.827	100%	$2.880±0.079^{B}$	0
10%	6.671±0.580	100%	$3.296±0.243^{A}$	Fiber pulled out

Note: CWF: cohesive wood failure. Data are average of five duplicates. A, B, C means significantly different, $\alpha < 0.05$, same letter means not significantly different.

Chapter 3. Soy-oil-based waterborne polyurethane improved wet strength of soy protein adhesives on wood

3.1 Abstract

Soy-oil-based waterborne polyurethane (WPU) is used to improve wet strength in shear test of wood bonded with an adhesive of soy protein isolate (SPI) by dispersing WPU into SPI slurry. WPU's effects on the physiochemical properties of WPU-SPI adhesives are characterized through Fourier transform infrared spectrum, transmission electron microscopy, thermal analysis, contact angle, and mechanical strength. Wet strength of the WPU-SPI adhesives increases by 66.7% compared to SPI control. Moreover, the microstructure of WPU has effects on the interactions between WPU and SPI. In this study, smaller and more uniform distributed WPU0002 is easier to interact and form stronger crosslinking network with protein than WPU0500. The stronger interaction between WPU0002 and protein results in increased viscosity and bond strength. The WPU-SPI blended adhesives show significantly improved wet strength, demonstrating their potential as wood adhesives.

3.2 Introduction

The necessity to develop greener materials to reduce the dependence on petroleum feedstock is growing. Not only is petroleum feedstock a limited resource, it also contributes to environmental pollution and human disease. Soy-protein-based adhesive has been commercially available as a replacement of urea formaldehyde. For example, Soyad from Solenis^{TM} has been used in wood composites, which includes particleboard and medium-density fiberboard (1). Columbia Forest Products uses soy-based PureBond® for hardwood plywood manufacturing, which is formaldehyde-free and complies with the U.S. Green Building Council's Energy and Environment Design standards (2). Although soy flour is widely used as wood adhesives with excellent dry bond strength, the poor water resistance of soybean-protein-based adhesives has limited their application as high-performance wood adhesives compared with phenol-formaldehyde adhesives. There is a strong necessity to improve soy-protein-based adhesive to broaden its application.

The hydrophilic nature of amino acids results in the relative weak wet strength of SPI-based adhesives. It is hypothesized that blending SPI-based adhesives with functionalized hydrophobic soy oil through covalent and non-covalent interactions would increase SPI-based adhesive's water resistance.

Soy oil is naturally triglyceride with three fatty acid chains. The main fatty acids are unsaturated α-linolenic acid (C-18:3), linolenic acid (C-18:2), and oleic acid (C-18:1). It also contains the saturated fatty acids stearic acid (C-18:0) and palmitic acid (C-16:0). The native oil structure is not possible for polymerization reactions but can be functionalized through the reactive double bonds. Through the well-developed methods including hydroformylation, ozonolysis, and transesterification, hydroxyl groups can be successfully incorporated into the oil structure to increase the future reactivity of soy oil (3-5). Cargill's BIOH with various hydroxyl functionalities is one of the commercial polyols from soy oil (6). It has replaced ingredients derived from petroleum-based products in traditional foam, carpet backing, upholstered furniture, and so on. BIOH is one of the most important starting materials for polyurethane synthesis, which requires a di- or polyisocyanate with a polyol. Plant-oil-based waterborne polyurethanes (WPU) have been studied as coatings, adhesives, and foams since it is more environmental friendly than polyurethanes synthesized from petroleum based hydroxyl-bearing monomers and isocyanates. Because of the hydrophobic nature of the oil structure, polyurethanes derived from plant oil have enhanced hydrophobicity and thermal stability (7, 8). The storage stability of plant oil based WPU dispersions was has been shown to be over six months, and the initial decomposition temperature of WPU-based film was above in excess of 250 ℃ (9).

WPU is highly reactive and interactive with other chemicals and compounds through covalent bonding, hydrogen bonding, hydrophobic interactions, and physical entanglement. Therefore, the physiochemical properties of the reacted compounds can be enhanced through the crosslinking. Acrylic monomers were successfully grafted onto soy-oil-based WPU networks during emulsion polymerization. These WPU/acrylic hybrid latexes had a significant increase in Young's moduli and tensile strength compared with unmodified WPU (10). Lots of Numerous previous studies found that soy protein isolate (SPI) had good miscibility and compatibility with WPU. For example, SPI plastics with utilizing anionic WPU have tensile strengths up to 19 MPa and water

resistance σb(wet) /σb(dry)=0.4-0.5, which was much better than those of pure SPI sheets. The SPI/WPU films made from poly (butylene adipate) also had higher contact angles with excellent water resistance. The Wwater uptake of SPI/WPU blended films was dramatically reduced because of the incorporation of WPU into a protein matrix (11-13).

In this study, we examined the interactions between a soy-oil-based WPU and SPI and how WPU would improve the wet strength of SPI based adhesives. Figure 1 presents the chemical pathway of soy-oil-based polyol derived WPU-SPI blended adhesives. The objectives of our study are to 1) Make soy-oil-based WPU with excellent stability and dispersibility; 2) Study the wood bonding strength, water resistance, thermal, and rheological properties of WPU-SPI blended adhesives.

3.3 Materials and Methods

3.3.1 Materials

Defatted soy flour was purchased from Cargill (Cedar Rapids, IA). BIOH polyols (X-0002 and X-0500) were purchased from Cargill (Cedar Rapids, IA). The hydroxyl number of X-0002 is 117 mg KOH/g and that of X-0500 is 56 mg KOH/g. Isophorone diisocyanate (IPDI, 98%), trimethylamine (TEA, 99%), acetone (99%), and dime thylol propionic acid (DMPA, 98%) were purchased form Sigma-Aldrich (St. Louis, MO). Cherry wood veneers used for the wood test were provided by Veneer One (Oceanside, NY).

Preparation of SPI, WPU and WPU-SPI blend

3.3.1.1 SPI

SPI was extracted from the defatted soy flour. The fiber was removed by dispersing soy flour at pH 8.5 and then centrifuging the soy flour dispersion. SPI was precipitated at pH 4.5 by 2mol/L hydrochloric acid, and redissolved at pH 7.6 by 2mol/L sodium hydroxide, and then freeze-dried (freeze dryer Model 6211-0459; The Virtis Company. Inc., Gardiner, NY). Dried SPI was milled into powder, and the powder was passed through a U.S. #100 mesh sieve.

3.3.1.2 WPU

BIOH polyols X-0002 and IPDI were mixed into a three-neck flask equiped with a condenser tube (Rratio of NCO/OH was 1.4.). The sample was placed in, and heated using a silicon oil bath for 1 h (Heidolph MR Hei-Standard Magnetic Stirrer with Temperature Sensor, Elk Grove Village, IL). The silicon oil temperature was 85 °C. DMPA was added to the mixture after 1 h. The reaction stayed on conditions were maintained for 2 to 3 h, during which time acetone was added to reduce viscosity. The sample was cooled down to 45 ℃, and TEA was used to neutralize the DMPA. Finally, water was added to make the water dispersion, and acetone was evaporated overnight in a fume hood. The solid content of WPU was adjusted to 10% by adding more water.

3.3.1.3 WPU-SPI

2 g of SPI powder was suspended in 18 ml deionized water and stirred for one hour to make a uniform slurries slurry with 10% solid content. The pH of the SPI slurry was adjusted to 9.0 ± 0.1 with 2 mol/L sodium hydroxide using a digital pH analyzer. Varying amounts of WPU (10%, 30%, 50%, and 60%/70% of SPI dry base) were then added drop by drop to the SPI slurry. The pH of the slurry was maintained at 9.0 by adding 2 mol/L sodium hydroxide. The mixture was stirred for 2 h at room temperature (23 ºC). A series of WPU-SPI blended adhesives were thus made and coded as WPU0002-SPI 10%, WPU0002-SPI 30%, WPU0002-SPI 50%, and WPU0002-SPI 60%. The same process was repeated with the BIOH polyols X-0500 to make a series of WPU0500-SPI adhesives, which were coded as WPU0500-SPI 10%, WPU0500-SPI 30%, WPU0500-SPI 50%, and WPU0500-SPI 70%.

3.3.2 Characterization

3.3.2.1 Fourier transform infrared spectroscopy (FTIR)

The Ccontrol SPI and WPU-SPI slurries were freeze-dried and ground into fine powders for IR analysis. The blended WPU-SPI samples were first freeze-dried and then hot pressed at 170 ℃ for 10 min to mimic the adhesives' applied application condition. The IR spectra were recorded by a PerkinElmer Spectrum 100 FTIR spectrometer (Waltham, MA) in the MID-IR range (4000-600 cm^{-1}) with a universal attenuated total reflectance (ATR) sampling device. Each sample was scanned 32 times at a resolution of 2 cm^{-1}. Data from ATR is converted to sample absorption data.

3.3.2.2 Contact angle

Measurements were made using a CAM 100 optical contact angle meter (KSV Instruments, CT). A sample was dropped onto a glass surface, and the shape of the sample was immediately recorded by a CCD video camera and the contact angle was determined by fitting the Young-Laplace equation to the drop profile. The data showed in this study was an average of eight replicated tests.

3.3.2.3 Water resistance of cured WPU-SPI samples

A certain amount of WPU-SPI samples were coated onto glass plates with an even thickness and cured at 115 ℃ in the an oven for 30 min. The cured samples were soaked in water for 30 min and then dried. The differences between dry sample weight before and after being soaked in water were calculated. Solid Material lost resulting from the soaking process were was expressed as the percentage of sample weight dissolved extracted into by the water to the original sample dry weight.

3.3.2.4 Rheology properties

The apparent viscosities of the control SPI and WPU-SPI slurries were measured by a Bohlin CVOR150 rheometer (Malvern Instruments, Southborough, MA) with a parallel plate (PP20, 20-mm plate diameter). The distance between cone and plate was set as at 500 nm for all samples. Shear rate was in the range of 0.1 to 50 S^{-1}, and the testing temperature was 23 ℃. To prevent dehydration during testing, a thin layer of silicone oil was spread over the circumference of the samples.

3.3.2.5 Thermal analysis

Control SPI and WPU-SPI slurries were freeze-dried, and then the thermal hydrolysis curves of dry samples were determined using Tthermogravimetric analysis (TGA, PerkinElmer Pyris1 TGA, Norwalk, CT). For each sample, about 5 mg was loaded in the pan and heated from 50 to 700 ℃ at a rate of 10 ℃/min. Onset (To) and peak temperatures (Tp) were calculated by TGA software.

Thermal denaturation of control SPI and WPU-SPI were measured via differential scanning calorimetry (DSC, Q200, TA instrument, Schaumburg, IL). Samples (about 10 mg) were hermetically sealed in T zero aluminum hermetic pans. The samples were heated from -50 to 300 ℃ and then cooled down to -50 ℃ and heated again with a heating rate of 10 ℃/min.

3.3.2.6 Particle size analysis

The 10% adhesive slurries were directly used for particle size analysis. A laser scattering particle size distribution analyzer (LA-910, HORIBA Company, Kyoto, Japan) was used to record and calculate particle size distribution.

3.3.2.7 Transmission electron microscopy (TEM)

TEM microstructure observation was carried out using a Philips CM 100 (FEI Company, Hillsboro, OR). Newly prepared WPU-SPI blended adhesives were diluted to 1% with deionized water and then sonicated for 5 min before imaging. Formvar/carbon-coated 200-mesh copper grids were used to absorb diluted samples and stained with 2% (w/v) uranyl acetate for 45-60 s at room temperature.

3.3.2.8 Wood specimen preparation and shear strength measurements

Cherry wood pieces were preconditioned in a chamber (Electro Tech Systems, Inc., Glenside, PA) at 23 ℃ and 50% RH for at least one week before use. About 1 ml SPI adhesive was brushed onto the surface of cherry wood pieces; the dimensions of each piece were 50 mm × 127 mm×5 mm (width×length×thickness). Wood pieces were allowed to rest at room temperature for 15 min and then layered and pressed with a hot press at 170 ℃ and 1.4 MPa for 10 min. Wood assemblies were removed and cooled at room temperature and then stored in a chamber at 23 ℃ and 50% RH for 1 day. Each wood assembly was cut into five pieces with dimensions of 50 mm×20 mm (length×width) and then further conditioned for two days before the dry strength test. Two of the five pieces were used for dry strength test, and the other three were used for a wet strength test. Three duplicated wood assemblies were made for each adhesive sample.

For dry strength tests, wood specimens were tested with an Instron Tester (Model 4465, Canton, MA) according to ASTM Standard Method D2339-98 at a crosshead speed of 1.6 mm/min (14). Bonding strength was recorded as stress at the maximum load. Wood failure was estimated in accordance with the standard method of determining the percentage of wood failure in adhesive-bonded joints (15). For wet strength tests, the specimens were soaked in water at room temperature for 48 h. Wet strength was tested immediately after soaking, on the basis of ASTM Standard Methods D1183-96 and D1151-00 (16).

3.4 Results and Discussion

3.4.1 FTIR spectra of SPI, WPU and their mixtures

FTIR spectra are shown in Figure 2. The characteristic peaks for SPI are as follows: amide I at 1634 cm^{-1}, which corresponds mainly to C=O stretching vibration (80%) with a minor contribution from C-N stretching vibration; amide II at 1515 cm^{-1}, which arises from N-H bending (60%) and C-N stretching vibration (40%) (17, 18). For WPU, the major peaks are from C=O, C-N, and N-H. The carbonyl group of WPU0500 was broad and seemed to be composed of two bonds at 1745 and 1715 cm^{-1}, which were from free C=O stretching and hydrogen bonded C=O, respectively (19). The sharp peak at 1712 cm^{-1} with WPU0002 was assigned to the stretching of hydrogen bonded carboxyl groups and they were similar with that of WPU0500 containing both free and hydrogen bonding C=O. The N-H bending and C-N stretching of polyurethane contributed to peaks at 1536 and 1537 cm^{-1}. After blending with WPU, amide bonds of SPI (1634 cm^{-1} and 1515 cm^{-1}) shifted to higher frequency (1645/1641 cm^{-1} and 1530 cm^{-1}) because strong intermolecular interactions between amide groups and polyurethane occurred and changed the chemical environment. The sharp carbonyl absorption turned into flat shoulder peaks besides amide I at a frequency of about 1736 cm^{-1}, which has less content of hydrogen bonding. The new shape and position of carbonyl absorption showed that C=O was in an entirely different chemical environment, for instance, it has less involving of N-H bonds from polyurethane as electron donor but more interaction with bonds from protein. FTIR spectra suggested that there were some intermolecular interactions between WPU and SPI.

3.4.2 Contact angle

Contact angle analysis was used to estimate the surface hydrophobic properties of the WPU-SPI blended adhesives. Contact angle changes with increasing WPU content are shown in Figure 3. For the pure SPI slurry, the contact angle was about 33 ± 2º (average of the two control tests), that was relatively hydrophilic and easier to wet the glass surface. The contact angles of WPUs were difficult to measure because of the polarity effect between WPU and glass surface. But after WPUs interacted with SPI, their contact angles increased up to 52 ± 2º and 50 ± 2º for WPU0002-SPI and WPU0500-SPI respectively. Interactions between SPI and WPU would change protein conformations and create a new and more hydrophobic surface with hydrophobic polyurethane

segments. It is possible that this new hydrophobic surface is affected by the interactions between WPU and protein and that too much WPU would decrease the interactions.

3.4.3 Water resistance of WPU-SPI film curing on glass plate

WPU-SPI blended adhesives were cured at 115 ℃ for 30 min on glass plates and then soaked in water for 30 min. The hydrophobic segments from the WPU are supposed to prevent water from breaking down and dissolving the cured SPI and thus reduce the solid lost in water. When blended with WPU, samples clearly exhibited much reduced levels of material extraction (Figure 4). The error within duplicated tests for SPI and 25%WPU-SPI were high because the cured samples were broken down into pieces, and the weights of some small pieces that became detached from the main body of the sample were impossible to measure. On the contrary, the 50%WPU-SPI sample maintained its shape very well with less material extracted and dispersed into the water. The above results demonstrated that with the incorporation of a certain amount of WPU, the SPI films had better water resistance than the control SPI film.

3.4.4 Viscosity analysis

Viscosity describes the resistance of adhesives to flow. It is an important factor determining a products' handling properties and ability to wet a substrate surface. When intermolecular attractions become stronger, samples will show a higher viscosity (20). The apparent viscosity against shear rate was measured and plotted as indicated in Figures 5 and 6. The viscosity of the SPI slurry was very low and constant with increasing shear rate in this test range. All blended samples had a higher viscosity than SPI with viscosity increasing substantially as the WPU content was increased from 10% to 50%. The highest value occurred with the 50% WPU0002-SPI system, which was still flowable and easy to apply onto a substrate surface. For WPU-SPI samples the viscosity first increased with shear rate and then decreased presenting shear thinning characteristics at higher shear rates. The shear thinning behavior benefits adhesive application by making it easier to spread the adhesive onto a substrate surface. The increased viscosity demonstrates the growing interactions between WPU and SPI and the stronger cross-linking network between molecules. At pH 9.0, protein is partly unfolded with increased hydrodynamic volume and contact area (21). The hydrophobic segments from WPU were likely to interact with

the hydrophobic amino residues from SPI and thus formed bigger aggregates, which were more resistant to flow. Because of the hydroxyl, amine, and carboxyl groups in the mixed system, WPU and SPI could form hydrogen bonds and electrostatic interactions, which enhanced the crosslinking network as shown by the FTIR data in Figure 2. It was noticed that samples made with WPU0002 had significantly higher viscosities than WPU0500 (Figure 5 and 6). The possible reasons for this could be that WPU0002 has a larger contact surface due to its smaller molecular weight and thus more interacting groups, which benefit the interactions between WPU and SPI. Higher viscosity indicated stronger interaction between molecules or residues. The contact angle of WPU0002-SPI was bigger than that for WPU0500-SPI (Figure 3) because with higher viscosity, WPU0002-SPI formed more hydrophobic liquid drops (22, 23).

3.4.5 Thermal properties analysis

DSC is a useful tool to characterize the thermal transitions of polymers. Differences in thermal transitions are related to composition and structural changes. Figure 7 shows that pure SPI had two endothermic peaks at temperatures of 186 and 217 ℃ in the first scan (Table 1), which were assigned to denaturation peaks of 7S and 11S subunits, respectively. Because 11S has a higher molecular weight and was the major compound of soy protein, it attains a higher denaturation temperature and enthalpy change. In the second scan, SPI had a very strong peak at 81℃ and a weaker peak at 150 ℃. These two peaks were believed to be melting peaks because during the cool down, protein could crystallize into different crystals, which melt when temperature increases. For WPU, there were two thermal transition peaks in the first scan. The first peak was 55 and 66 ℃ for WPU0002 and WPU0500 respectively. According to previous studies, this is the glass transition temperature and it varies with different polyurethane structure. The higher Tg of WPU0500 indicated that it had a higher molecular weight and crosslinking density than WPU0002 (24, 25). The higher thermal transition peak of WPU0500 in comparison to WPU0002 corresponded to TEM images showing that the aggregate size of WPU0500 was much larger than that of WPU0002 (Figure 11). Another peak from the WPU thermogram in the first scan was exothermic at temperatures of 197 and 204 ℃ for WPU0002 and WPU0500 respectively. This indicated a crosslinking reaction between free functional groups at the ends of the urethane prepolymer. The ∆Hd (-80.07J/g) change with WPU0002 was 3.5 times higher than that for

WPU0500 (∆Hd=-27.28 J/g, Table 1). The main reason for the difference is that WPU0002 was smaller in molecular weight and had more free functional groups available for further crosslinking reactions (26). In the second scan, the WPU curves were rather smooth with a small glass transition at 6 and 12 ℃ for WPU0002 and WPU0500 respectively.

The 50%WPU and SPI mixture had a slightly lower (about 5 ℃) glass transition temperature and smaller ∆Hd than the pure WPU in the first scan, which indicated that interactions between protein and polyurethane molecules had changed the former crosslinking of WPU. Compared with pure WPU, crosslinking reactions within the WPU and SPI mixture occurred at a higher temperature, with ∆Hd reducing substantially. This suggested that crosslinking reactions between polyurethane molecules were weakened. A possible reason was that the interaction of WPU with protein had partly blocked the free functional groups of the WPU, which would otherwise participate in crosslinking reactions. The denaturation temperature of SPI also changed because protein conformation was disrupted due to its interaction with WPU. In the second scan, WPU0002-SPI had a much stronger melting peak than WPU0500-SPI. This melting peak was even stronger than that of pure SPI with a lower melting temperature. The new melting peak was from new crystal structure resulting from interactions between SPI and WPU0002. The differences between WPU0002-SPI and WPU0500-SPI in thermal behavior suggest they must have different interacting processes and different microstructures (Figure 7 and Table 1).

3.4.6 Thermogravimetric analysis (TGA)

Thermogravimetric analysis gives information on thermal stability and decomposition as determined by weight loss. Figure 8 shows the derivative TGA curves of WPU, SPI, and their blends. SPI had only one decomposition peak from 304 ℃ to 358 ℃. In the beginning of degradation, non-covalent bonds including hydrogen bonds, electrostatic interactions, and hydrophobic interactions were disrupted, and covalent bonds between C-N, C (O)-NH, C (O)-NH2 and $–NH_2$ on amino acid residues and peptide backbones decomposed as temperature increased. The complete decomposition of protein released various gases such as CO_2, CO, and NH_3 (27, 28). WPU had two degradation peaks, which might be assigned to the two major segments with different thermal stability. The first one at 324 ℃ is similar for both WPU0002 and WPU0500, while the second peak with WPU0500 (415 ℃) was much higher than that of

WPU0002 (388 ℃). The higher decomposition temperature of WPU0500 indicated that this had a more thermally stable segment which may result from more regular urea and urethane segments (29).

For WPU-SPI blends, the degradation peaks, although broadened, were still similar in shape, which meant that WPU and SPI had good compatibility. It was also noticed that there was a weak peak at a higher temperature, around 440 ℃, for both blended samples, which suggests that SPI and WPU may combine into more stable and larger aggregates through interactions such as covalent linkages and electrostatic and hydrophobic interactions.

3.4.7 Particle size distribution and morphology of WPU-SPI adhesives

3.4.7.1 Particle size distribution

Because of the interactions between WPU and SPI molecules, the blended samples were expected to have different aggregate structures. For the WPU0500-SPI samples, including WPU0500 alone, had exhibited similar frequency in particle size curves (Figure 9) with the highest frequency around a particle size of 40 μm. Compared with SPI, the WPU0500-SPI blended samples had a slightly higher frequency when particle size <40 μm and a little lower frequency when particle size >40 μm. WPU0500 was smaller than SPI and their mixture should have a particle size between WPU0500 and SPI. While the WPU0002-SPI blends had a quite different size distribution pattern (Figure 10), the size of WPU0002 was too small to be measured using the light scattering method and curves were moved to a larger size with multiple peaks after WPU0002 was blended with SPI (Figure 10). For example, 10%WPU0002-SPI had the highest frequency at 60 μm and another peak value around 400 μm. Therefore, there were two dominant sizes in the sample. The 50% WPU0002-SPI was relatively uniform with a major peak at 100 μm.

Since the particle size of WPU0002 was quite small, there was larger contact surface with SPI, which would facilitate interaction and result in more massive aggregates. The particle size data agreed well with the viscosity data. Stronger interactions between WPU0002 and SPI led to larger sizes and higher viscosity, while interactions between WPU0500 and SPI had a small influence on particle size and viscosity.

3.4.7.2 Morphology

Soy protein is globular in shape, and the protein aggregates formed exhibit a continuous linear chain network as shown in Figure 11 A. Proteins were connected to the surrounding molecules through hydrophobic interactions, hydrogen bonds, and electrostatic interactions. The darker color indicates that more layers of protein aggregates were stuck together. Figure 11 B and C are for WPU0002 and WPU0500, respectively. The WPUs were both round in shape with varied particle sizes, but WPU0500 was noticeably larger than WPU0002. As the measurement results show, for WPU0002, the larger particles were around 60 nm and the smaller ones were only around 16 nm, while for WPU0500, the larger ones were over 500 nm and even the smaller ones were 50 nm on average. WPU particles also had connections with each other, which resulted in larger aggregates. Multiple factors can affect the particle size of WPU, for example, the ratio between hydroxyl and isocyanate groups, carboxyl groups' content, and ionic, nonionic hydrophilic segments (30, 31). The main reason for the different particle sizes in our WPU samples was the functionalities of BIOH 0002 and 0500.

With regard to microstructure, proteins were smaller and less unfolded in nature with WPU0002-SPI (Figure 11 D), whereas with WPU0500-SPI, a multiple layered linear chain network was observed (Figure 11 E). For WPU0002-SPI, proteins adhered to the surface of WPU particles, and the small particle size of WPU0002 made it easier to approach and interact with the protein crosslinking network and form new connections. For WPU0500, the particles were enclosed by a protein network. The WPU0002 had a more uniform distribution in the protein than WPU0500 because of its smaller size.

3.4.8 Dry and wet strength wood specimens

Both SPI and WPU-SPI blended adhesives exhibited good dry shear bond strength characteristics as shown in Table 2. However the bond strength for WPU was low and thus not shown in table 2 and figure 12. WPU0500 had a dry strength of 4.76 ± 0.42 MPa and wet strength of 1.85 ± 0.21 MPa; WPU0002 has a dry strength of 1.85 MPa ± 0.21, and a wet strength of 0.09 ± 0.06 MPa For the dry tests, samples are all exhibited 100% cohesive wood failure. All the samples in of WPU0002-SPI had a higher value than WPU0500-SPI. It is possible that samples tested at

different times were influenced by the systematic error associated with both instrumentation and wood materials variability However, it is possible that WPU0002 treated adhesives had a stronger adhesion property.

When WPU content reached to 50%, both WPU0002-SPI and WPU0500-SPI experienced increased wet strength (Figure12). The wet strength was increased to 3.81 ± 0.34 MPa, i.e. about 66.7% more than that of pure SPI. The highest value occurred with 50% WPU samples. 30% and 50% WPU0002-SPI and 30% and 50% WPU0500-SPI samples had fiber pulled out of the wood surface (Figure 13). Interactions between SPI and WPU could benefit adhesion performance. Their interactions can be due to covalent bonds between active functional groups such as amine and carbonyl as well as non-covalent linkages such as hydrophobic interaction and hydrogen bonds (Figure 2). Through these interactions, the protein might change to a more unfolded conformation so as to extend the contact area with WPU. Cavities between protein and wood resulting from the dissolution of hydrophilic amino acid residues into water are the main reason for poor wet strength. On the one hand, once the hydrophobic WPU adheres onto the protein surface, it would prevent water from penetrating into the interfacial surface between adhesive and wood. On the other hand because WPU was synthesized from hydrophobic soy oil, it is hard to dissolve in water so fewer cavities would form. However, when WPU content increased to 60% or 70%, the wet strength began to decrease. One possible reason for this is the decrease of adhesion groups from protein, which weakens the splice between adhesive and wood. The interaction between protein and WPU might also weaken if there was too much WPU. The WPU0002-SPI had a higher wet strength than WPU0500-SPI, which may relate to the differences in their physical properties such as aggregate sizes and viscosity. Particle size is related to mechanical properties (32, 33). In the wet strength test, WPU0002-SPI blends had a higher strength than WPU0500-SPI on each blended level. A more uniform distribution of hydrophobic segments could better prevent water from penetrating into the interphasial region between adhesive and wood. On the other hand, the smaller and more open proteins would promote adhesive penetration into wood and thus increase bond strength.

3.5 Conclusions

Soy-oil-based waterborne polyurethanes (WPU) have been successfully merged with soy protein into homogeneous adhesives. These WPU-SPI blends showed improved wet strength up to

3.81±0.34 MPa with fiber failure. The compatibility between WPU and SPI was the result of hydrogen bond and electrostatic and hydrophobic interactions. Based on FTIR and thermal behavior changes observed by DSC, it was inferred that a new crosslinking network may form between WPU and SPI. Microstructure and particle size information based on TEM images indicated that the smaller WPU0002 had more interactions with soy protein and that this contributed to improved mechanical properties. The WPU-SPI blended adhesives are safe, biodegradable, and renewable; therefore, they have great potential for the adhesive industries.

3.6 Reference

1. http://solenis.com/en/markets-served/specialties-wood-adhesives.
2. http://www.columbiaforestproducts.com/product/purebond-classic-core.
3. I. Cvetkovic, J. Milic, M. Ionescu and Z. S. Petrovic, Hemijska Industrija, 2008, 62, 319-328.
4. Z. S. Petrovic, J. Milic, Y. Xu and I. Cvetkovic, Macromolecules, 2010, 43, 4120-4125.
5. C.-S. Wang, L.-T. Yang, B.-L. Ni and G. Shi, Journal of Applied Polymer Science, 2009, 114, 125-131.
6. www.bioh.com
7. A. Zlatanic, L. Charlene, W. Zhang, Z. S. Perovic., Joural of Polymer Sciece, Part B: Polymer Physics, 2004, 42, 809-819
8. K. M. S. Meera, R. M. Sankar, S. N. Jaisankar., The Journal o Physical Chmistry B, 2013,117, 2682-2649
9. B. Ni, L. Yang, C. Wang, L. Wang and D. E. Finlow, Journal of Thermal Analysis and Calorimetry, 2010, 100, 239-246.
10. Y. Lu and R. C. Larock, Biomacromolecules, 2007, 8, 3108-3114.
11. H. Tian, Y. Wang, L. Zhang, C. Quan and X. Zhang, Industrial Crops and Products, 2010, 32, 13-20.
12. N. G. Wang and L. Zhang, Polymer International, 2005, 54, 233-239.
13. M. Zhang, F. Song, X.-L. Wang and Y.-Z. Wang, Colloids and Surfaces B-Biointerfaces, 2012, 100, 16-21.
14. Annual Book of ASTM Standards (2002), D2339-98, ASTM, International, West Conshohocken, PA, Vol. 15.06, pp 158-160
15. Annual Book of ASTM Standards (2002) D1183-96. ASTM, International, West Conshohocken, vol 15.06, pp 70–73
16. Annual Book of ASTM Standards (2002) D1151-00. ASTM, International, West Conshohocken, vol 15.06, pp 67–69

17. A. A. Bunaciu, S. Fleschin and H. Y. Aboul-Enein, Current Analytical Chemistry, 2014, 10, 132-139.

18. M. Jackson and H. H. Mantsch, Critical Reviews in Biochemistry and Molecular Biology, 1995, 30, 95-120.

19. Y. Lu and R. C. Larock, Biomacromolecules, 2008, 9, 3332-3340.

20. C. J. van Oss, Journal of Molecular Recognition, 2003, 16, 177-190.

21. K. Monkos, Biochimica Et Biophysica Acta-Proteins and Proteomics, 2005, 1748, 100-109.

22. Meincken M., Klash A., Seboa S., and Sanderson R. D., Applied Surface Science, 2006, 2, 805-809.

23. Tam K. C., Farmer M. L., Jenkins R. D., and Bassett D. R., Journal of Polymer Science, Part B Polymer Physics., 1998, 36, 2275-2290.

24. T. K. Chen, J. Y. Chui and T. S. Shieh, Macromolecules, 1997, 30, 5068-5074.

25. B. S. Chiou and P. E. Schoen, Journal of Applied Polymer Science, 2002, 83, 212-223.

26. D. J. Hourston, M. Song, F. U. Schafer, H. M. Pollock and A. Hammiche, Polymer, 1999, 40, 4769-4775.

27. S. N. Das, M. Routray and P. L. Nayak, Polymer-Plastics Technology and Engineering, 2008, 47, 576-582.

28. V. Schmidt, C. Giacomelli and V. Soldi, Polymer Degradation and Stability, 2005, 87, 25-31.

29. C. Li, X. Luo, T. Li, X. Tong and Y. Li, Polymer, 2014, 55, 6529-6538.

30. C. K. Kim and B. K. Kim, Journal of Applied Polymer Science, 1991, 43, 2295-2301.

31. S. H. Son, H. J. Lee and J. H. Kim, Colloids and Surfaces a-Physicochemical and Engineering Aspects, 1998, 133, 295-301.

32. D. E. Fiori, D. A. Ley and R. J. Quinn, Journal of Coatings Technology, 2000, 72, 63-69.2

33. N. G. Wang, L. N. Zhang and Y. S. Lu, Industrial & Engineering Chemistry Research, 2004, 43, 3336-3342.

3.7 Figures and Tables

Figure 3.1 Proposed chemical scheme of possible interactions between WPU and SPI: covalent linkage; hydrogen bond; hydrophobic interaction; physical entanglement

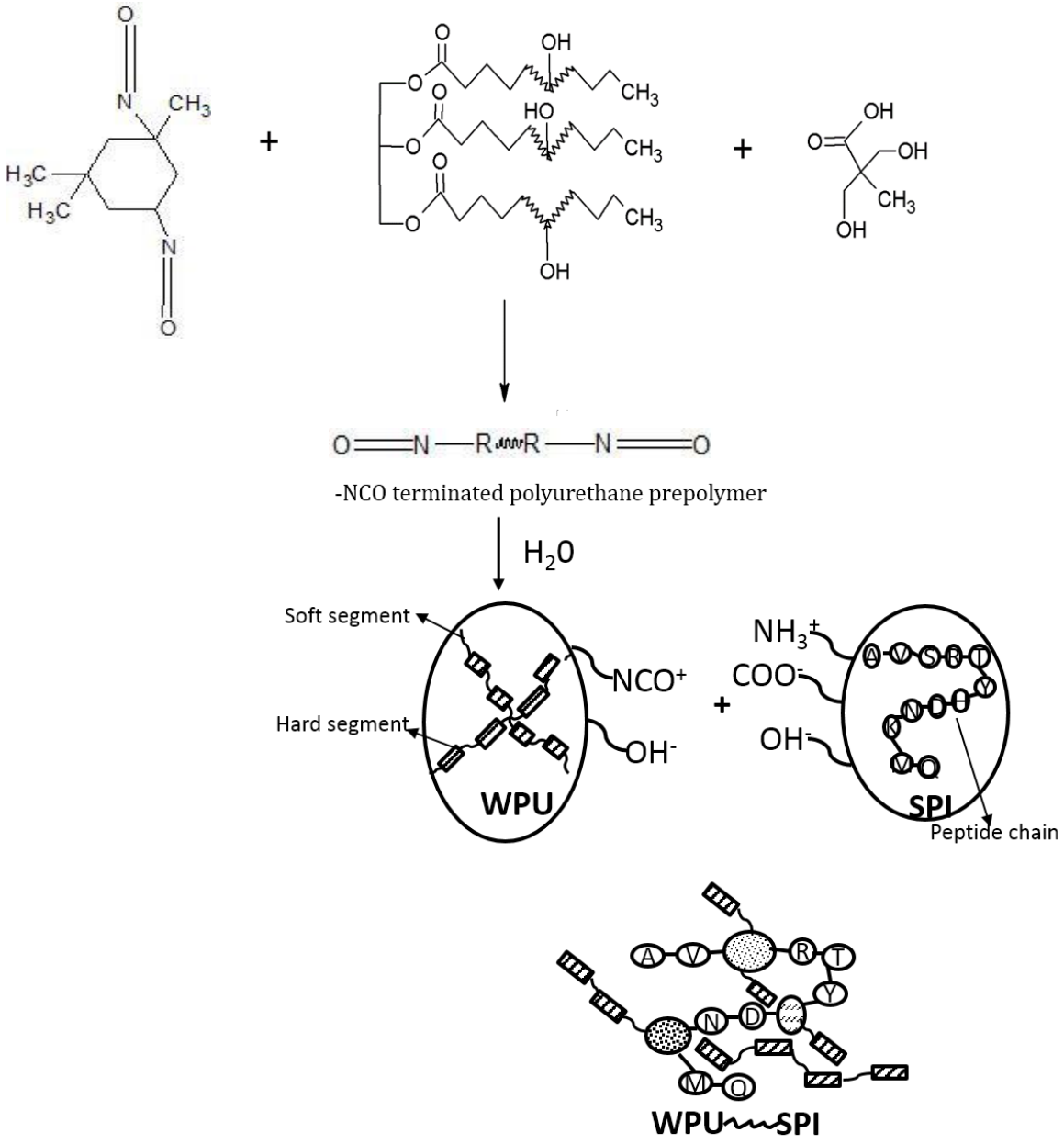

Figure 3.2 FTIR spectra of SPI, WPU, and WPU-SPI

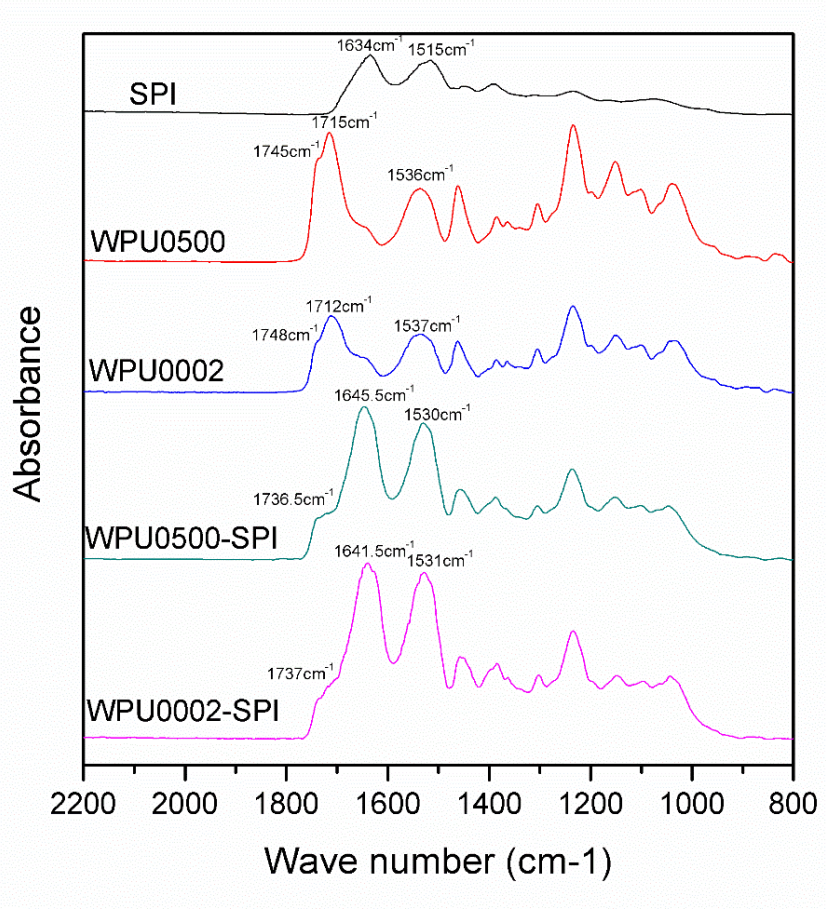

Figure 3.3 Contact angle of WPU-SPI blended adhesives as a function of WPU content

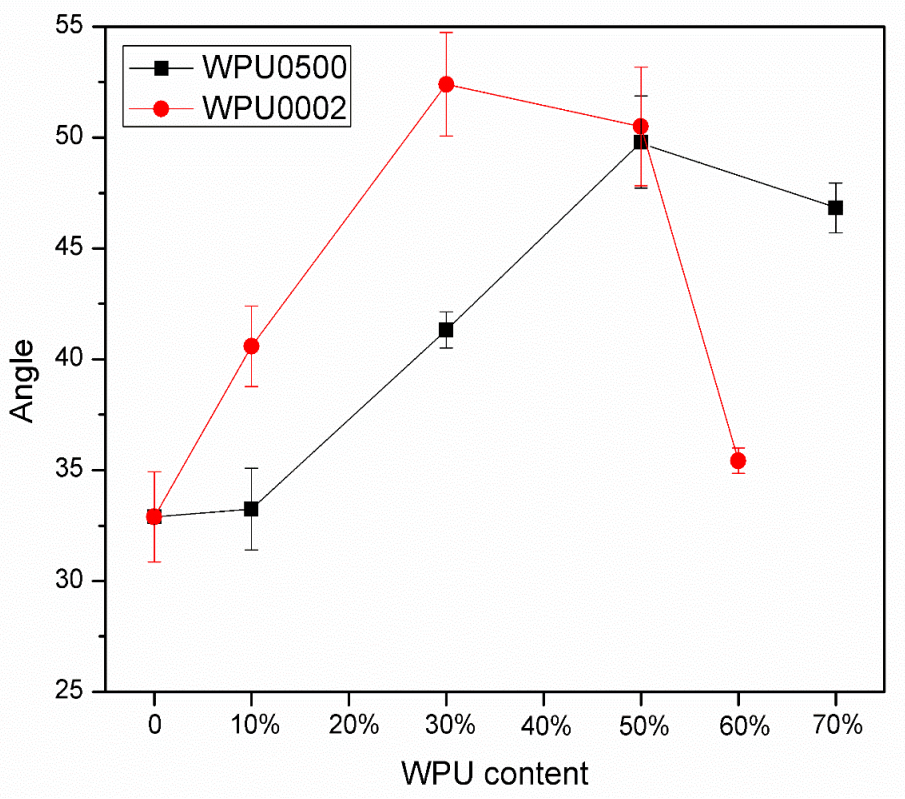

Note: Numbers in horizontal axis means dry base wt% of WPU in samples. The same applies to following figures

Figure 3.4 WPU-SPI blended samples' solid lost in water

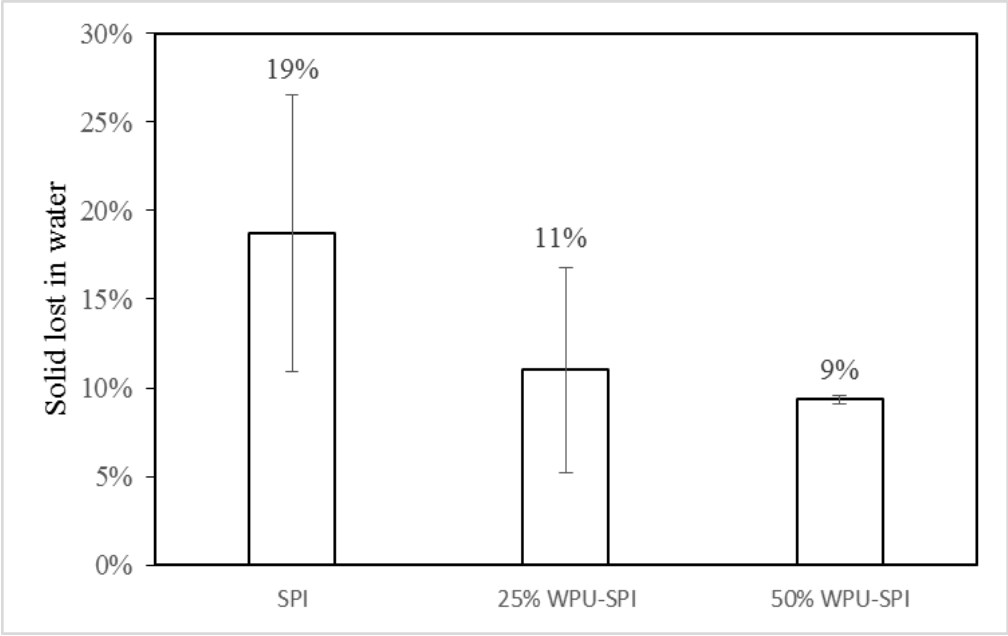

Figure 3.5 Apparent viscosity of WPU0002-SPI blended adhesives as affected by shear rate

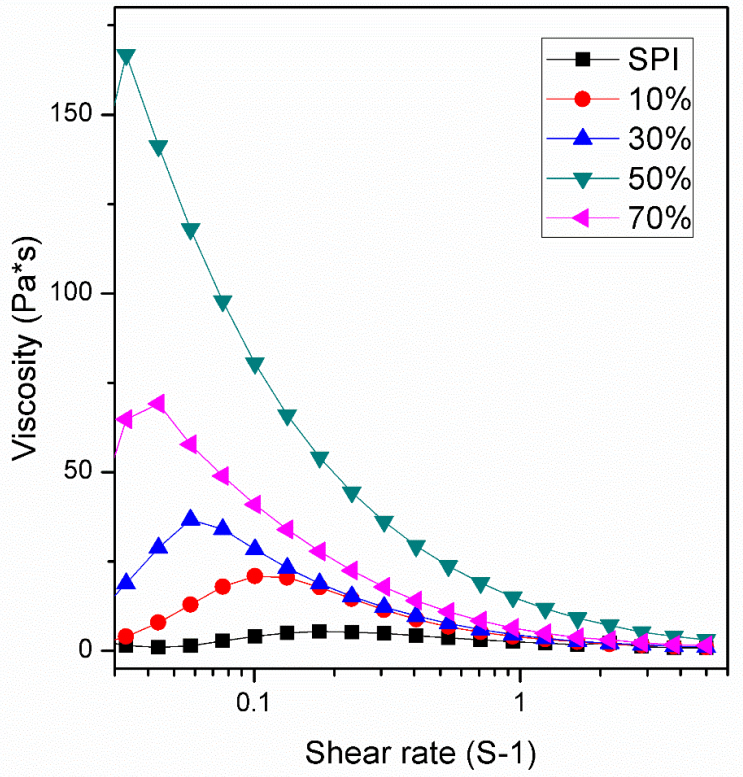

Figure 3.6 Apparent viscosity of WPU0500-SPI blended adhesives as affected by shear rate

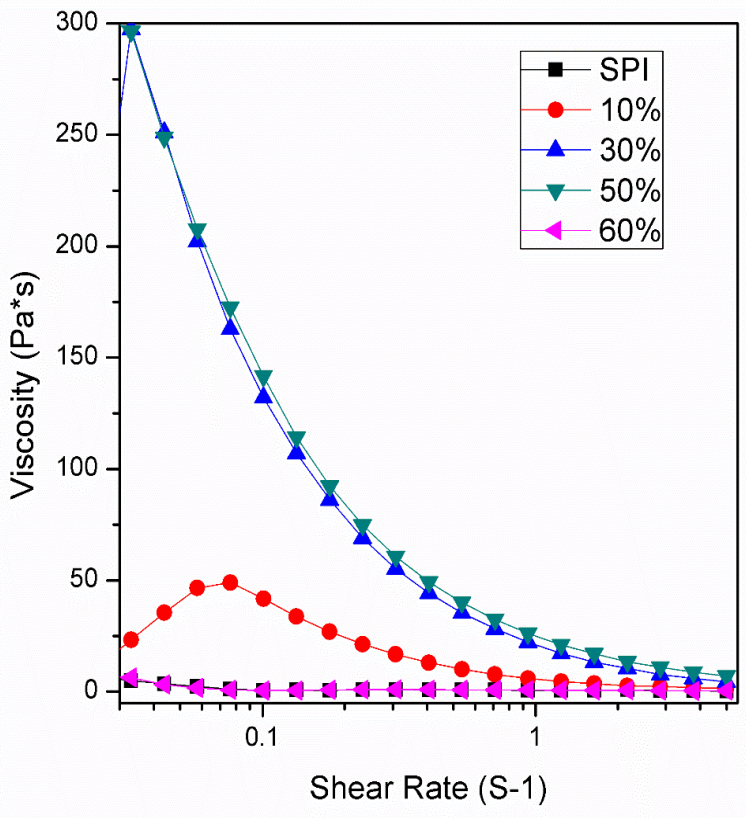

Figure 3.7 DSC thermogram of SPI, WPU, and WPU-SPI blends. Graph on left is the first scan; graph on right is the second scan.

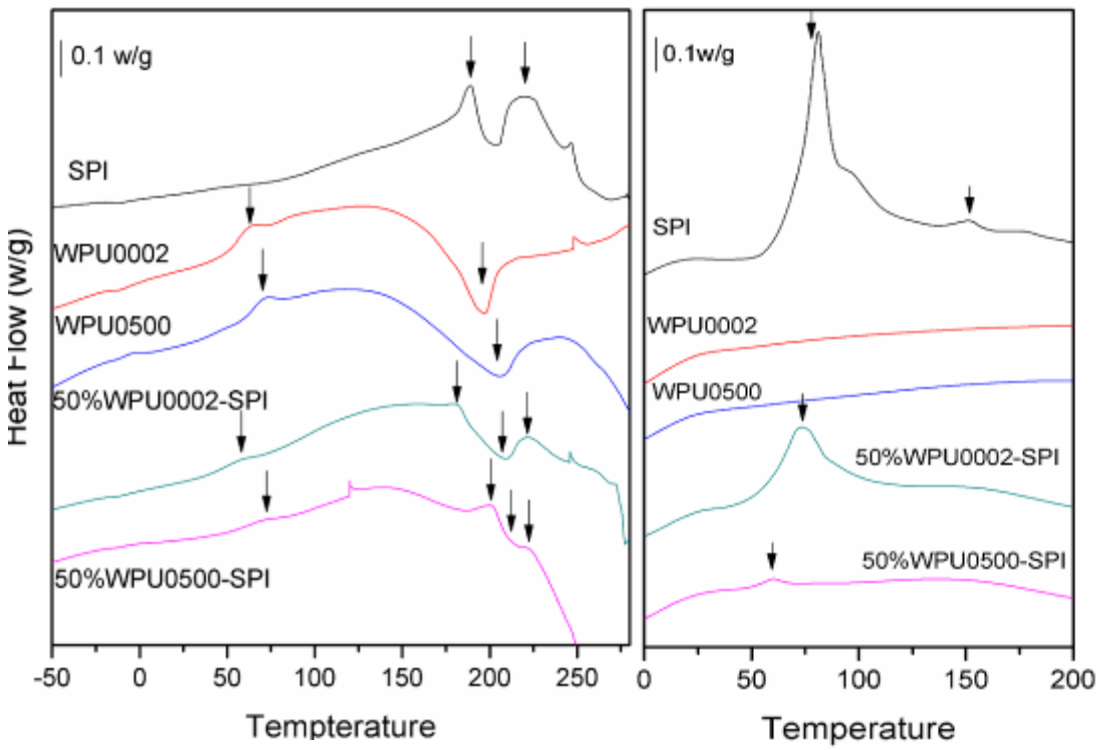

Figure 3.8 DTGA curves of WPU, SPI, and WPU-SPI blend

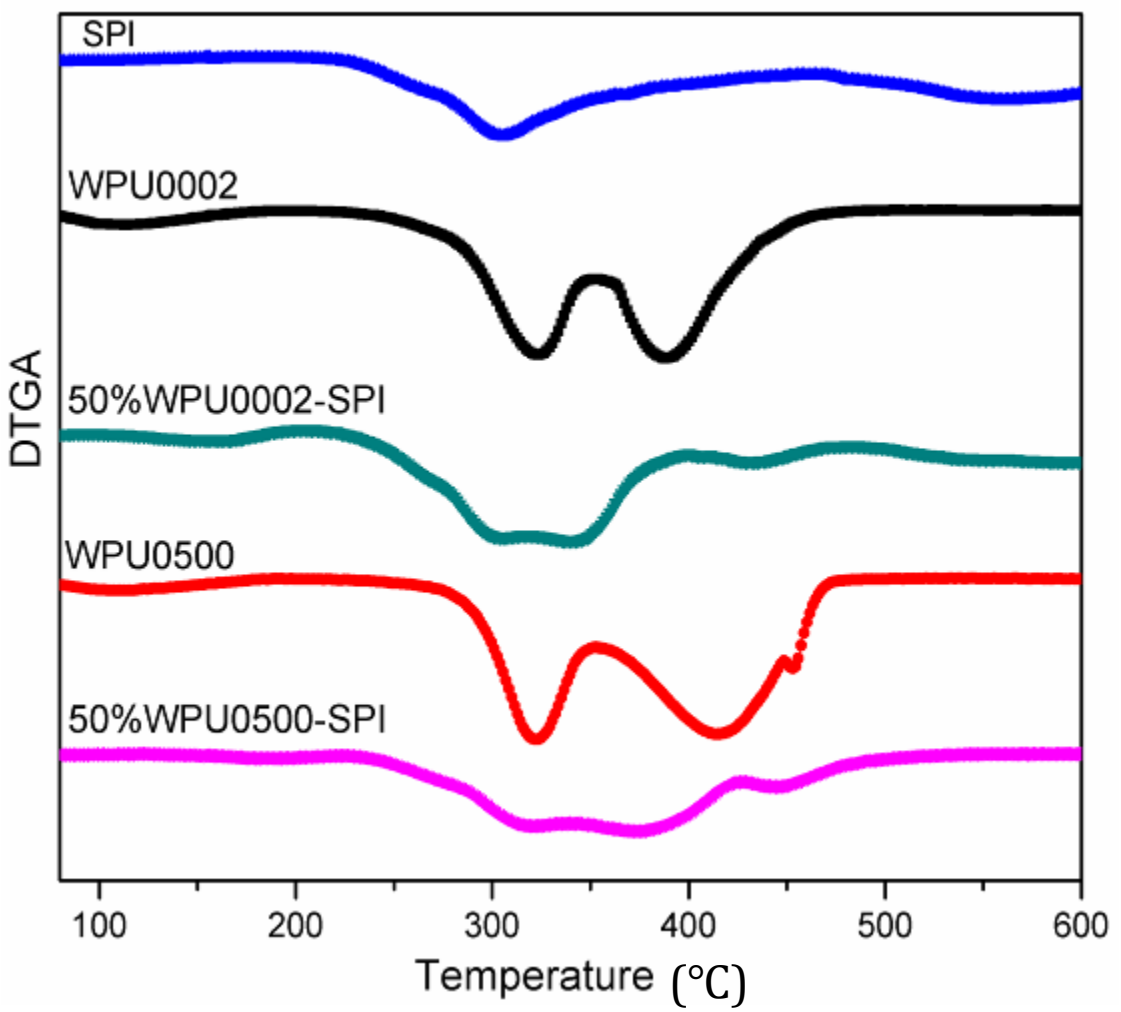

Figure 3.9 Particle size distribution of SPI, WPU0500, and WPU0500-SPI adhesives

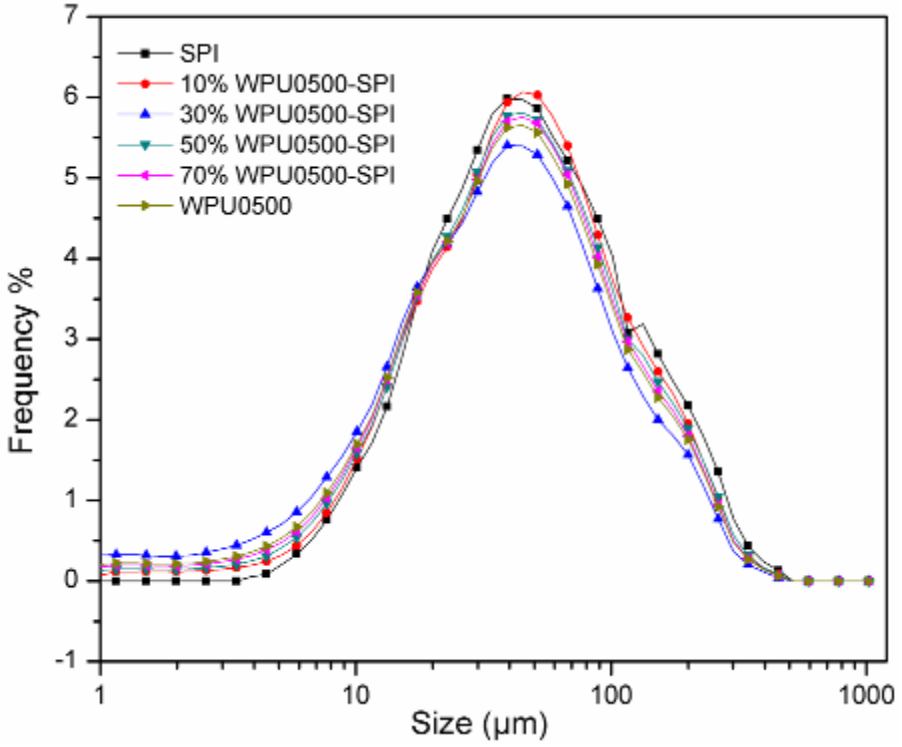

Figure 3.10 Particle size distribution of SPI, WPU0002, and WPU0002-SPI adhesives

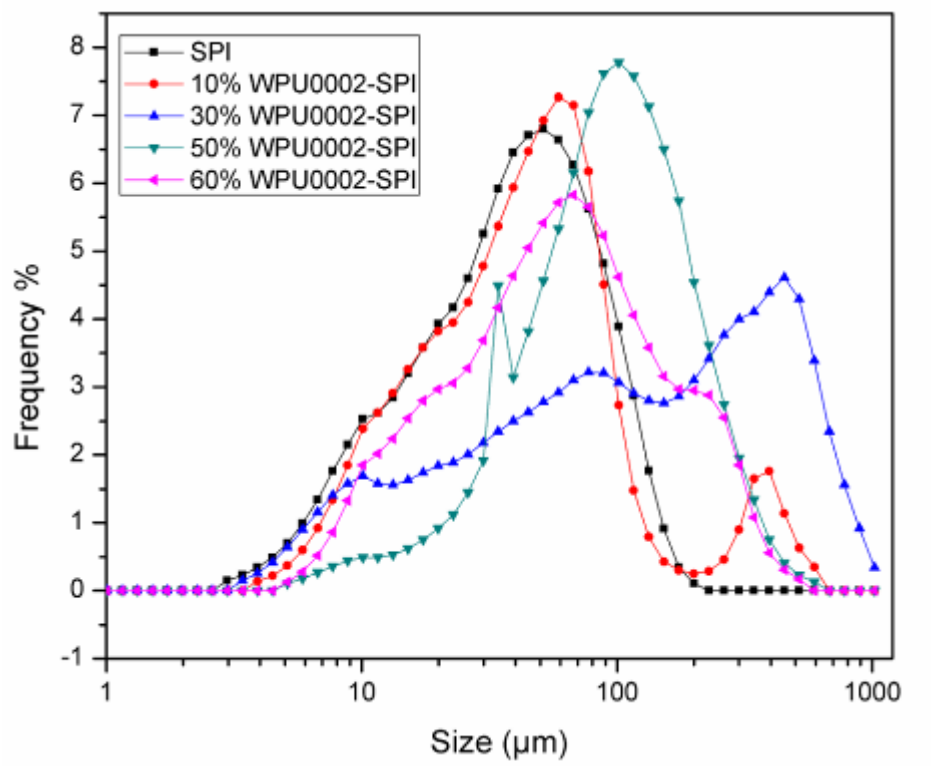

Figure 3.11 TEM images: A: SPI; B:WPU0002;C:WPU0500;D:WPU0002-SPI; E:WPU0500-SPI

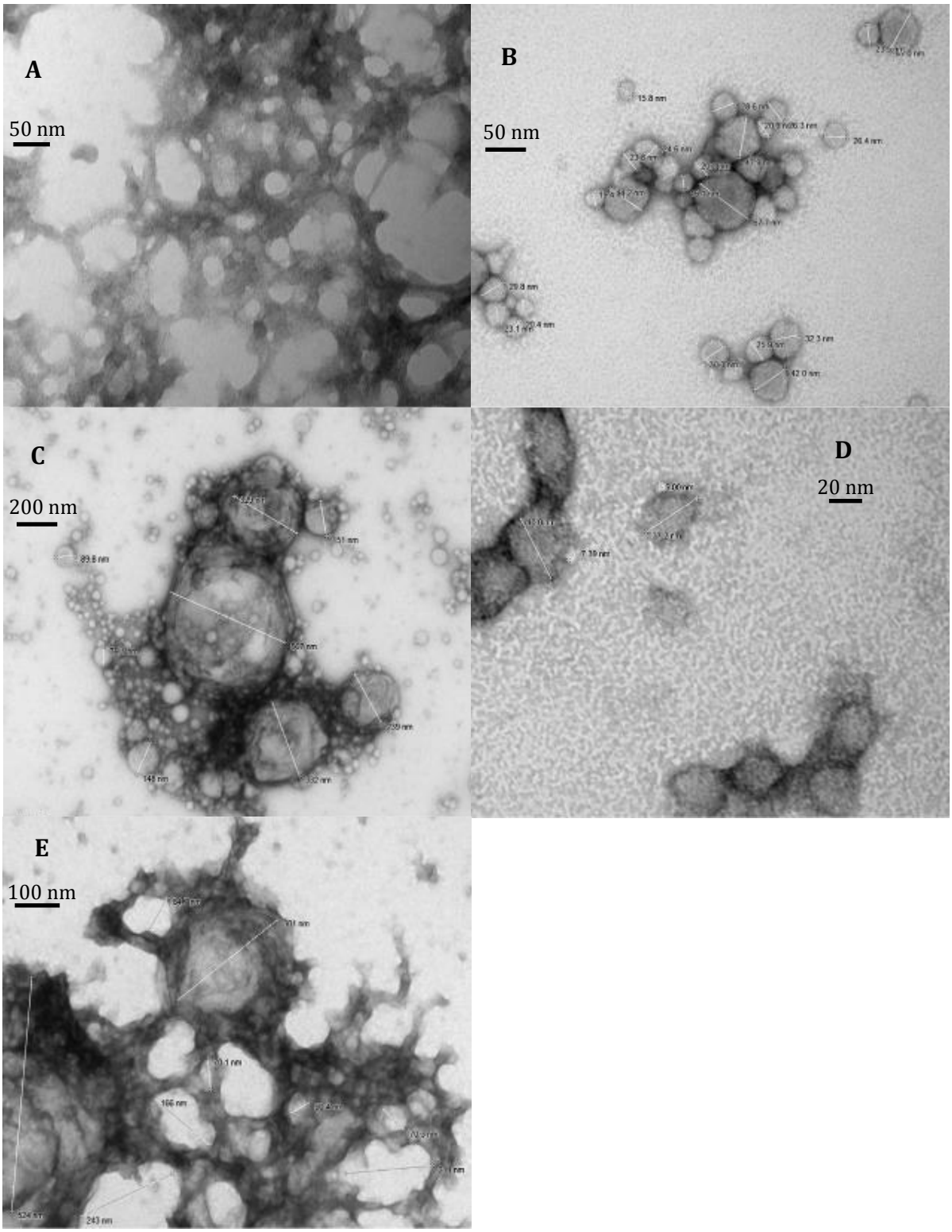

Figure 3.12 Wet shear bond strength of WPU-SPI blended adhesives

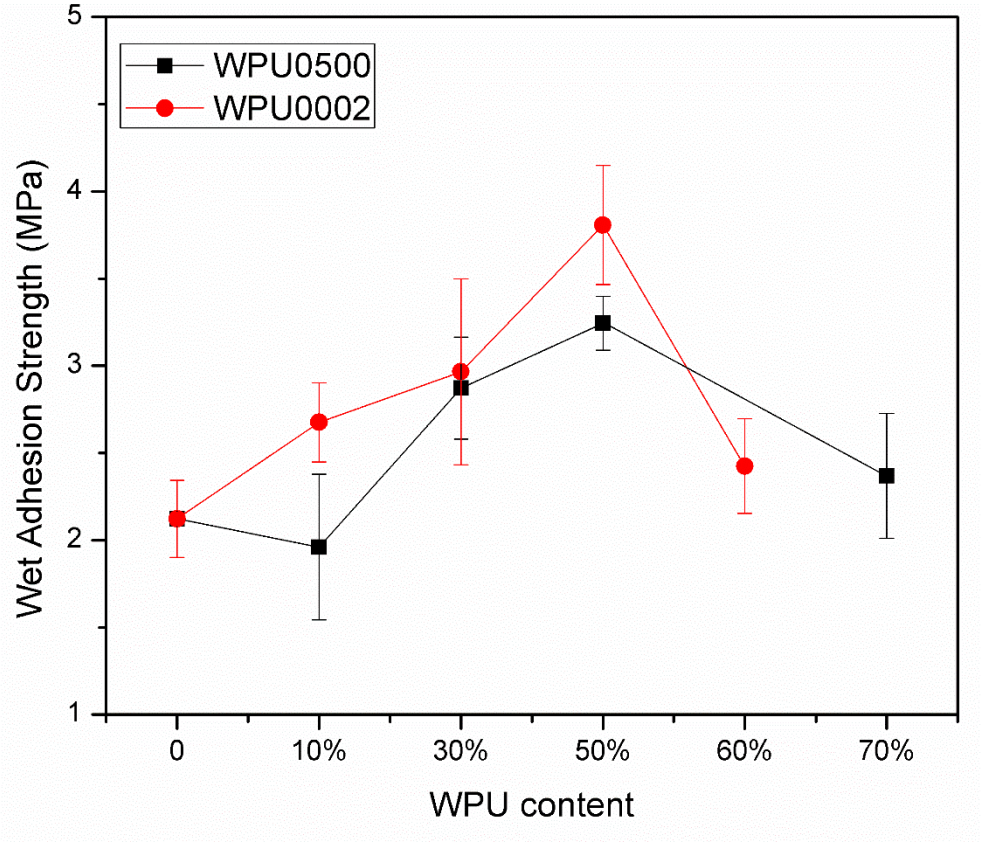

Figure 3.13 Wood surface after dry and wet bond strength test

Table 3.1 Peak temperatures and enthalpy change for DSC thermogram

	First scan									
	Peak 1 (℃)		ΔH_d		Peak 2 (℃)					
Sample ID	T_{d1}	T_g	T_d (J/g)	T_gJ/(g. ℃)	T_{d2}	ΔH_d (J/g)	Peak 3 (℃)	ΔH_d (J/g)	Peak 4 (℃)	ΔH_d (J/g)
SPI	186		4		217	12				
WPU 0002		55		0.37	197	-80.07				
WPU0500		66		0.16	204	-27.28				
50%WPU 0002-SPI		49		0.11	181	0.50	207	-5.86	222	3.24
50%WPU 0500-SPI		62		0.08	202	1.98	212	-1.14	223	0.50
	Second scan									
	Peak (℃)		ΔH_d		Peak (℃)		ΔH_d (J/g)			

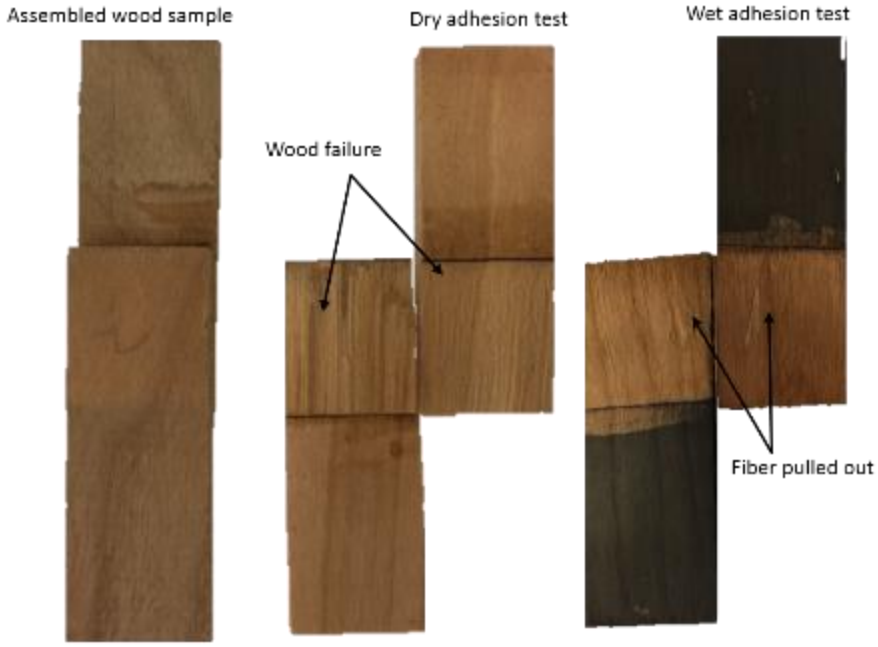

Sample ID	T_m	T_g	(J/g)	J/(g. ℃)	T_m	
SPI	81		29.92		150	1.42
WPU0002		6		0.75		
WPU0500		12		0.40		
50%WPU 0002-SPI		10		0.47	74	43.02
50%WPU 0500-SPI		16		0.30	60	1.53

Notes: Td1 and Td2 means protein denaturation temperature; Tg means glass transition temperature; Tm means melting temperature; ΔHd means enthalpy change.

Table 3.2 Dry shear bond strength of WPU-SPI blended adhesives

Sample ID	Strength (MPa)	Cohesive Wood Failure	Sample ID	Strength (MPa)	Cohesive Wood Failure
SPI	5.78 ± 0.37	100%			
10% WPU0500-SPI	5.41 ± 0.62	100%	10% WPU0002-SPI	6.76 ± 0.56	100%
30% WPU0500-SPI	4.80 ± 0.42	100%	30% WPU0002-SPI	5.94 ± 0.38	100%
50% WPU0500-SPI	6.49 ± 0.55	100%	50% WPU0002-SPI	7.30 ± 0.61	100%
70% WPU0500-SPI	5.21 ± 0.25	100%	60% WPU0002-SPI	6.36 ± 0.74	100%

Chapter 4. Camelina protein enhanced by polyelectrolyte interaction and its plywood bonding properties

4.1 Abstract

Camelina protein is a major by-product after oil extraction from camelina seeds and has drawn research attention as an economical material for bio-industrial implications. The present study investigates the influence of polyelectrolyte interaction on camelina protein structure and effects on wood bonding performance when used as a bio-adhesive. Infrared spectroscopy (IR) and transmission electron microscopy (TEM) images revealed that after interacting with polymeric amine epichlorohydrine (PAE), a cationic polyelectrolyte, camelina protein is partly unfolded with more flexible chain structures. PAE works as a bridge among different protein molecules primarily through electrostatic and hydrophobic interactions. Separation by size exclusion chromatography showed that soluble PAE modified proteins are smaller in molecular size. PAE modified proteins had reduced solubility, possibly indicated increased hydrophobicity. PAE treatment of camelina protein greatly improved both dry and wet adhesion strength when used as an adhesive. Two aliphatic structures with hydrophobic chains were introduced into the PAE modified protein system to further improve the water resistance. This study demonstrates the possibility of camelina as a green resource for the adhesive industry.

4.2 Introduction

Camelina is a native flowering plant found in the Mediterranean region of Europe and Asia. Camelina is known as an oilseed crop, which is planted in many areas including Austria, China, Finland, Germany, Ukraine and United States. Camelina seed contains about 39% oil of which 90% is made up of polyunsaturated fatty acids (1). Current research has focused on the utilization of camelina oil as bioenergy, for example, as jet fuel and biodiesel, as well as use as a biolubricant and in animal feed. Camelina based fuel has an 80% reduction in net carbon emissions and the fuel has been used in commercial airlines and military planes in North America (2). The successful industrial utilization of camelina oil may stimulate increased planting of more camelina and at the same time increase the need to exploit byproducts from the oil extraction process.

Defatted camelina meal contains roughly 40% protein, 12% fiber and small amount of gum and vitamins (3). According to a recent study, there are three main protein fractions including albumins, globulins, and glutelins in camelina protein with varied solubility and structure (4). Camelina protein is currently mainly used as animal feed additive. Based on the similarity of amino acid composition between soy protein and camelina proteins, camelina proteins would be useful new resources to replace soy protein in biomaterials. Modified camelina meals have improved physicochemical properties when used as thermal plastics, composite sheets, and wood adhesives (5, 6). However, the mechanical strength of native camelina protein based adhesive is too weak for industrial application. To improve the use of camelina proteins as adhesives, modifications to the native protein structure and properties need to be made. Disrupting native compact, globular protein structures and producing, more open, flexible and interwoven polypeptide chains can improve protein attachment to solid surfaces and distribute the concentration of stresses generated at the interface into the bulk solid (7). Polyelectrolyte chemicals bear electrolyte groups containing either cations or anions with different chain lengths and other functional groups in the main chain. Protein-polyelectrolyte interactions arise from interactions between a three-dimensional fixed and heterogeneously charged protein with a flexible charged chain strand of the polyelectrolyte. Strong bonding is formed through electrostatic interactions among charged groups and hydrophobic interactions among hydrophobic segments of the polyelectrolyte and hydrophobic patches of proteins (8, 9). Therefore, the three-dimensional network of protein may be strengthened. Based on previous work, aliphatic chains can be introduced into the protein-polyelectrolyte system to further increase the water resistance of protein based adhesives. (10, 11). Thus, a chemical crosslinker, Tetrakis(hydroxymethyl)phosphonium chloride (T), was also introduced to modify camelina protein and further improve adhesive performance. T is an economical, amine-reactive, aqueous cross-linker for protein based molecules. The T-amine reaction mechanism was studied using primary and secondary amino acids (12). The high reactivity and water solubility of T is essential to work with camelina protein.

The goals of the present study were to investigate ways to improve the use of camelina protein as a bio-adhesive through the interactions between cationic amine-epichlorohydrine and camelina protein. Specific objectives of this study were to 1) reveal the mechanism of how polyelectrolyte, chemical cross-linker, and aliphatic chains could influence the structure of camelina protein; 2)

characterize the plywood bonding strength, rheology, and other physiochemical properties of camelina protein based adhesives.

4.3 Experimental Section

4.3.1 Materials

Camelina meal was purchased from Field Brothers Inc (Pendroy, MT, US) and contained 15% lipids (db), 32.4% crude protein (db), and 11.0% moisture (db). Polymeric amine epichlorohydrine (PAE) was provided by Wuhu Hangchen Trading Co. Ltd (WuHu, China). PAE is in aqueous solution at a 12.7% solid content and pH 3.9. Undecylenic acid (99%, UA) was purchased from Sigma–Aldrich (St. Louis, MO). Tetrakis(hydroxymethyl)phosphonium chloride (T, 80% water solution), hydrochloric acid (HCl), sodium hydroxide (NaOH), and hexane were purchased from Fisher scientific (Waltham, MA, US). The water borne polyurethane was made from BiOH® polyols according to our previous studied methods (11). Cherry wood veneers with dimensions of 50 mm × 127 mm × 5 mm (width × length × thickness) were provided by Veneer One (Oceanside, NY). Yellow pine veneers with dimension of 300 × 300 × 3.5 mm were purchased from Ashland Company (Covingtion, KY US).

4.3.2 Characterization

Size exclusion chromatography (SEC)

The molecular weight of protein with/without modification were measured using a high performance liquid chromatography (HPLC) system (1260 with high sensitivity detector, Agilent, Palo Alto, Cal.) as described in Bean et al, 2006 (19) except that a 300 × 7.8 mm BioSep 4000 column and security guard column (Phenomonex, Torrance, Cal.) were used. The column was run at room temperature 30 ℃. The mobile phase was a pH7.0 sodium phosphate buffer (50mM) with 1% sodium dodecyl sulfate (SDS, w/v) and flow rate was maintained at 1 ml/min. The samples were first freeze dried and then redissloved in 1mL of a pH 7.0 sodium phosphate buffer (12.5 mM) with 1% SDS at a constant weight of 5 mg. Proteins including bovine serum albumin (66 kDa), carbonic anhydrase (29 kDa), lysozyme (14 KDa), and vitamin B12 (1350 Da) were used as standards for the estimation of camelina protein weight distribution.

Infrared spectroscopy (IR)

The control and modified camelina protein based adhesives were freeze dried after reaction and ground into fine particles. The IR spectrum were recorded using a Smiths Detection Sensor IR equipped with universal attenuated total reflectance. (London, England) in the range of 4000 - 800 cm^{-1}. Each spectrum was scanned 256 times at a resolution of 4 cm^{-1}. The spectra data were average of three replicates. Baseline and ATR correction were done to the spectra. Data from ATR is converted to sample absorption data.

Rheology

The shear rate dependent viscosities of camelina protein and modified camelina protein based adhesives were measured by a Bohlin CVOR150 rheometer (Malvern Instruments, Southborough, MA) with a parallel plate (PP20, 20 mm plate diameter).The distance between cone and plate was set as 500 nm for all samples. Shear rate was in the range of 0.1 to 100 S^{-1}, and the testing temperature was 23 ℃. To prevent dehydration during testing, a thin layer of silicone oil was spread over the circumference of the samples.

Morphology

Transmission electron microscopy (TEM)

The microstructure of aqueous samples were observed using a model CM100 TEM (FEI Co., Hillsboro, ORE) operated at 100 KV. Fresh prepared samples were diluted into 0.1% with deionized water and then sonicated for 3 min right before imaging. The sonicated sample was then absorbed onto Formvar/carbon-coated 200-mesh copper grids (Electron Microscopy Sciences, Fort Washington, Pa.) and stained with 2% (w/v) uranyl acetate (Ladd Research Industries, Inc., Burlington, Vt. US) for one minute at room temperature. The stained sample was allowed to dry for about 15 min before taking TEM images.

Scanning electron microscopy (SEM)

The samples were cured using the wood pressing temperature (170 ℃) to mimic the adhesive application conditions. The cured samples were milled into powder to view the microstructure on a Hitachi S-3500N (Hitachi Science System, Ibaraki, Japan) SEM instrument. The sample powder

was affixed to an aluminum stub with two sided adhesive tape and coated with an alloy of 605 gold and 40% palladium. (Desk Ⅱ Sputter/Etch Unit, Moorestown, NJ, US). The accelerating voltage of the testing was 5 KV.

Particle size analysis

Freshly prepared control and modified camelina protein adhesive samples were tested on a laser-scattering particle size distribution analyzer (LA-910, HORIBA company, Kyoto, Japan). Particle sizes were recorded and calculated into particle size distribution graphs. Three repetitive tests were done on each sample.

Turbidity

Control and modified camelina protein adhesive samples were diluted into 0.1% with deionized water and these solutions were stirred for one hour at room temperature before testing. The absorbance of protein solutions was measured at 600 nm with a UV-VIS Spectrophotometer (SHIZMADAU Corp. Tokyo, Japan). All measurements were done in three repetitions and the averages were reported.

Thermogravimetric analysis (TGA)

The control and modified camelina protein based adhesives were freeze dried after modification and milled into fine powder. The thermal hydrolysis curves of dry samples were record using thermogravimetric analysis (TGA, PerkinElmer Pyris1 TGA, Norwalk, CT). Around five mg of each sample was loaded into the TGA pan and heated from 50 to 700 ℃ at a heating rate of ten ℃/min. Heating processes were under nitrogen atmosphere. Data was plotted as the derivative thermogravimetric analysis (DTGA). The onset, end, and peak temperatures of each peak were calculated by TGA data processing software.

Wood bonding performance tests

Two layer wood specimen Cherry or yellow pine wood pieces were preconditioned at 23 ℃ and 50% RH in a chamber (Electro Tech Systems, Inc., Glenside, PA, US) for at least one week prior to use. According to previous studies, the camelina protein adhesives were brushed on wood at

2.36 mg/cm2. The wood pieces were rested for 15 min before assembling together. To avoid the influence of hot press condition on adhesion strength, a relative higher temperature of 170 ℃ and a longer time of 10 min were used at a pressure of 1.4 MPa. The wood assemblies were cooled at room temperature and conditioned at the chamber at 23 ℃ and 50% RH for one day before cutting.

Each wood assembly was cut into five small pieces at a dimension of 50 mm × 20 mm (length × width). Two of the small wood pieces were further conditioned and used for dry strength testing. Three of the small wood specimen were soaked in water at room temperature for 48 h. Wet strength was tested immediately after soaking. Adhesion strength was expressed as the stress at maximum load. Wood failure was evaluated in accordance to the standard for estimating the percentage of wood failure in adhesive-bonded joints (14). Wood specimens were tested with an Instron tester (Model 4465, Canton, MA) based on ASTM Standard Method D2339-98 at a crosshead speed of 1.6mm/min (15). Water resistance of the two layer wood specimen was measured based on ASTM Standard Methods D1183-96 and D1151-00 (16). Dry strength data were the average of four replicates and wet strength data were the average of six replicates.

Three layer wood specimen The 300 × 300 × 3.5mm dimension yellow pine veneers were preconditioned in a 27 ℃, 30% RH chamber at least one week before wood adhesion test. The three veneers were layered up in a way that grain lines of the middle panel were perpendicular to the grain lines of the top and bottom panels. Around 20 to 22 g/ft2 (wet basis) adhesive was brushed on the two faces of the middle veneer panel only. The assembled wood specimen was standing for 15 min before hot press. The hot press conditions were 150 ℃, 10 min at 1.03 MPa.

The bonded three layer wood specimen were conditioned in a chamber at 23 ℃ and 50% RH for two days and then cut into ten small pieces (82.6 × 25.6 mm) and four large wood pieces (50 × 127 mm) based on the ASTM standard method D906-98 (17). Four of the small wood pieces were used to test dry adhesion strength. Water resistance was evaluated in terms of wet shear adhesion strength and three cycle soaking test (18). Six of the small wood pieces were soaked in water for 24 h at 23 ℃ and then wet adhesion was tested immediately after soaking. The four large pieces were used for three cycle test. In each cycle, the wood pieces were soaked at 23 ℃ for four hours and then dried at 50℃ with air circulation for 19 h. After drying, the wood pieces were evaluated

for delamination. The delamination score is rated from zero to ten. Zero means no delamination, five is the maximum allowable delamination to pass the test, and ten means completely veneer separation. Any individual value higher than 5 is considered as fail to pass the three cycle test.

4.3.3 Preparation of Camelina Protein

Camelina protein was extracted according to previous method with slight modifications (13). Camelina meal was defatted using hexane at a ratio of 1:10 (w/v) for two hours with three repeated cycles. The defatted camelina meal (DCM) was then spread into thin layers (under 2mm) to allow hexane to evaporate in a fume hood for 48 hours. DCM was suspended into water at a ratio of 1:30 (w/v) and stirred for two hours. Centrifuge the DCM slurry to remove the water soluble gum and other impurities. The sedimentation was then dispersed into water at ratio of 1:30 (w/v) and the pH was adjusted to 12.0 using 3 Mol/L NaOH with continuous stirring for two hours to dissolve protein and then centrifuge. The supernatant was adjusted to pH4.5 using 3 Mol/L HCl to precipitated protein. To remove the salts, protein was washed with distilled water for twice and then redissloved at pH7 for freeze drying. The final protein isolate had about 83% protein as measured by Elemental Analyzer (Perkin Elmer 2400 Series Ⅱ CHNS/O, Waltham, MA) using 6.5 nitrogen to protein conversion factor.

4.3.4 Preparation of modified camelina protein based adhesives

Camelina protein was dispersed into water at a 10% solid content at different pH values and allowed stabilize at the pH for 30 min. Varied amounts of PAE (3%, 5%, 10%, 15%, volume ratio to C slurry) solution were then add to the protein slurry. The pH of the slurry was maintained using sodium hydroxide. Camelina protein slurry was stirred under the same conditions without PAE to use as control.

The adhesive formulation was further improved by introducing a cross-linker and hydrophobic aliphatic chains. The protein was first dispersed in water and then different amount of T, UA or WPU was added to the slurry. The pH of the slurry was maintained at 8 for UA and WPU, 4.5 and 8 for T, using NaOH & HCl and the mixture was stirred for two hours. Next, 10% of PAE was added to the CT/CU/CW mixture and the pH was maintained at 4.5 or 8. The CTP/CUP/CWP

adhesives were further stirred for another four hours. All the preparation procedures were done at room temperature (23 ℃).

4.4 Results and Discussion

4.4.1 Molecular weight of control and modified camelina protein studied by size extraction chromatography (SEC)

SEC was used to characterize the molecular weight (Mw) distribution of control and modified camelina proteins solubilized in SDS buffer. In Fig.1, control camelina protein had three major peak at 5.1 min, 8.1 min, and 9.0 min. According to the standard molecular weight marker, peak at 8.1 min represented fraction of 66 KDa, peak at 8.9 represented fraction of 29 KDa, peak at 9.8 min represented fraction of 14 KDa, and peak at 11.7 min represented fraction of 1,350Da. Peak at 5.1 min indicated camelina protein fractions with molecular weight distribution much larger than 66 KDa, which likely represents polymeric and oligomeric proteins composed of smaller protein subunits. In samples with PAE modification, the large peak at 5.1 min dramatically decreased and all other peaks shifted to lower molecular weights, indicating that within the SDS soluble proteins, PAE modification resulted in a shift to smaller proteins. Samples with UA and WPU had slightly larger Mw than CP but still under 29 KDa. This slightly different molecular weight distribution of the SDS-soluble proteins in UA and WPU may be due to UA and WPU partially blocking the protein surface and reducing the efficiency of PAE modification.

The SEC chromatograms of samples with cross-linker T are shown in Fig.2. SDS soluble proteins with T added had a narrower molecular weight range with the lower peak area after 10 min shifted to the 8-10 min range in the CTP and CT compared with CP. The sharp peak at 12min in Fig.4 was free cross-linker. CT and CTP had very similar SEC curves which indicated that the covalent bonding between T and protein was stronger than the uncovalent interactions between PAE and protein.

Chromatograms in Fig 1 and 2 were normalized to be able to easily compare the SEC chromatograms from the samples. The total peak area from the SEC analysis is shown in Fig 3. Demonstrating that after PAE modification, protein solubility in SDS was greatly reduced compared to the control PAE modification may have promoted the unfolding of camelina protein

and more hydrophobic groups exposed to limit the solubility. Modifications may have also resulted in the inability of SDS to bind to the proteins, limiting solubility. From Fig.2 and Fig.3, we could see after modifying protein with T, the protein samples had larger Mw but higher solubility. The surface hydrophobic groups should reach its maximum with only PAE modification.

4.4.2 IR spectra of control and modified camelina protein

In the IR spectra (Fig. 4) of cured PAE, we found typical amide I and amide II bonds at 1644 and 1551 cm^{-1}. In the unmodified camelina protein, the amide bonds were located at 1646 and 1542 cm^{-1} respectively. The amide I is corresponded to C=O stretching vibration with minor contribution from C-N stretching, and amide II arises from N-H bonding (60%) and C-N stretching (40%) (26, 27). The small peak at 1716 cm^{-1} in PAE spectra was attributed by the stretching vibration of C=O in ester groups. In the drying process, the carboxyl groups at the end of polyamideamine chains reacted with the hydroxyl groups on the azetidinium ring and formed the new ester groups (28). There was also an ester peak at 1745.6 cm^{-1} in camelina protein spectra corresponded to the residual of camelina oil. Both PAE and protein had the strong and broad peaks from the stretching of N-H but at different position.

In the spectra of CP, the amide bonds moved to lower position at 1640 and 1535.5 cm^{-1}, which indicated the changes in chemical environments because of the interactions between PAE and protein molecules. But the relative peak area ratio under amide I and amide II remained the same, indicating no covalent bonds between protein and PAE. To further study the structure changes in protein, Fourier self-deconvolution spectrum were calculated in the range of amide I bond. The major peaks in deconvolution amide bond were not changed for camelina protein after modification by PAE. The analysis of deconvolution amide I band proved that protein secondary structure stayed the same after PAE modification. The electrostatic and hydrophobic interactions between PAE and protein only altered protein tertiary conformation and partly unfolded protein. The acid carboxyl groups (-COOH) in protein can react with the azetidinium ring in PAE and form new ester carboxyl groups (-O-C=O) and thus the carboxyl absorbance peak shifted to 1737 cm^{-1} (29).

The spectrum of camelina protein modified with both PAE and UA/WPU/T are shown in Fig. 5. The acid carboxyl group from –COOH in UA at 1712 cm^{-1} was not shown in the CUP spectra, which indicated that carboxyl groups reacted with the amine group ($-NH_2$) in protein. The major interactions between protein and WPU are physical entanglement and hydrophobic interactions of side chains. IR spectrum demonstrated that covalent linkage and side chains interactions from UA and WPU promoted protein unfolding and conformation changes. The CTP and CT spectra were quite different in amide bonds position and relative intensity compared with C or CP. Molecular aggregation will influence the amide bonds vibration and thus move their absorption position in the IR spectra. The amide I and II peak area ratio in CTP and CT are 2.52 and 2.43 respectively while the ratio of C and CP are only 2.09 and 1.91 respectively. The increased ratio between amide I and II reveals that the intensity of amide II bond decreases due to the amine group reacting with cross-linker T.

4.4.3 Viscosities of control and modified camelina protein

Viscosity is an important parameter referring to handling and surface wetting ability of adhesives. Intermolecular interactions including hydrogen bonds, hydrophobic interactions, and electronic static forces mainly determine the intrinsic viscosity. With stronger intermolecular interactions, the protein molecules tend to be in larger sizes with more self-association (31, 32). The intrinsic viscosity against shear rate in the range of 0.1 to 100 S^{-1} were measured and plotted in Fig.6. Viscosity of camelina protein showed shear thinning properties and all the viscosities of modified samples were within the range for good industrial applications (33). After PAE modification, camelina protein had lower viscosity because of the positive charged groups from PAE forming electrostatic interaction with charged protein chains. The decrease of charged patches and increase of net charge on protein surface led to less attraction and more repulsion of surrounding molecules and therefore less self-association and lower viscosity (34).

Both UA and WPU have the long aliphatic chains and interact with polypeptide chains from CP. After addition of UA and WPU, the adhesives' viscosity increased mainly because of the intermolecular chain entanglement and hydrophobic interaction. As a small molecule, the reaction efficiency between UA and CP is much higher than that of WPU and the chain flexibility of UA is higher than WPU. Therefore, the increase of viscosity for UA treated adhesive is more obvious

than WPU treated adhesive. T crosslinked different protein chains together and thus increased intramolecular interactions and molecular weight, which resulted in higher viscosity.

4.4.4 Microstructures of control and modified camelina proteins

It has been reported that the majority of camelina proteins have are globular structures (37). For the current study, camelina protein was extracted as mixture of different fractions. The protein conformation in 1% aqueous solution was studied by TEM. Different camelina protein molecules crosslinked together into large aggregates and formed a continuous layered network as shown in Fig. 7. The darker color in TEM image shows more layers of the sample molecules. In the images of CP, two distinct types of structures were evident. The majority was the protein structures, the minority club-shaped structures were free PAE. Protein aggregates with PAE treatment had more flattened shapes and open, loose networks. PAE was uniformly distributed into protein and formed a bridge between protein molecules. The conformation changes of camelina protein observed by TEM demonstrated that partly unfolded camelina protein with more flexible structure would improve wood bond strength. The compact camelina protein structure was disassociated and unfolded by the stimulation of electrostatic and hydrophobic interactions between PAE and protein. The unfolded protein had more surface available for contact with wood and more exposed adhesion groups to react with wood. PAE also worked as a linkage to enhance the inner crosslinking of protein molecules.

The microstructures of cured protein adhesives were viewed by SEM (Fig.8). The samples were cured at hot press temperature and hand milled into small particles. Both samples formed compact disks after thermal curing, which indicated that the protein molecules were well crosslinked together. In the up-left side enlarge picture, the surface and sectional view were shown. The curved control camelina protein showed a smooth fracture surface with a few small particles attached on its surface. The PAE treated sample showed a coarse fracture surface with fluctuant layers. Absorbing polyelectrolyte into protein structure leads to a disordered and increased roughness of cured protein structure (38). Proteins in PAE treated samples were unfolded and had more flexible chains. Therefore, when protein cured, they tended to form anomalous crosslinking.

4.4.5 Particle size analysis

As an important physical characteristic, particle size reflects useful information including the changes in conformation, aggregate states, and denaturation. The particle size distribution of adhesive can influence the process of protein penetrating into wood cells and further effect the adhesion strength. Fig. 9 shows the particle sizes distribution of camelina protein adhesives with different formulation. The majority of the native protein particles had a size under 10 μm but had particles as large as 100 μm. After PAE modification, the frequency of particles under 10 μm decreased and converted to larger size around 100 μm to 400 μm. PAE can noncovalently link protein molecules together through electrostatic and hydrophobic interactions. In the CWP sample, WPU would have first covered the protein surface subsequently making it difficult for PAE to link protein molecules and thus, the CWP and C had almost the same particle size distribution curves. UA, as a small molecule, covalently grafted on protein. The UA chains interacted with other chains to help crosslink protein molecules and it didn't hinder the PAE coming to protein and thus, the CUP particle size was between 10 to 100 μm. CT particle size distribution shifts to larger size compared with CUP because T was an active, small molecule cross-linker. When T and PAE were combined together, the protein molecules crosslinking effects were even more obvious.

4.4.6 Turbidity

Turbidity is a useful optical parameter to predict protein aggregation behavior caused by either covalent crosslinking, noncovalent interactions, or physical entanglement (30). The turbidity of camelina protein with different chemical modifications is summarized in Table 1. The native camelina protein had very low absorbance at 600 nm, which indicated relatively high solubility and low aggregation. All the modified camelina protein had remarkable increase in absorbance at 600 nm. The interaction between PAE and protein through charged groups stimulated the unfolding process of protein and the exposed protein side chains would further interact with each other through hydrophobic interactions (8, 9). This process favored protein association and resulted in low solubility. WPU and UA brought more alkyl side chains into the protein system and these alkyl side chains mainly interact with protein through physical entanglement and hydrophobic interactions. T covalently crosslinked protein molecules together with the reaction on

amine groups. Thus, WPU, UA, and T further increase the aggregation process resulting in higher turbidity.

4.4.7 Thermal degradation analysis of control and modified camelina protein

Thermal analysis gives the information of sample decomposition as a function of temperature. The thermal stability of an adhesive is important reference for further process conditions such as hot press temperature. Fig. 10 showed the derivative weight loss curve of samples when heated under nitrogen. The details of peak temperature are summarized in Table 2. Free and bound water evaporated under 100 ℃. Since the water content of protein samples was very low, the water loss peaks were not obvious. Treatment C had two degradation stages assigned to protein subunits with different stabilities. During the heat process, the noncovalent intramolecular interactions including electrostatic interactions, hydrogen bonds, and hydrophobic interactions were first decomposed and then the covalent bonds such as C-N, C(O)-NH, C(O)-NH_2, and NH_2 broke and released CO_2, CO, and NH_3 (35, 36). Peak 1 in CP samples was broad with higher peak temperature than in C. After reacting with PAE, the composition of peak 2 in camelina protein disappeared, which meant it converted into structures decomposed at lower temperature. The electrostatic and hydrophobic interactions between PAE and protein stimulated protein unfolding into loosen structures with less thermal stability. Also, the CP surface covered with PAE molecules had less opportunities for protein-protein self-association. Because WPU itself had two decomposed peak at 324 and 338 ℃ assigned to hard and soft segments in WPU structure, (11) the CWP adhesive had one broad decomposed peak broadened from 273 to 480 ℃. Since the interactions between CP and WPU were mainly hydrophobic interactions and physically entanglement, their decomposed peaks merged together instead of forming a new peak at a higher temperature. Grafting UA on protein surface hardly affected the thermal stability of CP. Both CTP and CT had even lower peak temperatures comparing with other samples. The cross-linker T also resulted in protein with less thermal stable structures.

4.4.8 Wood bonding performance of camelina protein based adhesives

4.4.8.1 The effect of PAE on adhesion property of camelina protein

The adhesion properties of camelina protein were affected by PAE significantly. Dry and wet wood bonding strength of different amount of PAE modified camelina protein adhesives are summarized in Table 3. The native camelina protein had a very low dry bond strength of 2.39 ± 0.52 MPa and hardly any wet strength at all. The poor wood adhesion property of camelina protein could be due to its highly compact structure (20). After modification with 10% PAE, the dry wood bond strength was increased to 5.39 ± 0.50 MPa with 100% wood failure. The wet wood bond strength was dramatically increased from 0.37 ± 0.22 to 2.35 ± 0.17 MPa. PAE is a positive charged aqueous polyelectrolyte, which ensured good compatibility with camelina protein slurry. The charged protein segments are inclined to crosslink with charged chains of PAE. The charged chains of PAE may absorb onto the protein through physical entanglement and/or noncovalent bonding (21). Electrostatic interactions likely serve an essential role in the binding of charged PAE chains with the protein. The initial electrostatic association may form salt bridges or hydrogen bonding between protein and polyelectrolyte, which promotes partial protein unfolding resulting in more conformational flexibility and molecular mobility (22, 23). The more open structure of PAE modified protein would provide more contact area and adhesion groups to react with wood, and therefore increase the bond strength.

Protein structure is sensitive to pH conditions. At the isoelectric pH, protein is in the most compact state with lowest solubility. With the increasing of pH, protein will be partly unfolded, charged, and easier to disperse in water (24). The data in Table 4 showed that at pH 8.0 camelina protein had higher dry bond strength with 100% cohesive wood failure. Mild Alkaline pH alter protein charge, and therefore possibly structure, which in turn facilitates interaction with PAE and wood surfaces, which leads to the increased wood bonding strength. Wet bond strength at pH 9.0 decreased to 1.54 ± 0.27 MPa, possibly due to increasing charge on the proteins and increasing interaction with water, weakening bond strength.

4.4.8.2 Synergistic effect of PAE with aliphatic compounds and chemical cross-linker on adhesion property of camelina protein

From previous studies it is known that addition of aliphatic chains to proteins results in increased hydrophobicity of protein and therefore increases in wet bond strength of protein based adhesives (10, 11). In the present study, camelina protein was first reacted with 10% PAE at pH 8 and then

different amount of UA/WPU were added to the PAE modified adhesive. UA can grafted onto protein through the reaction of carbonyl group from UA and amine group from protein, which can be detected using IR. WPU can interact with protein through hydrogen bonding, hydrophobic interactions and physical entanglement. From table 5 and 6, it can be seen that the addition of UA/WPU increased both dry and wet bond strength. The hydrophobic chains from UA or WPU could prevent water penetration into the adhesive surface and thus increase water resistance. Also, the chemical crosslinking and physical entanglement of UA or WPU with protein may have enhanced the three dimensional network of PAE modified camelina protein. The highest wet adhesion strength was increased up to 3.12 ± 0.20 MPa with wood fiber pulled out. Too much UA or WPU would block the functional groups which should react with wood cells and resulted in low bond strength.

Chemical crosslinking could also enhance the three dimensional structure of protein. T is active to react with amine group on protein and link different protein segments together (13).From the data shown in table 7, crosslinked camelina protein had higher dry and wet adhesion strength than native protein and crosslinking effect was not influenced by pH condition. But little synergistic effect was found between T and PAE.

4.4.8.3 Three layer wood adhesion performance

Formulations with significant difference were selected to do three layer wood adhesion test and further characterization. Sample names were coded as following camelina protein: C; camelina protein + 10% PAE: CP; camelina protein+7%UA+10%PAE: CUP; camelina protein + 30%WPU +10%PAE: CWP; camelina protein +10% T: CT; camelina protein + 10%T+ 10% PAE: CTP.

Table 8 shows the three layer wood adhesion and three-cycle soaking results. The dry strength of native camelina protein was acceptable to use as plywood adhesive but camelina protein hardly had any wet adhesion strength. Wet adhesion strength of PAE modified camelina protein was dramatically increased to 1.30 ± 0.23 MPa, which met commercial standards and was higher than modified soy protein adhesion strength (25). When WPU was added into the PAE modified camelina protein, the adhesion performance was further improved. The multiple chains of WPU enhanced the adhesive structure mainly through physical entanglements and hydrophobic

interactions. When adding UA into the PAE modified camelina protein, the dry strength decreased and wet strength was comparable to C and CP. Single chains of UA may have covalently grafted onto the protein surface, which partly blocked adhesion of the protein directly to the wood surface. The hydrophobic chain of UA still protects protein from water penetration, which ensured a relatively high wet adhesion strength, 1.12 ± 0.31 MPa. When protein was covalently crosslinked by T, both dry and wet adhesion strength decrease because larger protein aggregates have relatively small reactive surface with wood cells.

4.5 Conclusion

Compared with soy protein, camelina protein (CP) is more economical and doesn't cause potential political and economic concerns regarding famine and therefore could potentially serve as a new primary source of protein in biomaterial field. Camelina protein was successfully modified into adhesive meeting industrial standards for application on plywood in terms of adhesion strength. Due to the constrained globular structure of control camelina protein, it had poor dry and wet adhesion strength. PAE works on opening camelina protein structure into flexible chains with more adhesive groups and hydrophobic packs on the surface confirmed by TEM imaging and SEC data. The open and flexible protein structure with more functional groups available for reaction had better adhesion performance. Hydrophobic chains from WPU and UA further improved water resistance of protein. The CWP sample had improved dry strength to 2.75 ± 0.22 MPa and wet strength to 1.40 ± 0.25 MPa on three layer plywood. CUP has lower try strength compared with CWP because UA partly covering adhesion groups and resulting in weak three dimensional network in cured adhesive. CT and CTP samples prove that too much crosslinking in protein structure impeded the adhesion performance. Modified camelina protein adhesive is not only safe and renewable but also economic compared with soy source materials.

4.6 Reference

1. Putnam, D.H., J.T. Budin, L.A. Field, and W.M. Breene. 1993. Camelina: A promising low-input oilseed. p. 314-322. In: J. Janick and J.E. Simon (eds.), New crops. Wiley, New York

2. Johnson, Andrew, September 2, 2011. "Blue Angels Use Biofuel at Patuxent Air Show.". United States Department of Defense (press release). Retrieved September 3, 2011 Howell, Katie, November 23, 2009. "KLM Carries Passengers in Biofuel Test Flight". The New York Times

3. Sampath, A., 2009. Chemical Characterization of Camelina Seed Oil. Master dissertation. The State University of New Jersey, Graduate School-New Brunswick Rutgers

4. Li, N., Qi, G., Sun, X.S., Wang, D., Bean, S., Blackwell, D. Isolation and characterization of protein fractions isolated from camelina meal. T. ASABE, 2014, 57, 169–178

5. Jun Tae Kim, and Anil N. Netravali. Non-Food Application of Camelina Meal: Development of Sustainable and Green Biodegradable Paper-Camelina Composite Sheets and Fibers. Polymer composites, 2012, 33: 1969–1976. doi:10.1002/pc.22337

6. Narendra Reddy., et al. Extraction, Characterization of Components, and Potential Thermoplastic Applications of Camelina Meal Grafted with Vinyl Monomers. Agricultural and food chemistry, 2012,60(19),4872-4879

7. Van Der Leeden, M. C., Rutten, A. A. C. M., & Frens, G. How to develop globular proteins into adhesives. Journal of Biotechnology. 2000, 79, (3):211-221 http://doi.org/10.1016/S0168-1656 (00)00238-8

8. Chodankar, S., Aswal, V. K., Kohlbrecher, J., Vavrin, R., & Wagh, A. G. Structural study of coacervation in protein-polyelectrolyte complexes. Physical Review E, 2008, 78(3), 031913

9. Fan, Y., Tang, S., Thomas, E. L., & Olsen, B. D. Responsive Block Copolymer Photonics Triggered by Protein–Polyelectrolyte Coacervation. American Chemistry Socisty NANO, 2014, 8(11), 11467-11473

10. Liu, H., Li, C., & Sun, X. S. Improved water resistance in undecylenic acid (UA)-modified soy protein isolate (SPI)-based adhesives. Industrial Crops and Products, 2015, 74, 577–584

11. Liu, H., Li, C., & Sun, X. S. Soy-oil-based waterborne polyurethane improved wet strength of soy protein adhesives on wood. International Journal of Adhesion and Adhesives, 2017, 73, 66–74

12. Chung, C., Lampe, K. J., & Heilshorn, S. C. Tetrakis(hydroxymethyl) Phosphonium Chloride as a Covalent Cross- Linking Agent for Cell Encapsulation within Protein-Based Hydrogels. Biomacromolecules, 2012, 13(12):3912-6

13. N. Li, G. Qi, Isolation and characterization of protein fractions isolated from camelina meal, American Society of Agricultural and Biological Engineers, 2014, 57(1): 169-178 2014

14. ASTM International, 2002. Standard Practice for Estimating the Percentage of Wood Failurein Adhesive Bonded Joints. Annual Book of ASTM Standards, D5266-99 Vol 15 (06), West Conshohocken, PA, pp. 143

15. ASTM International, 2002. Annual Book of ASTM Standards, D2339-98 Vol 15 (06), West Conshohocken, PA, pp. 158–160

16. ASTM International, 2002. Annual Book of ASTM Standards, D1131-00 Vol 15 (06), West Conshohocken, PA, pp. 67–69.

17. Annual Book of ASTM Standards, 2004. D906-98, ASTM International. West Conshohocken, PA, Vol. 15.06, pp 1-4

18. ANSI/HPVA HP-1-2004, Hardwood Plywood & Veneer Association. 2004 American National Standard- Hardwood and decorative plywood. ANSI/HPVA HP-1-2004

19. Bean, S. R., Ioerger, B. P., Park, S. H., & Singh, H. Interaction between sorghum protein extraction and precipitation conditions on yield, purity, and composition of purified protein fractions. Cereal Chemistry, 2006 83(1), 99-107.http://dx.doi.org/10.1094/CC-83-0099.

20. Ningbo Li, Adhesion properties of camelina protein fractions isolated with different methods. Industrial crops and products, 2015, 69:263-272

21. Zhong, Z., Sun, X. S., & Wang, D. Isoelectric pH of Polyamide – Epichlorohydrin Modified Soy Protein Improved Water Resistance and Adhesion Properties. Applied polymer, 2007, 103(4): 2261-2270, http://doi.org/10.1002/app

22. Chodankar, S., Aswal, V. K., Kohlbrecher, J., Vavrin, R., & Wagh, A. G. Structural study of coacervation in protein-polyelectrolyte complexes. Physical Review E, 2008, 78(3), 031913. 18.

23. John Oakes. Protein–surfactant interactions. Nuclear magnetic resonance and binding isotherm studies of interactions between bovine serum albumin and sodium dodecyl sulphate. Journal of the Chemical Society, 1974, 70, 2200-2209.

24. Fan, B., Zhang, L., Gao, Z., Zhang, Y., Shi, J., & Li, J. Formulation of a novel soybean protein-based wood adhesive with desired water resistance and technological applicability. Applied polymer, 2016, 43586, 1–10. http://doi.org/10.1002/app

25. N. S. Hettiarachchy, U. Kalapathy, D. J. Myers. Alkali-modified soy protein with improved adhesive and hydrophobic properties. Journal of the American Oil Chemists' Society, 1995, 72(12):1461-1464

26. Bunaciu, A.A., Fleschin, S., Aboul- Enein, H.Y. Infrared microspectroscopy applications – review. Current Analytical Chemistry, 2013, 10 (1), 132–139; Jackson,

27. M., Mantsch, H.H., The use and misuse of FTIR spectroscopy in the determination of protein-structure. Crit. Rev. Biochemistry and molecular biology, 1995, 30 (2), 95–120

28. Kong, J., & Yu, S. Fourier Transform Infrared Spectroscopic Analysis of Protein Secondary Structures. Acta biochimica et biophysica sinica, 2007, 39 (20745001), 549–559. http://doi.org/10.1111/j.1745-7270.2007.00320.x

29. Moreno, A., Mas-oliva, J., Bolanos-garcia, V. M., & Salvador, C. O. Turbidity as a useful optical parameter to predict protein crystallization by dynamic light scattering. Journal of molecular structure, 2000, 519:243-256

30. Obokata, T., & Isogai, A. The mechanism of wet-strength development of cellulose sheets prepared with polyamideamine-epichlorohydrin (PAE) resin, Colloids and surfaces A: physicochemical and engineering aspects, 2007, 302, 525–531. http://doi.org/10.1016/j.colsurfa.2007.03.025

31. Yadav, S., Shire, S. J., & Kalonia, D. S. Factors Affecting the Viscosity in High Concentration Solutions of Different Monoclonal Antibodies, Journal of pharmaceutical sciences, 2010, 99(12), 4812–4829. http://doi.org/10.1002/jps;

32. C. J. van Oss. Long-range and short-range mechanisms of hydrophobic attraction and hydrophilic repulsion in specific and aspecific interactions. Journal of Molecular Recognition, 2003, 16, 177-190.

33. Luo, J., Li, C., Li, X., Luo, J., Gao, Q., & Li, J. A new soybean meal-based bioadhesive enhanced with 5, 5-dimethyl hydantoin polyepoxide for the improved water resistance of plywood. RSC Advances, 2015, 5(77), 62957–62965. http://doi.org/10.1039/C5RA05037E

34. Yadav, S., Laue, T. M., Kalonia, D. S., Singh, S. N., & Shire, S. J. The Influence of Charge Distribution on Self-Association and Viscosity Behavior of Monoclonal Antibody Solutions. Molecular pharmaceutics, 2012, 9(4), 791-802

35. Das, S.N., Routray, M., Nayak, P.L. Spectral, thermal, and mechanical properties of furfural and formaldehyde cross-linked soy protein concentrate: a comparative study. Polymer-plastics technology and engineering, 2008, 47 (6), 576–582.

36. Schmidt, V., Giacomelli, C., & Soldi, V. Thermal stability of films formed by soy protein isolate-sodium dodecyl sulfate. Polymer degradation and stability, 2005, 87, 25–31.

37. Li, N., Qi, G., Sun, X. S., Wang, D., Bean, S., & Blackwell, D. Isolation and characterization of protein fractions isolated from camelina meal, American Society of Agricultural and Biological Engineers, 2015, 57(1), 169–178.

38. Caruso, F., Furlong, D. N., Ariga, K., & Ichinose, I. Characterization of Polyelectrolyte - Protein Multilayer Films by Atomic Force Microscopy , Scanning Electron Microscopy , and Fourier Transform Infrared Reflection. Absorption Spectroscopy, 1998, 7463(22), 4559–4565.

4.7 Figures and tables

Figure 4.1 SEC molecular weight distribution of C, CP, CUP, and CWP

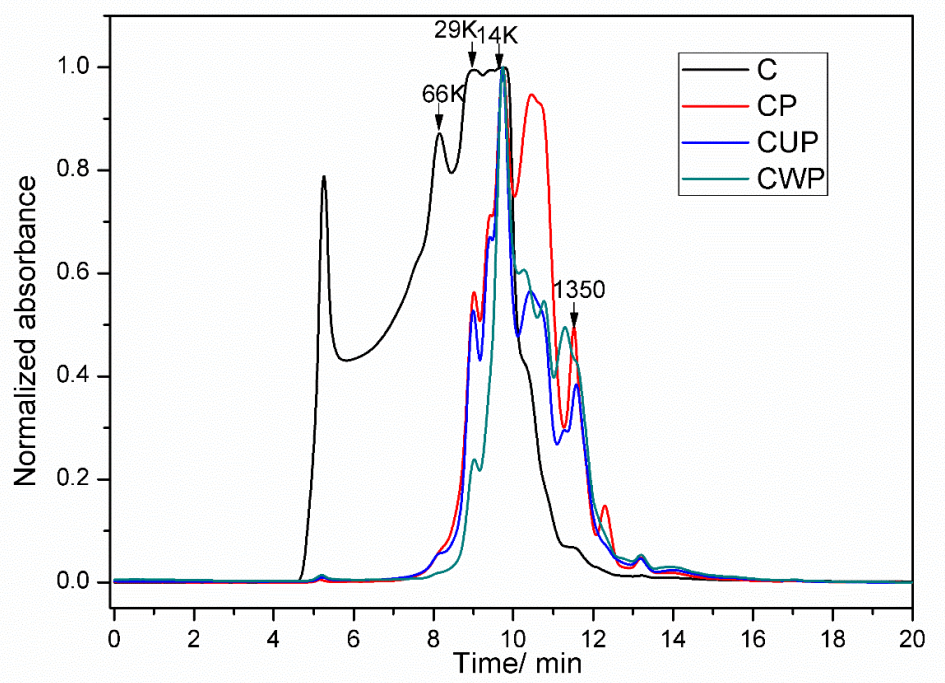

Figure 4.2 SEC molecular weight distribution of C, CPT, and CT

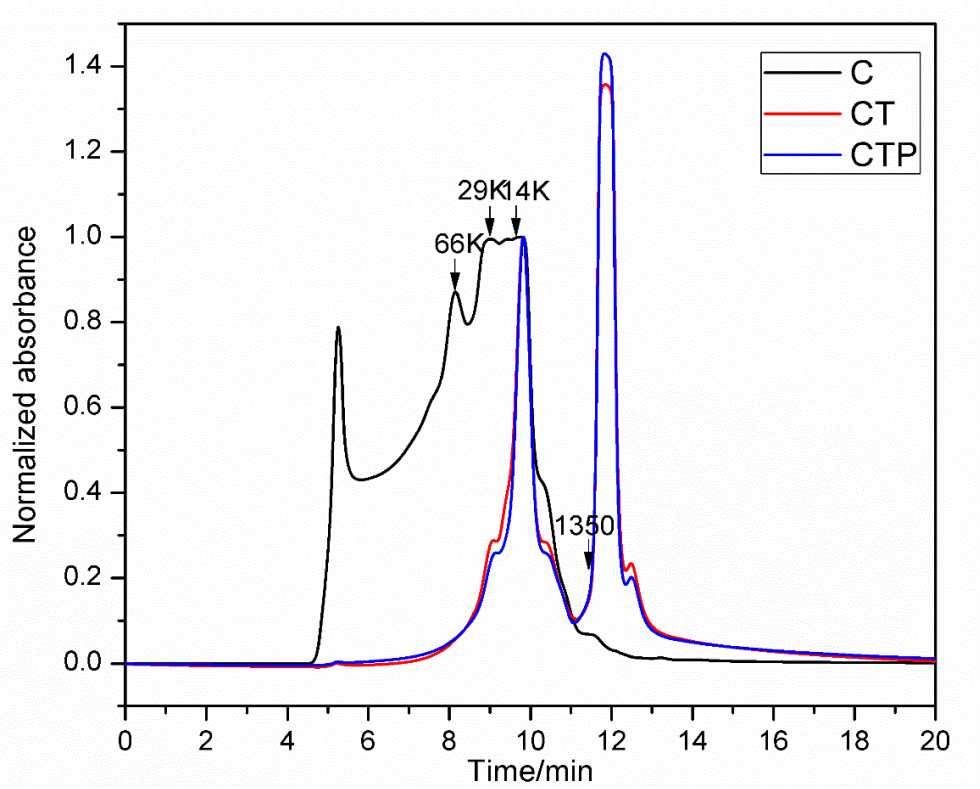

Figure 4.3 Total SEC peak area of control and modified camelina protein

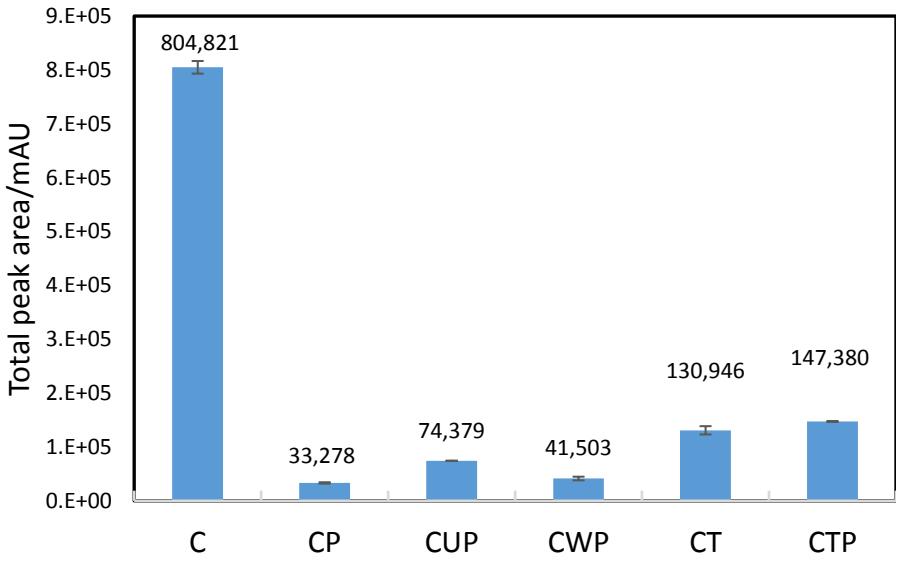

Figure 4.4 IR spectra of PAE, C, and CP

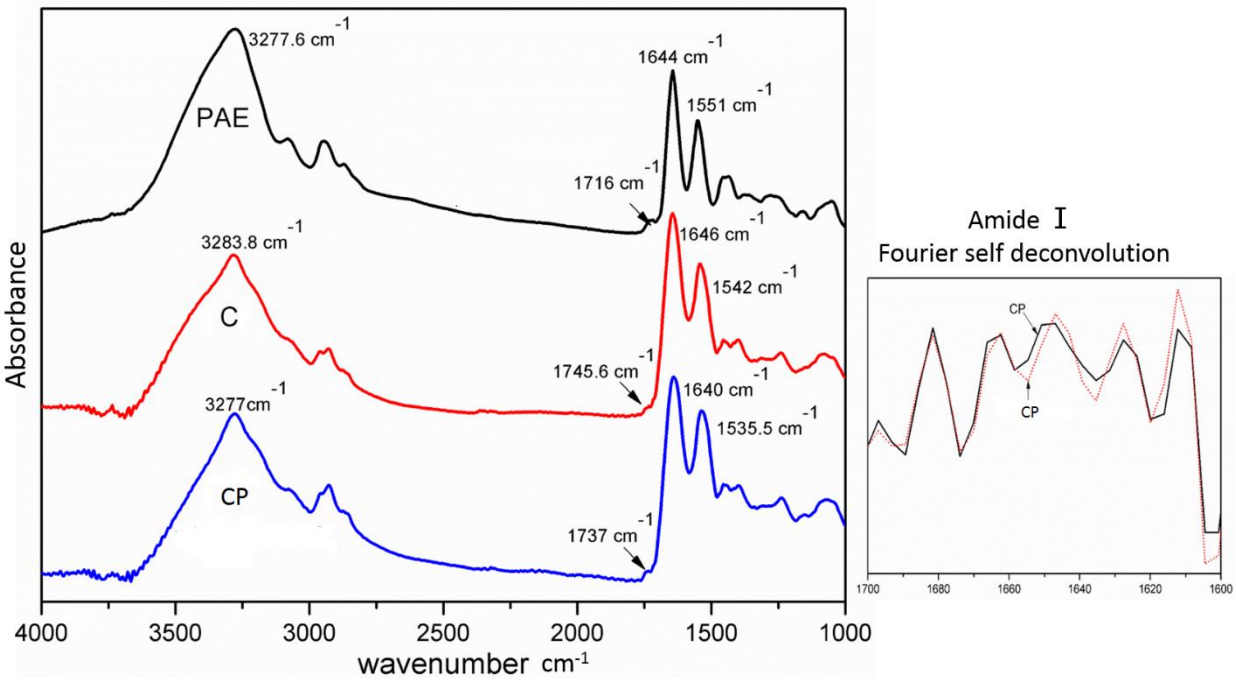

Figure 4.5 The infrared absorbance of camelina protein with different modification

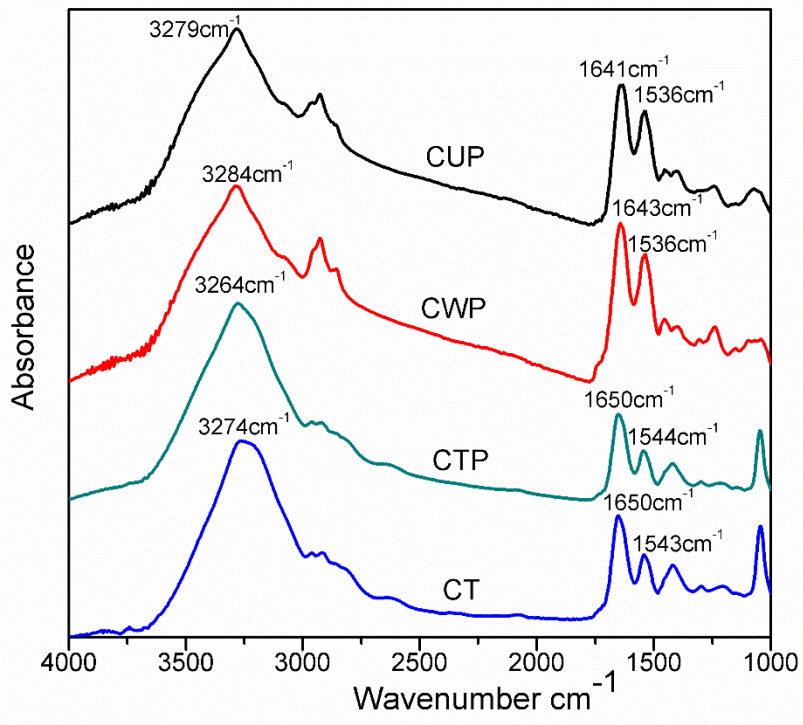

Figure 4.6 Shear rate dependent viscosities of camelina protein adhesives with different formulations

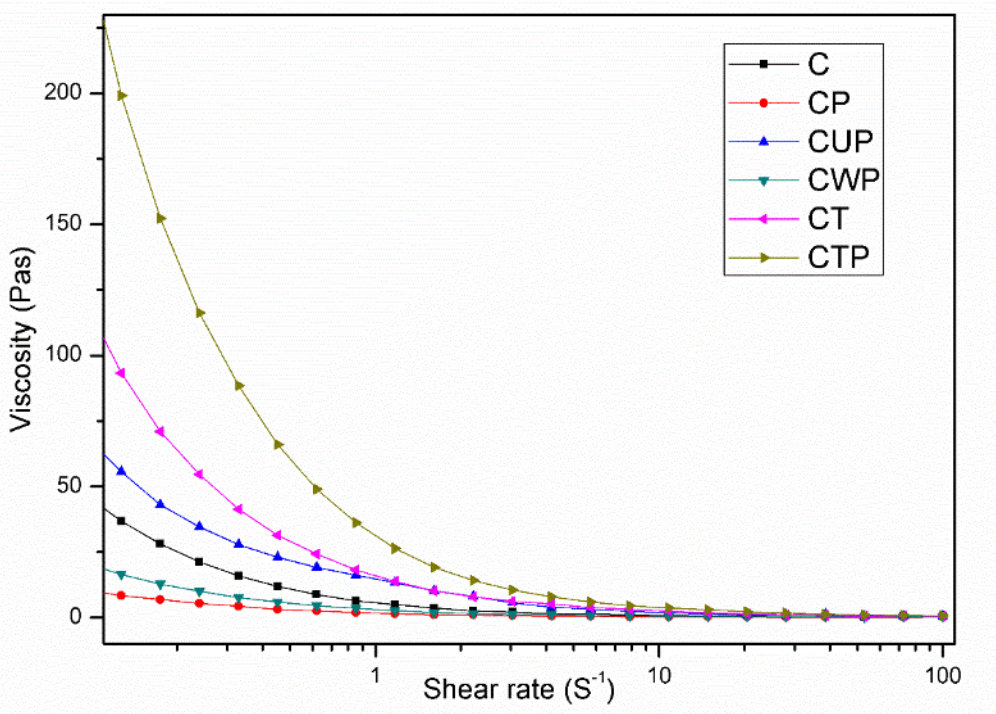

Figure 4.7 TEM images of camelina protein and sample modified with PAE

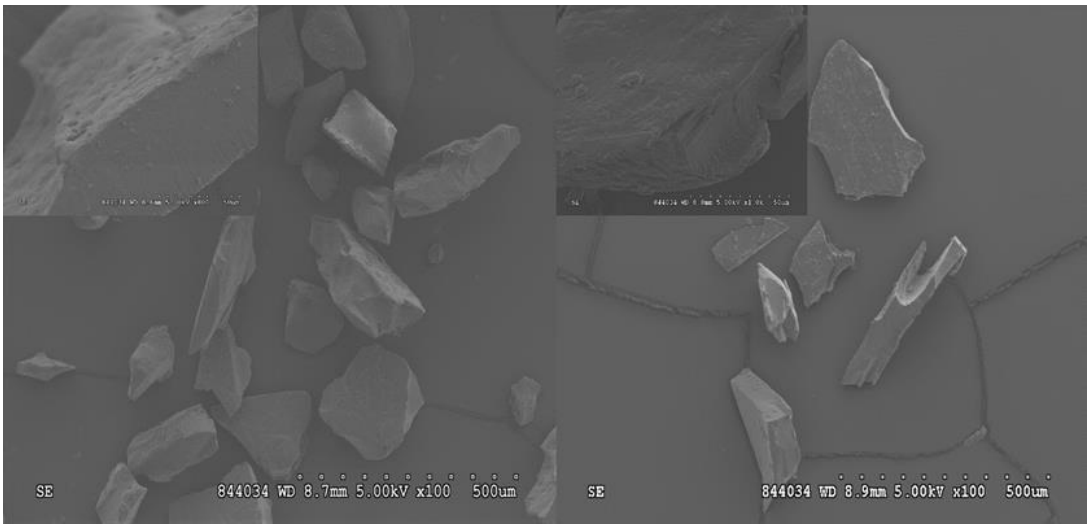

Note: Left: C Right: CP+10%PAE

Figure 4.8 SEM images of CP and PAE treated CP

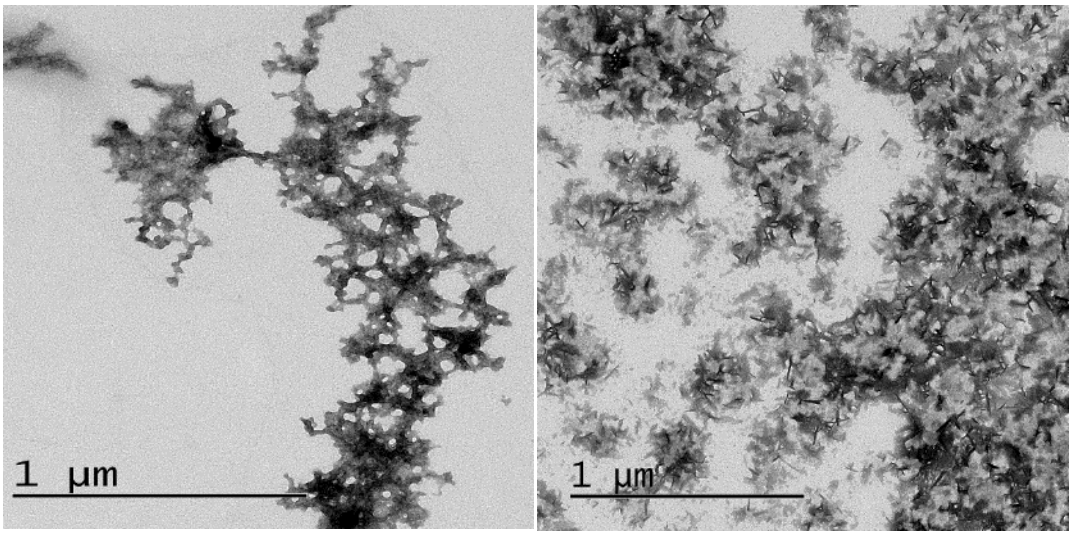

Note: Left: CP Right: CP+10%PAE

Figure 4.9 Particle size distributions of camelina protein adhesives with different formulations

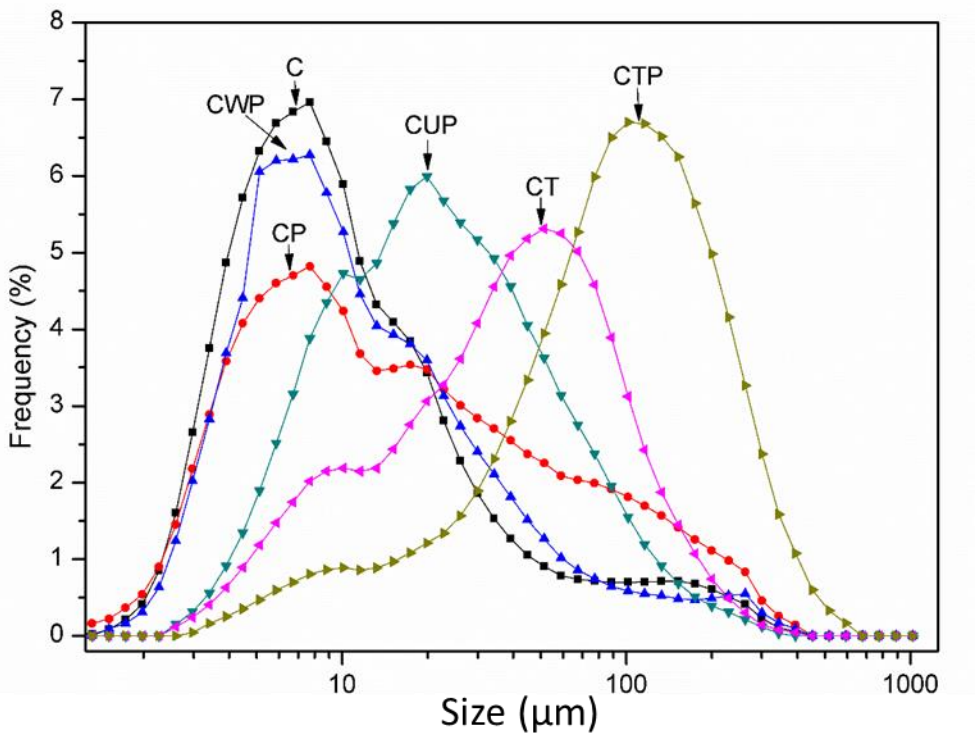

Figure 4.10 Derivate thermal degradation analysis curves of control and modified camelina proteins

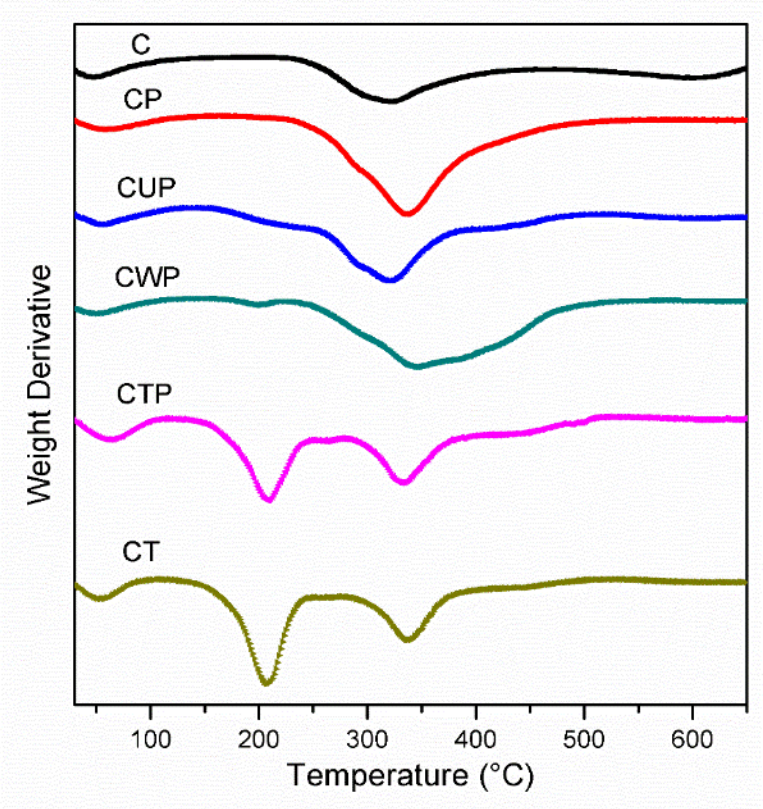

Table 4.1 The turbidity of camelina protein adhesives with different formulation

sample	absorbance	Solubility	association
C	0.20±0.02	High	Low
CP	0.75±0.05	Low	High
CWP	0.84±0	Low	High
CUP	0.89±0.04	Low	High
CT	0.86±0.02	Low	High
CTP	0.89±0.03	Low	High

Table 4.2 Derivative thermogravimetric peaks temperature data of control and modified camelina proteins

Sample ID	Peak 1 (℃)			Peak 2 (℃)		
	One set	End	Peak	One set	End	Peak
C	255	374	321	550	639	599
CP	268	400	338			
CUP	264	365	321			
WP	273	480	347			
CTP	182	237	208	303	365	333
CT	178	231	207	306	363	337

Table 4.3 Two layer cherry wood adhesion strength of camelina protein modified with different amount PAE at neutral pH

Sample ID	Dry Strength (MPa)	CWF	Wet Strength (MPa)	CWF
CP	2.39 ± 0.52C	0	0.37 ± 0.22D	0
CP+3% PAE	4.14 ± 0.39B	Fiber pulled out	1.66 ± 0.12C	0
CP+5% PAE	4.10 ± 0.64B	Fiber pulled out	2.00 ± 0.17B	0
CP+10% PAE	5.39 ± 0.50A	100%	2.35 ± 0.17A	0
CP+15% PAE	5.11 ± 0.48A	67%	2.34 ± 0.15A	0

Note: CWF means cohesive wood failure. Dry strength data were the average of six duplicates and wet strength data were the average of nine duplicates. Capital letters after data were results for statistical analysis. $\alpha = 0.05$

Table 4.4 Two layer cherry wood adhesion strength of camelina protein modified with 10% PAE at different pH

Sample pH	Dry Strength (MPa)	CWF	Wet Strength (MPa)	CWF
4	3.98 ± 0.60B	0	1.79 ± 0.28BC	0
6	5.14 ± 0.49A	67%	1.94 ± 0.34B	0
7	5.45 ± 0.50A	100%	2.34 ± 0.17A	0
8	5.36 ± 0.37A	100%	2.34 ± 0.44A	0
9	5.18 ± 0.60A	67%	1.54 ± 0.27C	0

Table 4.5 Synergistic effect of PAE with UA on two layer yellow pine wood adhesion performance at pH8

Sample Name	Dry strength (MPa)	CWF	Wet strength (MPa)	CWF
CPI+10%PAE	6.32 ± 0.18BC	100%	2.59 ± 0.17B	0
CPI+5%UA+10%PAE	7.40 ± 0.44A	100%	2.78 ± 0.12AB	0
CPI+7%UA+10%PAE	6.86± 0.69AB	100%	2.87 ± 0.21A	0
CPI+10%UA+10%PAE	5.89 ± 0.17CD	100% weak	2.28 ± 0.25C	0
CPI+15%UA+10%PAE	5.80 ± 0.05D	100% weak	2.29 ± 0.20C	0

Table 4.6 Synergistic effect of PAE with WPU on two layer yellow pine wood adhesion performance at pH8

Sample Name	Dry strength (MPa)	CWF	Wet strength (MPa)	CWF
CPT+10%PAE	6.32 ± 0.18	100%B	2.59 ± 0.17B	0
CPI+20%WPU+10%PAE	7.59 ± 0.19	100%A	3.05 ± 0.17A	0
CPI+30%WPU+10%PAE	6.91 ± 0.32	100%AB	3.12 ± 0.20A	Fiber pulled out
CPI+40%WPU+10%PAE	6.43 ± 0.60	100%B	2.80 ± 0.50AB	0
CPI+50%WPU+10%PAE	5.41 ± 0.80	100%C	2.60 ± 0.22B	0

Table 4.7 Synergistic effect of PAE with T on two layer yellow pine wood adhesion performance at Ph4.5 and Ph8

Sample Name	Dry Strength (MPa)	CWF	Wet strength(MPa)	CWF
CP+10%T ph4.5	3.79±0.29	50% WF	2.16±0.35	0
CP+10%T+10%PAE 4.5	3.96±0.75	75% WF	2.47±0.23	83%WF,17%FIBER
CP+10%T Ph8	3.79±0.29	Weak WF	2.16±0.53	0
CP+10%T+10%PAEph8	5.4±0.45	Weak WF	2.35±0.23	Fiber pulled out

Table 4.8 Three layer wood test results of selected adhesive formulations and literature reference data

Adhesion strength results			
Sample Name	Dry strength (MPa)	Wet strength (MPa)	Reference
C	2.12 ± 0.17	NA	
CP	2.55 ± 0.22	1.30 ± 0.23	
CWP	2.75 ± 0.22	1.40 ± 0.25	
CUP	1.45 ± 0.16	1.12 ± 0.31	
CTP	1.30 ± 0.34	0.69 ± 0.08	
CT	1.56 ± 0.06	0.23 ± 0.16	
Polyamide modified SPI	2.71 ± 0.23	1.12 ± 0.13	Bo Fan, 2016 Ref. 25
Commercial standards	0.98	0.98	Japan JIS K6806-2003
Interior-use plywood	0.7	0.7	China GB/T 17657-1999

Three cycle soaking results						
Sample Name	Cycle 1		Cycle 2		Cycle 3	
	Score	Pass	Score	Pass	Score	Pass
C	2.25	100%	4.50	75%	8.00	0
CP	0	100%	0	100%	0	100%
CWP	0	100%	0.50	100%	1.00	100%
CUP	0	100%	0.50	100%	0.88	100%
CTP	4.25	100%	5.88	50%	6	0
CT	5.75	75%	6.25	0	NA	NA

Chapter 5. Adhesion and physicochemical properties of camelina meal with different modification

5.1 Abstract

Camelina meal is the byproduct after oil extraction from camelina seed. Camelina meal has drawn research attention because it is an economical resource for biomaterials. The major components in camelina meal are protein, carbohydrate, and oil, which is proved by Fourier transfer infrared spectrum (FTIR) in this study. Native camelina meal hardly has any adhesion strength. Polymeric amine epichlorohydrine (PAE) and Laccase were used to modify camelina meal. The modified camelina meal showed dramatically improved adhesion strength and potential to imply for wood adhesive industry.

5.2 Introduction

For over 150 years petroleum has been the foundation for the majority of the resins on the market. The United States' dependence on petroleum is depleting the sources much faster than they can be restored. Due to the unbalanced relation between supply and demand, oil prices have doubled since 2010. The over-use of this chemical has created two major issues within the industry. First, the emissions from petroleum-based product production and petroleum burning are a leading source of pollution. Secondly, it is inability to replenish petroleum source. There is strong necessity to release modern industry from its dependence on depleting resources. Synthetic petrochemical adhesives not only generate severe problems including environmental pollution and detrimental to human health but also limited resource. Due to their biodegradability, worldwide availability and relative low prices, plant based resins are now attractive raw materials for many applications.

Since the formaldehyde based adhesives containing residual toxic chemicals, many researches have been done to find more natural and renewable resources for wood adhesives industry (1, 2). Soy has been considered as the most promising plants for biobased materials and soy protein has a very long history to use as adhesive (3). Many green modification technics such as chemical unfolding and crosslinking, ultra sound unfolding, and enzyme catalyze have been studied to

improve the adhesion performance of soy protein and soy flour based adhesives(4-6). There are already commercial products developed from soy protein and soy meal. However, soy based biomaterials have the potential political and economic concerns regarding famine.

Camelina which contains 40% of protein in its defatted meal, haven't been extensively used and could potentially serve as a new primary source of protein. P. Moriel has studied using camelima coproducts to replace conventional corn-soybean meal supplements in the diets of developing replacement beef heifers (7). Camelina would be a desirable new resource to replace soy protein in biomaterial field. Camelina [Camelina sativa L. Crantz] is an annual oil seed plant growing in North America since 4000 BCE. The unique oil composition and properties make camelina oil a great resource for biofuels and jet fuel. Camelina meal which is the byproduct after oil extraction is mainly used as animal feed with a value about \$100 Mg^{-1} (8). The non-food research of camelina meal are still limited. J.T. Kim used recycled newspaper as a reinforcing agent to improve tensile properties and increase water resistance of the camelina meal-based biodegradable composite sheets and fibers (9). Ningbo Li and Guangyan Qi isolated gum from camelina seed and studied the effects of glycerol and nanoclay on camelina gum based films. The physically crosslinked network in modified camelina gum proved to increase affinity between the camelina gum matrix and intercalated nanoclay and thus make contribution to mechanical strength of camelina gum based film (10, 11). The vinyl monomers grafted camelina meal was made into thermoplastic films with excellent wet tensile strength (12).

Previous studies proved that camelina meal which is rich in carbohydrate, protein, oil, and other trace component is a promising resource for biomaterial. The adhesion properties of camelina meal has not been studied yet. In this study, protein and carbohydrate in camelina meal were modified to open the original structure and crosslink to form strong network to enforce the adhesion strength. It found that laccase could catalyze fiber or lignin crosslinking and had the possibility for industrial bonding and modification of carbohydrates (13). Polymeric amine epichlorohydrine (PAE) can stimulate the unfolding of protein and further conformation changes through electrostatic and hydrophobic interactions (14, 15). The goal of the present study are to discover and characterize the adhesion performance of camelina meal modified with laccase and PAE.

5.3 Materials and methods

5.3.1 Materials

Camelina meal was provided by commercial processor (Field Brothers Inc., Pendroy, MT, U.S.) and it was milled into particle size < 0.5mm using a cyclone sample mill (Udt Corp., Fort Collins. CO, U.S.). The Camelina meal content around 15% (db) oil, and 32% protein. Polymeric amine epichlorohydrine (PAE) was provided by Wuhu Hangchen Trading Co. Ltd (WuHu, China). PAE is in aqueous solution at a 12.7% solid content and pH 3.9. Laccase from agaricus bisporus was brought from Sigma-Aldrich, Inc. (St. Louis, MO, U.S.). Its catalyze ability is ≥ 4 U/mg.

5.3.2 Preparation of modified camelina meal based adhesives

Camelina meal was dispersed into water at 10% solid content at neutral pH 7.0. Varied amount of PAE solution (10%, 20% 30%, 40%, volume ratio to camelina meal slurry) were added into camelina meal slurry with consistent stirring. The pH of the slurry was maintained using 3M sodium hydroxide. Camelina meal slurry was stirred under the same conditions without PAE to use as control. The 30% PAE-camelina meal formulation was further modified with different amount of laccase (0.2% and 0.4% w/w). Laccase was added to 30% PAE-camelina meal slurry and the slurry was heating at 50 to 60 °C for 30 min with stirring. After heat treatment, 3M sodium hydroxide was added to adjust pH to 7.0. The modified adhesive sample was then stirring at room temperature for three hour before mechanical tests.

5.3.3 Wood bonding strength tests

Two layer wood specimen Cherry or yellow pine wood pieces were preconditioned at 23 ℃ and 50% RH in a chamber (Electro Tech Systems, Inc., Glenside, PA, US) for at least one week prior to use. According to previous studies, the camelina protein adhesives were brushed on wood at 2.36 mg/cm^2. The wood pieces were rested for 15 min before assembling together. To avoid the influence of hot press condition on adhesion strength, a relative higher temperature of 170 ℃ and a longer time of 10 min were used at a pressure of 1.4 MPa. The wood assemblies were cooled at room temperature and conditioned at the chamber at 23 ℃ and 50% RH for one day before cutting.

Each wood assembly was cut into five small pieces at a dimension of 50 mm × 20 mm (length × width). Two of the small wood pieces were further conditioned and used for dry strength testing. Three of the small wood specimen were soaked in water at room temperature for 48 h. Wet strength was tested immediately after soaking. Adhesion strength was expressed as the stress at maximum load. Wood failure was evaluated in accordance to the standard for estimating the percentage of wood failure in adhesive-bonded joints (16). Wood specimens were tested with an Instron tester (Model 4465, Canton, MA) based on ASTM Standard Method D2339-98 at a crosshead speed of 1.6mm/min (17). Water resistance of the two layer wood specimen was measured based on ASTM Standard Methods D1183-96 and D1151-00 (18). Dry strength data were the average of four replicates and wet strength data were the average of six replicates.

Three layer wood specimen The 300 × 300 × 3.5mm dimension yellow pine veneers were preconditioned in a 27 ℃, 30% RH chamber at least one week before wood adhesion test. The three veneers were layered up in a way that grain lines of the middle panel were perpendicular to the grain lines of the top and bottom panels. Around 20 to 22 g/ft^2 (wet basis) adhesive was brushed on the two faces of the middle veneer panel only. The assembled wood specimen was standing for 15 min before hot press. The hot press conditions were 150 ℃, 10 min at 1.03 MPa.

The bonded three layer wood specimen were conditioned in a chamber at 23 ℃ and 50% RH for two days and then cut into ten small pieces (82.6 × 25.6 mm) and four large wood pieces (50 × 127 mm) based on the ASTM standard method D906-98 (19). Four of the small wood pieces were used to test dry adhesion strength. Water resistance was evaluated in terms of wet shear adhesion strength and three cycle soaking test (20). Six of the small wood pieces were soaked in water for 24 h at 23 ℃ and then wet adhesion was tested immediately after soaking. The four large pieces were used for three cycle test. In each cycle, the wood pieces were soaked at 23 ℃ for four hours and then dried at 50℃ with air circulation for 19 h. After drying, the wood pieces were evaluated for delamination. The delamination score is rated from zero to ten. Zero means no delamination, five is the maximum allowable delamination to pass the test, and ten means completely veneer separation. Any individual value higher than 5 is considered as fail to pass the three cycle test

5.3.4 Characterization

5.3.4.1 Fourier transform infrared spectroscopy (FTIR)

The control and modified camelina meal based adhesives were freeze dried after reaction and ground into fine particles. The IR spectra were recorded by a PerkinElmer Spectrum 100 FTIR spectrometer (Waltham, MA) in the MID-IR range (4000-600 cm^{-1}) with a universal attenuated total reflectance (ATR) sampling device. Each sample was scanned 32 times at a resolution of 2 cm^{-1}. Data from ATR is converted to sample transmission data.

5.3.4.2 Rheology properties

The apparent viscosities of control SPI and WPU-SPI slurries were measured by a Bohlin CVOR150 rheometer (Malvern Instruments, Southborough, MA) with a parallel plate (PP20, 20-mm plate diameter). The distance between cone and plate was set as 500 nm for all samples. Shear rate was in the range of 0.1 to 100 S^{-1}, and the testing temperature was 23℃. To prevent dehydration during testing, a thin layer of silicone oil was spread over the circumference of the samples.

5.3.4.3 Thermogravimetric analysis (TGA)

Control and PAE-laccase modified camelina adhesive were freeze-dried, and then the thermal hydrolysis curves of dry samples were determined using Thermogravimetric analysis (TGA, PerkinElmer Pyris1 TGA, Norwalk, CT). For each sample, about 5 mg was loaded in the pan and heated from 50 to 700 ℃ at a rate of 10 ℃/min. Onset (To) and peak temperatures (Tp) were calculated by TGA software.

5.3.4.4 Differential scanning calorimetry (DSC)

Thermal denaturation of control and PAE-laccase modified camelina adhesive were measured via differential scanning calorimetry (DSC, Q200, TA instrument, Schaumburg, IL). Samples (about 2.5 mg) were hermetically sealed in Tzero aluminum hermetic pans. The samples were heated from 0 to 250 ℃ with a heating rate of 10 ℃/min.

5.4 Results and discussion

5.4.1 Bonding strength of camelina meal based wood adhesive

The influence of PAE on adhesion strength of camelina meal on two layer cherry wood. PAE improved the adhesion strength of camelina meal dramatically. Table 1 is the summary of dry and wet adhesion strength of control and modified camelina meal. The native camelina meal has very low dry strength and hardly has any wet strength. After modification with PAE, both dry and wet adhesion strength significantly increased. With 40% PAE, the dry adhesion strength increased to 4.84 ± 0.43 MPa, and wet strength increased to 2.62 ± 0.61 MPa. PAE is a positive charged aqueous polyelectrolyte, which ensured good compatibility with camelina meal slurry. Charged PAE chains could absorb onto protein and carbohydrate segments in camelina meal through electrostatic interaction and thus enforce the crosslinking network in camelina meal. The initial electrostatic association may form salt bridges or hydrogen bonding between protein/carbohydrate and polyelectrolyte, which promotes partial unfolding resulting in more conformational flexibility and molecular mobility (21, 22). The azetidinium groups from PAE and carboxyl groups from protein/carbohydrates also can form ester bonds during hot-press. Carboxyl with negative charge also serve as anionic retention sites of cationic PAE (23).

5.4.2 Synergistic effect of PAE with laccase on adhesion strength of camelina meal

The formulation with 30% PAE-camelina meal was further improved by adding laccase, which can contribute to the bonding of fiber. The adhesion performance of new formulation were tested on three layer plywood. Table 2 shows that addition laccase help with dry strength but has little effect on wet adhesion strength. When increase solid content from 10% to 15%, wet adhesion strength increased significantly up to 1.04 ± 0.19 MPa. Therefore, solid content has more impact on adhesion strength of camelina meal then chemical modification.

5.4.3 FTIR analysis of control and modified camelina meal

Camelina meal is the material after extracting oil from camelina seed. The FTIR spectrum of camelina meal in Figure 1 indicates three major components, protein, carbohydrate, and oil in camelina meal. The peaks at 1635 and 1539 cm^{-1} representing the vibrations of amides I and II, are from the protein in camelina meal (24). Peak at 1051 cm^{-1} is the C-O and C-C vibrations from

carbohydrates (25). The weak peak at 1743 cm^{-1} is from ester and reveal the existence of camelina oil. After modification with PAE and Laccase, the carbohydrate peak move to lower wavenumber which prove the functional groups changes in carbohydrates. The protein peaks remain the same after modification, which indicates that PAE and Laccase only influence the spatial structure not the peptide or amino acid structures.

5.4.4 Rheology properties of control and modified camelina meal

Viscosity is one of the most important factors when considering handling and surface wetting abilities of adhesives. The intrinsic viscosity against shear rate in the range of 0.1 to 100 S^{-1} were measured and plotted in Fig.2. The gum component in camelina meal makes camelina meal slurry gain very high viscosity. Viscosity of camelina meal at low shear rate (0.1 S^{-1}) can rich to 5000 cp. Viscosity of camelina meal showed shear thinning properties and all the viscosities of modified samples were within the range for good industrial applications (26). PAE and Laccase have on significant influence on camelina meal viscosity.

5.4.5 Thermal degradation analysis of control and modified camelina meal

Thermal analysis gives the information of sample decomposition as a function of temperature. The thermal stability of an adhesive is important reference for further process conditions such as hot press temperature. Figure. 3 and Table 3 shows the derivation weight loss information of camelina meal samples when heating under nitrogen. Figure 3 shows three major components in camelina meal degraded at different temperatures. The first peak at 77 °C in camelina meal was the loss of water and for other samples no obvious water loss peaks were found. The second component of camelina meal showed three ladder peaks between 251-373 °C. The noncovalent bonds including hydrogen bonds, electrostatic interactions, and other intramolecular interactions are first decomposed and then the covalent bonds broke and decomposed at a higher temperature (27, 28). The third component was decomposed at 616 °C which may assign to protein subunits with more stable crosslinking network. The PAE-Laccase modified camelina meal loss the three ladder peaks and peaks were broadened. PAE and Laccase interacted with protein and carbohydrates in camelina meal and disturbed the original structure and thus the modified camelina meal showed different thermal stability.

5.4.6 Differential scanning chromatography (DSC) study of camelina meal

Proteins are macromolecular assemblies can form well defined structures that undergo thermally-induced conformational changes. DSC measure the absorption of heat caused by the redistribution of non-covalent bonds and reveal the stability of protein and other macromolecules (29). The DSC peak in camelina meal at 75.3 °C with enthalpy change of 2.9 J/g is considered as protein denaturation peak. When adding PAE, the DSC peak temperature moves to 58.4 °C with much smaller enthalpy change 0.6 J/g. PAE first interacts with protein through electrostatic interactions among charged groups and then stimulates protein unfolding to loose structure, which makes protein less stable and easier for thermal denaturation. Laccase doesn't influence protein denaturation temperature very much but samples with both Laccase and PAE have higher enthalpy than sample with only PAE. Laccase has the potential to covalently link protein subunits or protein subunit with carbohydrate and therefore stabilize protein structure and increase the energy need for protein denaturation. DSC analysis of the thermal denaturation of camelina meal provides an insight into the unfolding of camelina protein and forces involved in conformation stability.

5.5 Conclusion

Compared with soy and other plants, camelina meal is more economical with little competition with food industry. FTIR spectra revealed that protein, carbohydrate, and ester were three main components in camelina meal. Native camelina meal hardly had any adhesion strength. But with PAE and Laccase modification, camelina meal got a dry strength of 1.86 ± 0.32 MPa and wet strength of 1.04 ± 0.19 MPa. PAE interacted with protein and carbohydrate through electrostatic and other non-covalent forces, which broke down the native spatial structure of protein and carbohydrate. Laccase worked as catalyst for oxidation and enforced crosslinking network of camelina meal. It was also found that solid content had significant influence on adhesion strength. Modified camelina meal shows great potential for implication in wood adhesive and serves as a new resource in biomaterial field.

5.6 Reference

1. Ciannamea E.M., Stefani P.M., Ruseckaite R.A. Medium-density particleboards from modified rice husks and soybean protein concentrate-based adhesives. Bioresour. Technol. 2010, 101, 818-25

2. Liu D., Chen H., Chang P.R., Wu Q., Li K., Guan L. Biomimetic soy protein nanocomposites with calcium carbonate crystalline arrays for use as wood adhesive. Bioresour. Technol. 2010, 101, 6235-41

3. KIM S., KIM H.-J. Curing behavior and viscoelastic properties of pine andwattle tannin-based adhesive. J Adhes Sci Technol. 2003, 17, 1369-83

4. Fei Song,* Dao-Lu Tang, Xiu-Li Wang, and Yu-Zhong Wang. Biodegradable Soy Protein Isolate-Based Materials: A Review. Bio Macromolecules 2011, 12, 3369-3380

5. J.M. Wescott, C. R. Frihart and A. E. Traska. High-soy-containing water-durable adhesives, Journal of adhesion science and technology, 2012, 859-873

6. Kai Gu, Jian Huang and Kaichang Li, Preparation and evaluation of particleboard bonded with a soy flour-based adhesive with a new curing agent. Journal of adhesion science and technology 2013, 2053-2064

7. P. Moriel, V. Nayigihugu, B. I. Cappellozza, E. P. Gonçalves, J. M. Krall, T. Foulke, K. M. Cammack, and B. W. Hess. Camelina meal and crude glycerin as feed supplements for developing replacement beef heifers. Journal of animal sicience, 2011,89, 4314-4324

8. Marisol Bertia, Russ Geschb, Christina Eynckc, James Andersond, Steven Cermake, Camelina uses, genetics, genomics, production, and management. Industrial crops and products, 2016, 94, 690-710

9. Jun Tae Kim,1 Anil N. Netravali, Non-Food Application of Camelina Meal: Development of Sustainable and Green Biodegradable Paper-Camelina Composite Sheets and Fibers. Polymer composites, 2012,1969-1976

10. Ningbo Li, Guangyan Qi, Xiuzhi Susan Sun, Donghai Wang. Characterization of gum isolated from Camelina seed. Industrial crops and products, 2016,83,268-274

11. Guangyan Qi, Ningbo Li, Xiuzhi Susan Sun, Yong-chen Shia, Donghai Wang. Effects of glycerol and nanoclay on physiochemical properties of camelina gum-based films. Carbohydrate polymers, 2016,152, 747-754

12. Narendra Reddy, Enqi Jin, Lihong Chen, Xue Jiang, and Yiqi Yang. Extraction, Characterization of Components, and Potential Thermoplastic Applications of Camelina Meal Grafted with Vinyl Monomers. Agricultural and food chemistry, 2012, 60, 4872-4879

13. Claus Felby, Jens Hassingboe, Martin Lundc. Pilot-scale production of fiberboards made by laccase oxidized wood fibers: board properties and evidence for cross-linking of lignin, Enzyme and microbial technology, 2002,31, 736-741

14. Chodankar, S., Aswal, V. K., Kohlbrecher, J., Vavrin, R., & Wagh, A. G. Structural study of coacervation in protein-polyelectrolyte complexes. Physical Review E, 2008, 78(3), 031913

15. Fan, Y., Tang, S., Thomas, E. L., & Olsen, B. D. Responsive Block Copolymer Photonics Triggered by Protein–Polyelectrolyte Coacervation. American Chemistry Socisty NANO, 2014, 8(11), 11467-11473

16. ASTM International, 2002. Standard Practice for Estimating the Percentage of Wood Failurein Adhesive Bonded Joints. Annual Book of ASTM Standards, D5266-99 Vol 15 (06), West Conshohocken, PA, pp. 143

17. ASTM International, 2002. Annual Book of ASTM Standards, D2339-98 Vol 15 (06), West Conshohocken, PA, pp. 158–160

18. ASTM ASTM International, 2002. Annual Book of ASTM Standards, D1131-00 Vol 15 (06), West Conshohocken, PA, pp. 67–69.

19. Annual Book of ASTM Standards, 2004. D906-98, ASTM International. West Conshohocken, PA, Vol. 15.06, pp 1-4

20. ANSI/HPVA HP-1-2004, Hardwood Plywood & Veneer Association. 2004 American National Standard- Hardwood and decorative plywood. ANSI/HPVA HP-1-2004

21. Chodankar, S., Aswal, V. K., Kohlbrecher, J., Vavrin, R., & Wagh, A. G. Structural study of coacervation in protein-polyelectrolyte complexes. Physical Review E, 2008, 78(3), 031913. 18.

22. John Oakes. Protein–surfactant interactions. Nuclear magnetic resonance and binding isotherm studies of interactions between bovine serum albumin and sodium dodecyl sulphate. Journal of the Chemical Society, 1974, 70, 2200-2209)

23. Takao Obokata, Akira Isogai, The mechanism of wet-strength development of cellulose sheets prepared with polyamideamine-epichlorohydrin (PAE) resin. Colloids and Surfaces A: Physicochem. Eng. Aspects, 2007, 302, 525-531

24. D.C. Lee, D. Chapman. Analysis of peptide and protein structures using Fourier transform infrared spectroscopy Methods Mol. Biol., 22 (1994), pp. 183–202)

25. R. Kizil, J. Irudayaraj, K. Seetharaman Characterization of irradiated starches by using FT-Raman and FTIR spectroscopy J. Agric. Food Chem., 50 (2002), pp. 3912–3918.

26. Luo, J., Li, C., Li, X., Luo, J., Gao, Q., & Li, J. A new soybean meal-based bioadhesive enhanced with 5, 5-dimethyl hydantoin polyepoxide for the improved water resistance of plywood. RSC Advances, 2015, 5(77), 62957–62965. http://doi.org/10.1039/C5RA05037E

27. Das, S.N., Routray, M., Nayak, P.L. Spectral, thermal, and mechanical properties of furfural and formaldehyde cross-linked soy protein concentrate: a comparative study. Polymer-plastics technology and engineering, 2008, 47 (6), 576–582.

28. Schmidt, V., Giacomelli, C., & Soldi, V. Thermal stability of films formed by soy protein isolate-sodium dodecyl sulfate. Polymer degradation and stability, 2005, 87, 25–31

29. Chiu MH, Prenner EJ. Differential scanning calorimetry: An invaluable tool for a detailed thermodynamic characterization of macromolecules and their interactions. Journal of Pharmacy and Bioallied Sciences. 2011; 3(1):39-59. doi:10.4103/0975-7406.76463

5.7 Figures and Tables

Figure 5.1 FTIR spectra of control and modified camelina meal

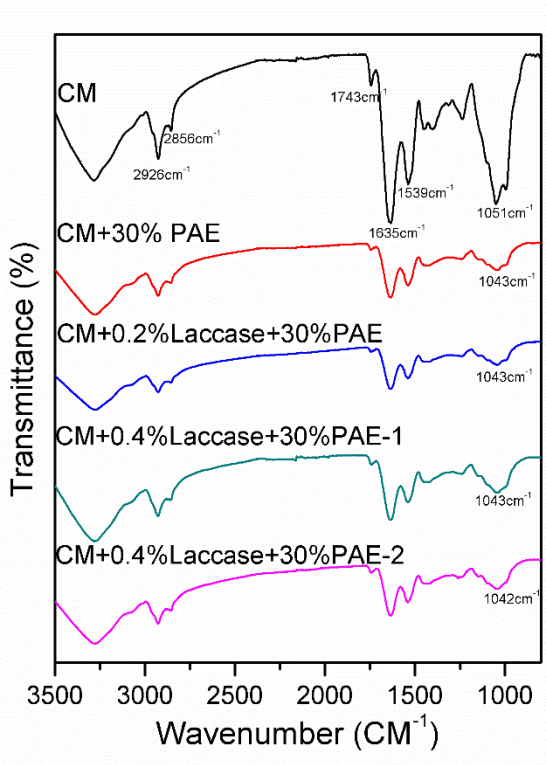

Figure 5.2 Shear rate dependent viscosities of control and modified camelina meal adhesives

Figure 5.3 Derivate thermal degradation analysis curves of control and modified camelina meals

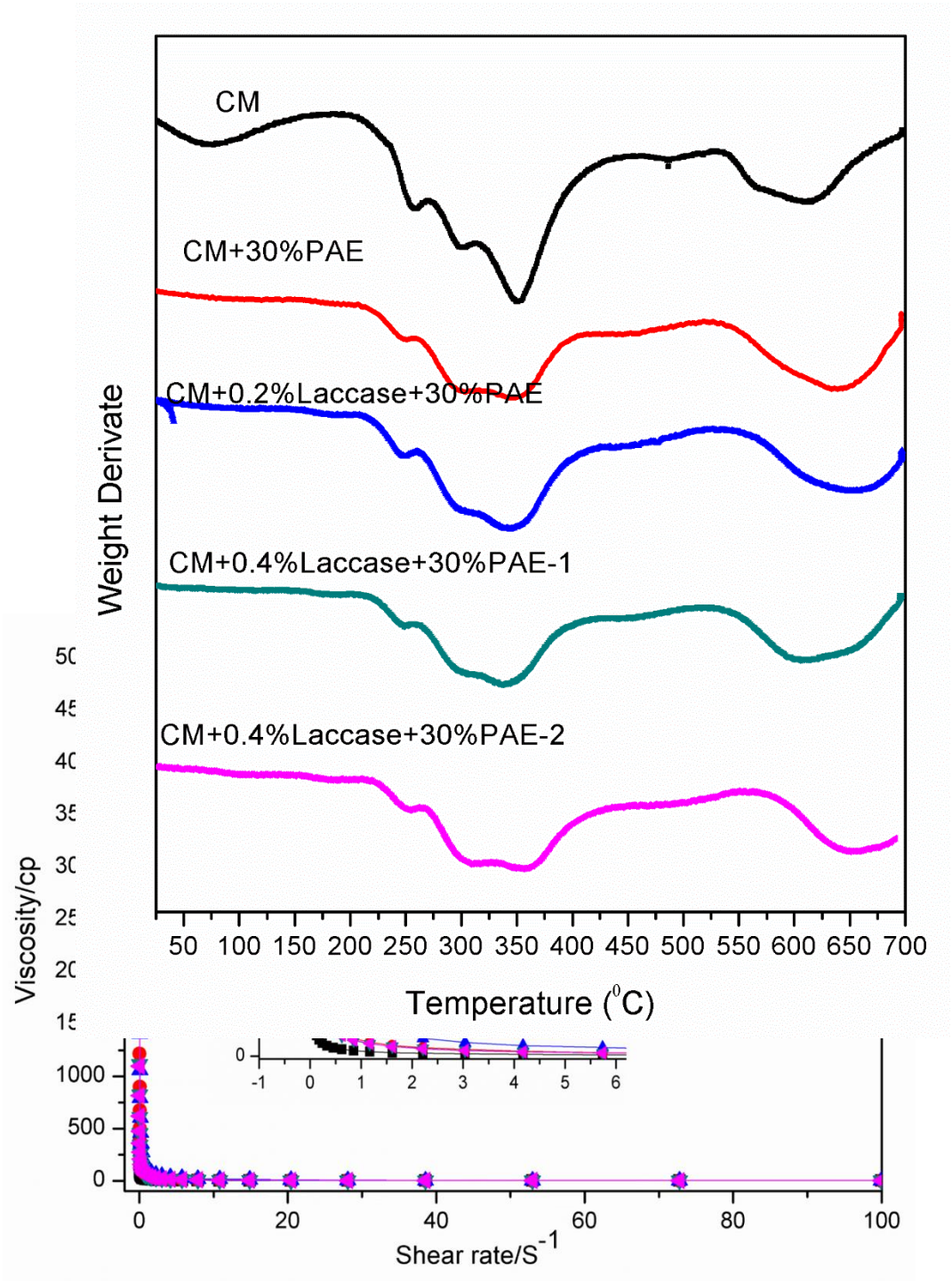

Figure 5.4 DSC of control and modified camelina meal

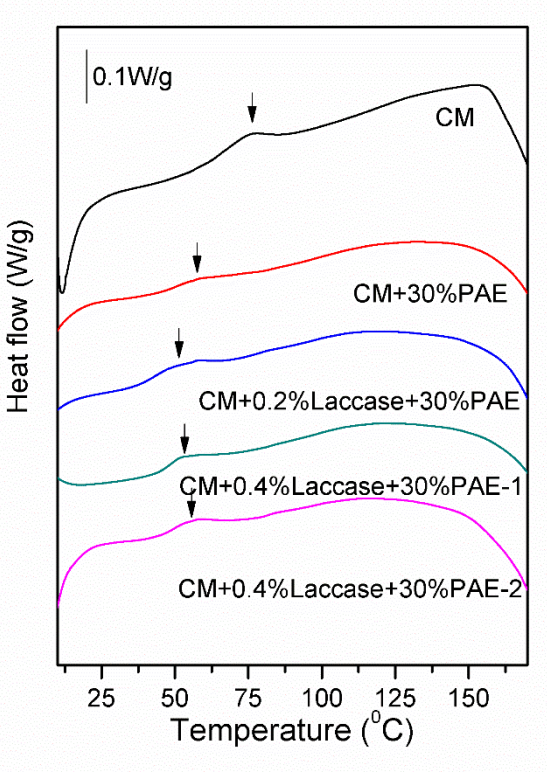

Table 5.1 Two layer cherry wood adhesion strength of camelina meal modified with different amount PAE at neutral pH

Sample ID	Dry Strength (MPa)	CWF	Wet Strength (MPa)	CWF
CM	1.17 ± 0.51C	0	NA	NA
CM+10% PAE	4.66 ± 1.09A	0	1.21 ± 0.31C	0
CM+20% PAE	4.10 ± 0.64AB	0	2.21 ± 0.14B	0
CM+30% PAE	4.54 ± 0.72A	0	2.33 ± 0.52A	0
CM+40% PAE	4.84 ± 0.43A	0	2.62 ± 0.61A	0

Note: CWF means cohesive wood failure. Dry strength data were the average of six duplicates and wet strength data were the average of nine duplicates. Capital letters after data were results for statistical analysis. $\alpha = 0.05$; CM is abbreviation for camelina meal.

Table 5.2 Three layer yellow pine wood adhesion strength of modified camelina meal

Adhesion strength results						
Sample Name	Dry strength (MPa)		Wet strength (MPa)			
CM	0.91 ± 0.12		NA			
CM+30%PAE	1.63 ± 0.16		0.49 ± 0.26			
CM+0.2%Laccase+30%PAE	1.76±0.44		0.27±0.22			
CM+0.4%Laccase+30%PAE	1.95 ± 0.50		0.47 ± 0.52			
15% solid content	1.86 ± 0.32		1.04 ± 0.19			
Three cycle soaking results						
Sample Name	Cycle 1		Cycle 2		Cycle 3	
	Score	Pass	Score	Pass	Score	Pass
CM	NA					
CM+30%PAE	0.25	100%	1.38	100%	2.34	75%
CM+0.2%Laccase+30%PAE	0.82	100%	4.5	100%	7	0
CM+0.4%Laccase+30%PAE	4.75	75%	5.62	50%	6.67	0
15% solid content	0	100%	0.88	100%	1	100%

Note: Higher score means larger delamination

Table 5.3 Derivative thermal degradation peaks of control and modified camelina meal

Sample ID	Peak 1 (℃)			Peak 2 (℃)			Peak 3 (℃)		
	Onset	End	Peak	Onset	End	Peak	Onset	End	Peak
CM	36	101	77	251	266	258	282	310	298
CM+30%PAE	53	78	74	229	257	245	272	266	293
CM+0.2%Laccase+30				241	256	250	271	387	344
CM+0.4%Laccase+30				244	252	248	267	383	338
CM+0.4%Laccase+30				245	260	253	273	400	355

Sample ID	Peak 4 (℃)			Peak 5 (℃)		
	Onset	End	Peak	On set	End	Peak
CM	328	373	351	546	644	616
CM+30%PAE	327	318	350	552	696	639
CM+0.2%Laccase+30				585	697	652
CM+0.4%Laccase+30				552	688	606
CM+0.4%Laccase+30				613	698	649

Table 5.4 DSC peaks of control and modified camelina meal

Sample name	Peak Temperature (°C)	ΔH (J/g)
CM	75.3	2.9
CM+30% PAE	58.4	0.6
CM+0.2%Laccase+30%PAE	50.6	1.6
CM+0.4%Laccase+30%PAE-1	52.8	1.56
CM+0.4%Laccase+30%PAE-2	50.8	1.3

Note: ΔH means enthalpy change

Chapter 6. Conclusion and future outlook

6.1 Conclusion

The physiochemical properties of oilseed proteins were successful modified to meet the application needs as wood adhesive. The forces stabilizing protein three dimensional structure including hydrophobic interactions, hydrogen bonds, and electrostatic interactions were altered by fatty acyl chains and polyelectrolytes. The water sensitive groups (WSG) were reduced by interacting or reaction with hydrophobic molecules. Introducing fatty acyl chains to protein increased the system hydrophobicity and then benefit mechanical properties of oilseed proteins. Polyelectrolytes could stimulate protein unfold and explore more active groups to further influence other protein characteristics. Both the interactions between protein and aliphatic chemicals, protein and polyelectrolytes improve the wet adhesion strength of protein based adhesive.

Undecylenic acid (UA) with 11-carbon chain was grafted onto soy protein through reaction between carboxyl from UA and amine from protein. The fatty acyl chain of UA had significantly increased the wet adhesion strength of soy protein from 2.04 MPa to 3.03 MPa testing on cherry wood. Hydrophilic amine groups replaced by hydrophobic fatty acyl chains was the main reason for improved water resistance of protein structure. Decreased particle size as observed by AFM and laser scattering particle sizer revealed that the cross linkage between protein molecules were decreased because the blocking effect of UA chains. The protein thermal denaturation and degradation peaks observed by DSC and TGA gave evidence for a less stable structure and the increased viscosity and modules proved protein unfolding and increased intermolecular interactions with UA.

Soy oil with three fatty acid chains was converted into waterborne polyurethane (WPU) and then interacted with protein to reduce the WSG. The oil based WPU had good compatibility and reactivity with aqueous protein. The main forces between WPU and protein were physical entanglement, hydrophobic interactions, and hydrogen bond. WPU modification had increased wet adhesion strength up to 3.81 ± 0.34 MPa with fiber pulled out compared with 2.01 ± 0.46 MPa of SPI testing on cherry wood. Also, the dry wood adhesion strength were improved from 5.78 ± 0.37 to 7.30 ± 0.61 MPa with 100% cohesive wood failure. A new crosslinking network structure were

built between protein and WPU. The particle size of different WPU had effects on the interactions with protein. The larger contact surface from smaller size WPU0002 facilitated the interaction with protein and led to a massive aggregates as observed by TEM images. Particle size and viscosity data agreed well with TEM images. WPU0002-SPI adhesive had larger particle size and higher viscosity while interaction between WPU0500 and SPI had little impact on particle size and viscosity.

UA and WPU had reduced the WSG on soy protein and improved its wet adhesion strength, however, these methods can't apply to camelina protein directly. The camelina protein is more compact than soy protein in structure. Native camelina protein has poor mechanical strength, 2.39 ± 0.52 MPa dry strength and 0.37 ± 0.22 MPa wet strength testing on cherry wood. Polymeric amine epichlohydrine (PAE) were used to unfold camelina protein and explore more reactive groups or adhesion groups. TEM images revealed that PAE worked as bridges among protein molecules and after PAE modification, protein had more flexible and loos structures. PAE modified camelina protein had an increased dry strength at 5.39 ± 0.50 MPa with 100% cohesive wood failure and wet strength at 2.35 ± 0.17 MPa testing on two layer cherry wood. The three layer yellow pine wood testing results of PAE treated camelina protein had a wet adhesion strength of 1.30 ± 0.23 MPa, which already met China and Japan standard for plywood application. When brought UA and WPU to the PAE pretreated camelina system, the wet adhesion strength were further improved to 2.87 ± 0.21 MPa and 3.12 ± 0.20 MPa testing on two layer yellow pine wood. For the three layer wood testing, WPU can further improved both dry and wet adhesion strength of PAE pretreated camelina protein to 2.75 ± 0.22MPa and 1.40 ± 0.25MPa respectively. But UA had negative effect on dry strength when testing on three layer yellow pine wood. Because the small UA molecule partly covered reactive groups on camelina protein and resulted in weak three dimensional network while WPU didn't directly cover reactive groups but strongly physical entangled with protein structure. When brought crosslinker, Tetrakis(hydroxymethyl)-phosphonium chloride, into the PAE pretreated camelina system, both dry and wet adhesion strength were decreased, which proved that crosslinking occupied too many reactive groups and not favored for adhesion strength.

Camelina meal is more economical to use as adhesive than extracted camelina protein. Native camelina meal hardly has any adhesion strength. After introducing PAE and laccase to camelina meal slurry at neutral pH, camelina meal got a dry strength of 1.86 ± 0.32 MPa and wet strength of 1.04 ± 0.19MPa on three layer yellow pine wood, which already met China and Japan standards. PAE interacted with protein and carbohydrates through charged groups and broken the spatial structure in camelina meal. Laccase could enforce meal structure by stimulating oxidation reaction of protein and carbohydrates.

Oilseed protein are great resource for bio-based adhesives. The methods studied in this dissertation has successful improve the wet mechanical performance of soy protein, camelina protein, and camelina meal, showing the potential for application in other proteins. The modified protein based adhesives meet industrial needs for good performance and environmentally-friendly characters.

6.2 Recommendation

The future study of this project could consider these following aspects:

1. The purity of the oilseed protein isolate is usually between 80% and 90%. The other contents include polysaccharose, fiber, and oil. The discontinues in structure between protein and other impurities may results in weak crosslinking network. Improving the linking between protein and the other polysaccharides, fiber and oil contents should enhance the networking structure of the curried protein based adhesive. The amine, carboxyl, and hydroxyl groups from protein are active for amidation, acylation, and condensation reactions. The suitable reaction condition and catalyzes for reaction between protein and other contents need to be studied.

2. Study the influence of temperature, charge density, and ionic strength on the interactions between protein and polyelectrolytes/fatty acyl chains. External conditions affect chemical reaction and covalent and non-covalent interactions between molecules. The extent of reaction directly influences protein conformation and then perform differently on adhesion properties.

3. In this dissertation, protein with polyelectrolytes or acyl chains was modified after extraction. Actually, during the alkali dissolution, protein is in a highly unfolded state with larger contact surface and more reactive groups on the surface. Modification during extraction should

increase the reaction efficiency and the unreacted chemical agents are easily removed during acidic precipitation.